Coordination Chemistry Reviews, 86 (1988) 43–134
Elsevier Science Publishers B.V., Amsterdam – Printed in The Netherlands

^{113}Cd NMR SPECTROSCOPY OF COORDINATION COMPOUNDS AND PROTEINS

MICHAEL F. SUMMERS *

Biophysics Laboratory, Center for Drugs and Biologics, Food and Drug Administration, 8800 Rockville Pike, Bethesda, MD 20892 (U.S.A.)

(Received 24 March 1987)

CONTENTS

ABBREVIATIONS AND DEFINITIONS

acac	Acetylacetonate
ALAD	5-Aminolevulinic acid dehydratase
AP	Alkaline phosphatase
As	Arsenate
α-Lact	α-Lactalbumin
BCA	Bovine carbonic anhydrase

* Present address: Department of Chemistry, University of Maryland, Baltimore County, Baltimore, MD 21228, U.S.A.

0010-8545/88/$32.20

BGP	Osteocalcin
bipy	Bipyridine
bnz	Benzyl
bnzSuc	Benzylsuccinate
BS	Benzenesulfonamide
BSA	Bovine serum albumin
BTA	Benzoyltrifluoroacetone
Bu	n-Butyl
buxan	Butylxanthate
Bz	Benzimidazole
CA	Carbonic anhydrase
Cal	Calmodulin
chx	Cyclohexyl
ChxDTA	*N,N,N′,N′*-Cyclohexanediaminetetraacetate
Con A	Concanavalin A
COO*	Bidentate-coordinated carboxyl group
CP	Cross polarization
CPA	Carboxypeptidase A
cryp	4,7,13,16,21,24-hexaoxa-1,10-diazabicyclo[8.8.8]hexacosane
Cys	Cysteine
dien	Diethylenetriamine
dtc	Dialkyldithiocarbamate
dtp	*O,O*-dialkyldithiophosphate
dtpb	*O,O*-dibutyldithiophosphate
dtph	*O,O′*-dicyclohexyldithiophosphate
dtpp	*O,O′*-diisopropyldithiophosphate
2D	Two-dimensional
δ	Isotropic chemical shift
δ_{11}, δ_{22}, δ_{33}	Principal shielding elements
$\Delta\delta$	Chemical shift anisotropy
EDTA	*N,N,N′,N′*-Ethylenediaminetetraacetate
EGTA	Ethylene glycol bis(β-*O*-aminoethyl ether)*N,N′*-tetraacetate
en	Ethylenediamine
Et_4en	*N,N,N′,N′*-Tetraethylethylenediamine
etxan	Ethylxanthate
etxth	*O*-ethyl xanthato
γ	Magnetogyric ratio, kHz gauss^{-1}
Gla	γ-Carboxyglutamic acid
Glc	Glucose
Glc-6-P	Glucose-6-phosphate

$GlcP_2$	Glucose-1,6-diphosphate
Gly	Glycine
HA	High-affinity binding site
HCAB	Human carbonic anhydrase B
HCAC	Human carbonic anhydrase C
HMQC	Heteronuclear multiple quantum coherence
HRP	Horseradish peroxidase
Hthi	Thiamine
I	Nuclear spin quantum number
ICaBP	Intestinal calcium binding protein
imid	Imidazole
Ins	Insulin
itc	Isothiocyanato
Ll	$(BzCH_2)_3N$; Bz = 2-substituted benzimidazole
LA	Low-affinity binding site
LADH	Liver alcohol dehydrogenase
MAMI	5-(1,2,5-Dithiazepan-5-ylmethylene)-4-methyl-2-ethylimidazole
MAS	Magic angle spinning
Mbz	2-Substituted 5,6-dimethylbenzimidazole
3-Medtb	3-Methyl-1,2-dithiobenzene
Meen	*N*-Methylethylenediamine
Meimid	*N*-Methylimidazole
Mes	4-Morpholineethanesulfonate buffer
Met	Methionine
mnt	$S_2C_2(CN)_2$
MT	Metallothionein
N	Isotopic natural abundance
NAD^+	Nicotinamide adenine dinucleotide, oxidized form
NADH	Nicotinamide adenine dinucleotide, reduced form
Neop	Neoprontosil
Parv	Parvalbumin
PF1	Prothrombin fragment 1
PFX	Prothrombin factor X
PGM	Phosphoglucomutase
Ph	Phenyl
phen	Phenanthroline
Pho C	Phospholipase C
Pi	Inorganic phosphate
P_i	Population of the ith species
pip	Piperidine
3PP	3-Phenylpropionate

PPase	Inorganic pyrophosphatase
PPPE	L-Phenylalanine phosphoramidate phenyl ester
Pr	Propyl
py	Pyridine
R	Alkyl
R_C	Receptivity relative to ^{13}C, $= \lvert\gamma_x^3/\gamma_c^3\rvert[N_x I_x(I_x+1)/N_c I_c(I_c+1)]$
R_2dtc	Dialkyldithiocarbamate
R_2dtp	*O,O'*-Dialkylthiophosphate
SBB	Monothiodibenzoylmethane
SD	Superoxide dismutase
STTA	Monothiothenoyltrifluoroacetone
T_1	Spin–lattice (longitudinal) nuclear relaxation constant
T_2	Spin–spin (transverse) nuclear relaxation constant
TFP	Trifluoperazine
TGA	Thioglycolic acid
TLA	Thiolactic acid
tmd	$NH_2(CH_2)_4NH_2$
tmtu	Tetramethylthiourea
tn	$NH_2(CH_2)_3NH_2$
Tn C	Troponin C
TPP	Tetraphenylporphyrin
trien	Triethylenetetramine
TTA	Thenoyltrifluoroacetone
W	Water molecule
W*	Water or substrate molecule
X	Halide
YE	Yeast enolase

A. INTRODUCTION

^{113}Cd NMR spectroscopy has received considerable attention since its utility as a metallobioprobe was demonstrated by Armitage, et al. in 1976 [1]. To date, ^{113}Cd NMR spectroscopy has been employed in studies of more than 24 different metalloproteins to examine the coordination environment in Zn, Ca, Cu, Cd, Hg, Mn, and Mg binding sites. In addition to providing information on the number and type of coordinating groups, ^{113}Cd NMR spectroscopy has afforded valuable information on protein conformational changes, accessibility of solvent and anions to the metal, and the nature of protein interactions with substrates and inhibitors. Several reviews which include selected aspects of the ^{113}Cd NMR literature have appeared [2–16].

The efficacy of ^{113}Cd NMR as a metallobioprobe is due in part to the ability of Cd (the oxidation state is +2) to form complexes with a wide

variety of conformations and ligand numbers. Generally, Cd-substituted metalloproteins retain, at least to some extent, their biological activity. Unlike other probes, such as Co, Cd^{2+} possesses a filled *d*-shell and thus coordination geometries are not subject to ligand field effects. In addition, ^{113}Cd has a spin of $\frac{1}{2}$ (thus, no quadrupolar contribution to NMR relaxation which broadens NMR signals), a reasonable magnetogyric ratio (γ) (-0.947 kHz gauss^{-1}; for comparison the value for ^{13}C is 1.07 kHz gauss^{-1}), and a natural abundance of 12.26% (compared to 1.108% for ^{13}C). Thus, ^{113}Cd has a receptivity relative to ^{13}C (R_C, see Abbreviations and Definitions) of 7.6. Finally, ^{113}Cd has a demonstrated chemical shift range of over 900 ppm, and the value of the chemical shift has been shown to depend on the nature, number, and geometric arrangement of the atoms coordinated to cadmium. ^{111}Cd also has properties suitable for NMR measurements ($I = 1/2$, $\gamma = -0.905$ kHz gauss^{-1}; $N = 12.75\%$). Since the receptivity of ^{111}Cd is less than that of ^{113}Cd, the majority of the NMR studies have been performed with the latter nuclide. However, for completeness, studies employing ^{111}Cd will also be included in this review.

Within four years of the first study of Cd-substituted proteins, some anomalies began to emerge. For example, in 1978 Armitage et al. reported a chemical shift for ^{113}Cd-substituted superoxide dismutase of 170 ppm [17]. In 1980, Ellis and co-workers reported a shift for the same enzyme of 311 ppm [18]. In addition, the chemical shifts obtained for some enzymes were dramatically different, even though X-ray structural analyses revealed very similar metal binding sites. It became clear early on that chemical dynamic problems could influence ^{113}Cd chemical shifts, thereby confounding analyses of shifts in terms of the structural properties of metal binding sites in proteins. Much effort has been subsequently made to circumvent the adverse effects of chemical exchange, including the application of solid-state NMR methods, the use of super-cooled solutions to slow down the chemical exchange processes, and the synthesis of compounds with less labile ligands. Recently, multi-pulse NMR experiments, including two-dimensional (2D) ^{1}H-detected heteronuclear multiple quantum coherence (HMQC) spectroscopy, have been successfully applied. The wealth of new information, mostly generated in the last decade, has provided the coordination chemist and the biochemist with a powerful tool for elucidating structural features of metal coordination sites in coordination compounds and proteins.

The first part of this review is intended to provide a comprehensive summary of research efforts employing ^{113}Cd NMR spectroscopy. The solid-state ^{113}Cd literature will be presented first, followed by the solution-state literature. Within these groups, data for coordination compounds and proteins will be presented separately. In the latter part of the review, chemical shift results obtained for solid- and solution-state samples will be

compared and trends between structural parameters and ^{113}Cd shifts identified. With these results, an attempt will be made to rationalize shifts observed for Cd-substituted metalloproteins. The structural information obtainable using recently developed two-dimensional (2D) solution NMR methods, including 2D heteronuclear multiple quantum coherence and ^{113}Cd-COSY will then be described and, finally, a brief overview will be presented.

B. SOLID STATE STUDIES

The different types of solid state NMR spectral data and the information they can provide will be briefly described. Solid-state results will then be presented separately for Cd coordination compounds and Cd-substituted metalloproteins. Except as noted, chemical shift values will be reported relative to the most widely utilized standard (0.1 M aqueous $Cd(ClO_4)_2$). Conversions to this reference have been made where appropriate and noted in the table legends.

The solid-state ^{113}Cd experiments which have been reported thus far can be arranged into two main groups including those which utilize non-oriented, powdered samples and those which utilize oriented single crystal samples. Cross polarization (CP) is usually employed to provide decoupling of the dipolar interaction with protons and for sensitivity enhancement. Solid-state ^{113}Cd NMR spectral lineshapes can be used to determine the principal shielding elements (δ_{11}, δ_{22}, δ_{33}) of the chemical shift tensor. Under conditions of magic-angle spinning (MAS) the isotropic chemical shift δ (eqn. (1)) can be obtained, which is equivalent to the shift observed

$$\delta = \tfrac{1}{3}(\delta_{11} + \delta_{22} + \delta_{33}) \tag{1}$$

in solution in the absence of chemical equilibria effects. For Cd in a nonsymmetric environment, with $\delta_{11} < \delta_{22} < \delta_{33}$, the chemical shift anisotropy ($\Delta\delta$) is defined as

$$\Delta\delta = \delta_{33} - \tfrac{1}{2}(\delta_{11} + \delta_{22}) \tag{2}$$

For a symmetric tensor, where $\delta_{22} = \delta_{11} = \delta_{\perp}$, then $\delta_{33} = \delta_{\parallel}$; for $\delta_{22} = \delta_{33} = \delta_{\perp}$, then $\delta_{11} = \delta_{\parallel}$. For these cases, the shift anisotropy is defined by

$$\Delta\delta = \delta_{\parallel} - \delta_{\perp} \tag{3}$$

In general, the principal elements of the shielding tensor are determined via computer fitting of the experimental powder spectra. In some cases, the relative shielding tensors (δ'_{11}, δ'_{22}, δ'_{33}; eqn. (4)) are reported.

$$\delta'_{nn} = \delta_{nn} - \delta \quad n = 1, 2 \text{ or } 3 \tag{4}$$

(i) Coordination compounds

Studies utilizing non-oriented samples and oriented, single crystal samples will be grouped separately. In general, results within each group will be presented as they appeared chronologically.

Studies with non-oriented samples

^{113}Cd NMR studies of non-oriented solid samples were published as early as 1969 by Look [19], where the spin–lattice relaxation properties (T_1) and Hall effects were examined as a function of temperature for cadmium oxide. ^{113}Cd chemical shifts were subsequently reported for Cd chalcogenides and Cd salts containing halides and oxo-anion donor ligands [20,21], Tables 1 and 2. The first systematic evaluation of solid-state shifts as a function of coordination properties was published in 1981 by Maciel and co-workers [22], where a large group of structurally (X-ray) characterized Cd compounds was examined. The NMR results, summarized in Table 1, provided the first of the so-called "benchmark" spectral data for analyzing solution spectra of Cd compounds and proteins. The chemical shift values observed were almost always different from those observed for solution-state samples due to the fact that the solution shifts reflect weighted averages of shifts for various species which are in equilibrium and exchanging rapidly.

There have been a number of studies directed at comparing X-ray structural and powder-pattern NMR data in order to determine the influence of structural features on shift. Two different Cd sites are present in

TABLE 1

Relative principal shielding elements (ppm) for some cadmium(II) salts [a]

Complex	$\delta_{11'}$	$\delta_{22'}$	$\delta_{33'}$	$\Delta\delta$	δ
$(Me_4N)_2CdBr_4$	−11	−11	22	33	395
$(Me_4N)_2CdI_4$	−28	−2	27	42	92
$(Et_4N)_2CdCl_4$	0	0	0	0	479
$(Et_4N)_2CdBr_4$	0	0	0	0	372
$(Et_4N)_2CdI_4$	−18	−18	36	54	81
Cd(n-buxan)$_2$	−116	10	106	159	440
Cd(etxan)$_2$	−173	24	148	222	410
$Cd(OH)_2$	−107	54	54	−161	150 (152) [b]
$Cd(NH_4)_2(SO_4)_2\cdot 6H_2O$	−30	−13	47	68	60
$Cd(ClO_4)_2\cdot 6H_2O$	0	0	0	0	0
Cd(acac)$_2$	−22	−4	28	41	−19
$Cd(NO_3)_2\cdot 4H_2O$	−120	60	60	−180	−100

[a] Ref. 22.

[b] Value in parentheses from ref. 21.

TABLE 2

Isotopic ^{113}Cd NMR chemical shifts of some crystalline powdered compounds [a]

Compound	δ (ppm)	Ligands	Geometry [b]
$(Et_4N)_2CdCl_2$	483	4Cl	tet.
$(Hthi)CdCl_4 \cdot H_2O$	460	4Cl	tet.
$CdCl_2 \cdot 5/2H_2O$ Cd(1)	213 (196) [c]	5Cl, 1O	oct.
Cd(2)	187 (175) [c]	4Cl, 2O	oct.
$[Cd(NH_3)_6][CdCl_5]$	134	5Cl	trig. bip.
$Cd(n\text{-buxan})_2$	445	4S	tet.
$Cd(etxan)_2$	414	4S	tet.
$Cd(et_2dtc)_2$	377	5S	trig. bip.
$(pip)_2CdBr_4$	396	4Br	tet.
$(Me_4N)_2CdBr_4$	391	4Br	tet.
$(Et_4N)_2CdBr_4$	374	4Br	tet.
$(Me_4N)_2CdI_4$	92	4I	tet.
$(Et_4N)_2CdI_4$	79	4I	tet.
$Cd(en)_3Cl_2 \cdot H_2O$	380	6N	oct.
$Imid_6Cd(OH)NO_3 \cdot 4H_2O$	272	6N	oct.
$Imid_6Cd(NO_3)_2$	238	6N	oct.
$Na_2Cd(EDTA)$	117, 107, 97	2N, 4O	oct.
$Cd(OH)_2$	158	6O	oct.
$Cd(NH_4)_2(SO_4)_2 \cdot 6H_2O$	61	6O	oct.
$Cd(HCOO)_2 \cdot 2H_2O$	26, 21	6O	oct.
$Cd(O_2CCHCHCO_2) \cdot 2H_2O$	12, −7	6O	oct.
$Cd(ClO_4)_2 \cdot 6H_2O$	0	6O	oct.
$CaCd(OAc)_4 \cdot 6H_2O$	−14	8O	dodec.
$Cd(acac)_2$	−18		
$Cd(OAc)_2 \cdot 2H_2O$	−46 (−58) [c]	7O	
$3Cd(SO_4) \cdot 8H_2O$	−45, −58 (147, −60) [c]	6O	oct.
Cd(cryp)	−62		
$Cd(NO_3)_2 \cdot 4H_2O$	−100 (−100) [c]	8O	
CdF_2 [d]	−223		
$CdCl_2$ [d]	211		
$CdBr_2 \cdot 4H_2O$ [d]	41		
CdI_2 [d]	−672		
CdO [d]	900		
CdS [d]	692 (808) [e]	4S	tet.
CdSe [d]	550		
CdTe [d]	283 [f]		
$CdCO_3$ [d]	−30		

[a] For details see ref. 22.

[b] Approximate geometry; see references to structures published in Table II of ref. 22.

[c] Values in parentheses from ref. 21. The reference has been changed to the $Cd(ClO_4)_2$ standard by changing the shift value of $Cd(NO_3)_2 \cdot 4H_2O$ (aq) from 0.0 ppm to $= -100.0$ ppm.

[d] From ref. 20.

[e] Value in parentheses from ref. 24.

[f] See also ref. 194.

$3CdSO_4 \cdot 8H_2O$, and δ values of -43.7 ± 2 ppm and 56.4 ± 2 ppm were observed for Cd in the A and B sites, respectively [23]. The shielding tensors were reported to exhibit axial symmetry; however, asymmetric shielding parameters of -139, -31, and 28 ppm for δ_{11}, δ_{22}, and δ_{33} were observed for $CdSO_4 \cdot H_2O$. A correlation was found between bonding distance anisotropies and NMR chemical shift anisotropies, and no correlation between average Cd–O distance and isotropic chemical shift was observed [23]. Single crystal studies of cadmium sulfate have also been reported (vide infra).

Similar structure–shift comparisons have been made for Cd complexes containing mercaptoethanol [24,25], Table 3. Originally, $[Cd_{10}(SCH_2CH_2OH)_{16}][(ClO_4)_4]$ was examined [24], which contains three distinct Cd sites. The A site (containing 3 S and 3 O donor atoms) gave an isotropic shift of 509 ppm, the B site (4 S and 1 O) gave a shift of 603 ppm and the C site (4 S) gave a shift of 774 ppm. Comparison of the NMR results with published X-ray data afforded the following conclusions: (i) shielding anisotropy provides a measure of the range of bond lengths for a given Cd, and (ii) the isotropic shift indicates the type of liganding atoms. Under high resolution conditions, the signals exhibited anomalous splittings. More recently, the perchlorate and sulfate salts $[Cd_{10}(SCH_2CH_2OH)_{16}][(ClO_4)_4]$ and $[Cd_{10}(SCH_2CH_2OH)_{16}][(SO_4)_2] \cdot H_2O$ were examined [25] and the NMR results are given in Table 3. A high-resolution X-ray crystal structure of the

TABLE 3

Isotropic chemical shift values (ppm) for the A, B, and C sites of $[Cd_{10}(SCH_2CH_2OH)_{16}]^{4+}$ salts [a]

Other components of sample	A (3S, 3O)	B (4S, 1O)	C (4S)
$[ClO_4]_4 \cdot 8H_2O$ [b]	403	496	650
	409	503	667
$[ClO_4]_4 \cdot 8H_2O$ [b]	404	497	650
	409	503	667
$[ClO_4]_4$ [c]	400	492	673
$[ClO_4]_4$ [d]	388	481	652
$[SO_4]_2 \cdot 4H_2O$	391	481	623
	401	507	705
$[SO_4]_2$ [c]	392	488	625
		504	657
			686

[a] Reference = 0.1 M aqueous $Cd(ClO_4)_2$; see ref. 25 for details.
[b] Different samples from ref. 25.
[c] $T = 80\,^{\circ}C$.
[d] From ref. 24.

perchlorate salt revealed 6 different Cd sites rather than 3; i.e. two similar but structurally inequivalent (due to small changes in bond angles and lengths) CdS_3O_4, CdS_4O and CdS_4 sites were found, which explained the anomalous "splitting" of the A, B, and C site ^{113}Cd signals reported earlier [24].

For the two CdS_4 sites of the cadmium perchlorate salt [25], the shift difference was 17 ppm and the largest angular difference was 6.7° for one of the S–Cd–S angles. The difference in the average Cd–S distances for the two sites was < 0.01 Å. However, a shift difference of 82 ppm was observed for the sulfate salt, where the difference in average Cd–S distance was 0.03 Å and the angular differences were the same as those observed for the perchlorate salt [25]. This interesting finding indicates that ^{113}Cd shifts are influenced less by changes in bond angles than by changes in Cd–L bond distances.

Ellis and co-workers [26,27] published detailed ^{113}Cd, ^{15}N, and ^{13}C NMR studies of Cd(TPP)py (TPP = tetraphenylporphyrin; py = pyridine) and Cd(TPP). Some of the work was done on a solution sample and those results are reported in the section on solution studies (vide infra). The solid-state ^{113}Cd spectra are shown in Fig. 1, and the shielding tensor elements for Cd(TPP) and Cd(TPP)py are given in Table 4. Clearly, py ligation affects the anisotropic shielding tensor elements differently, leading to −124 ppm and +112 ppm shift changes for $\delta_{\parallel}$ and $\delta_{\perp}$, respectively. These shift changes were attributed to the donor properties of py and the movement of Cd out of the 4N plane of the TPP macrocycle. The isotropic shift for Cd(TPP)py in the solid (+432 ppm) is in full agreement with the shift observed in $CDCl_3$ solution (427 ppm).

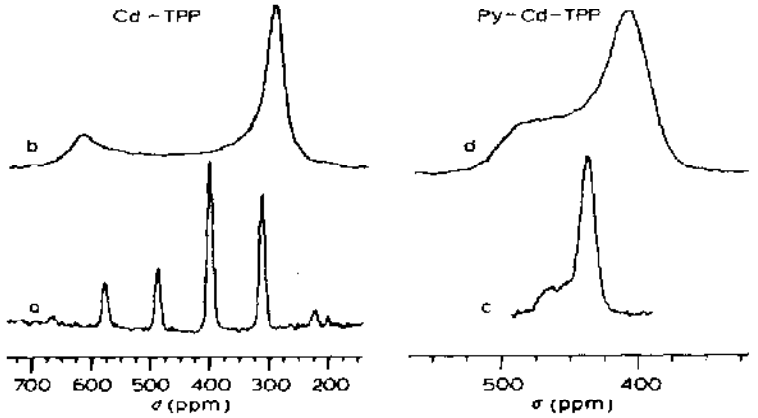

Fig. 1. Solid-state CP ^{113}Cd NMR spectra of Cd(TPP) (a and b) and its ^{15}N-pyridine adduct pyCd(TPP) (c and d). (a) and (c) MAS spectra; (b) and (d) powder patterns for the axially symmetric shielding tensors. From ref. 27.

TABLE 4

^{113}Cd Chemical shielding tensors (ppm) for Cd(TPP) and Cd(TPP) (py) [a]

	δ	$\delta_{\parallel}$	$\delta_{\perp}$	$\Delta\delta$
Cd(TPP)	399	626	285	341
Cd(TPP) (py)	432	502	397	105

[a] Ref. 26.

Isotropic solid-state ^{113}Cd shifts and X-ray structural information have been obtained for a number of Cd compounds [28–38] and the results are summarized in Table 5. In contrast to the above results of Ellis and co-workers [26,27] for the Cd(TPP)py, where nearly equivalent solid- and solution-state shifts were observed, Rodesiler et al. [36] found that the shifts of Cd(TPP)(pip) · *o*-xylene (pip = piperidine) for solid (467 ppm) and solution (438 ppm, $CDCl_3$) samples differed significantly (29 ppm) and these differences were attributed to relaxation of molecular distortions.

Recently, Munakata et al. [39] presented a detailed comparison of the solid-state and low temperature solution ^{113}Cd spectra for a series of CdL_n

TABLE 5

X-Ray structural and ^{113}Cd NMR data for Cd coordination complexes

Compound	Structural features [a]		^{113}Cd δ (ppm)	
			Solid	Solution
$Cd(2\text{-}NH_2CH_2py)_2(NO_3)_2$ [d]	$2NO_3$; 4N	oct.	222	
$Cd(Meimid)_6(NO_3)_2$ [e]	6N	oct.	230	177 (MeOH)
$Cd(p\text{-}ClPhCOO)_2(H_2O)_2$ [f]	2COO*; $2H_2O$	oct. [c]	24	−51 (MeOH)
$Cd(p\text{-}NO_2PhCOO)_2(H_2O)_2$ [f]	2COO*; $2H_2O$	oct. [c]	24	−53 (MeOH)
$Cd(p\text{-}ClPhCOO)_2(py)_2H_2O$ [f]	2COO*; 2N; $1H_2O$	pent. bipy.	30	
$[Cd(o\text{-}HOPhCOO)_2(H_2O)_2]_2$ [g]	2COO*[c]; $2H_2O$ (ax.)	pent. bipy.	−31	
$[Cd(o\text{-}HOPhCOO)_2py_3]_2$ [g]	2COO*, 3py;	pent. bipy.	61	−5 (MeOH)
Cd(succinato)$(H_2O)_2$ [h]	2COO* [c]; $2H_2O$	pent. bipy	−52	
$Cd(2,2'\text{-bipy})_2(NO_3)_2(H_2O)$ [i,j]	4N; $1NO_3$; $1H_2O$	oct.	122	172 (D_2O)
$Cd(2,2'\text{-bipy})_2(NO_3)_2$ [i,j]	4N; $2NO_3$	oct.	51	172 (D_2O)
$Cd(2,2'\text{-bipy})_2(itc)_2$ [j]	6N	oct.	216	122 (DMSO)
$[CdCl_3(H_2O)]_n$ [k]	1 axial Cl; 1 axial H_2O; 4 equat. bridging Cl	oct.	200	
$Cd(tmtu)_2(NO_3)_2$ [l]	2S; $2NO_3$	tet.	263	

[a] COO* = bidentate coordination.

[b] Intermediate between trigonal prismatic and octahedral.

[c] Two of the COO* oxygen atoms in the dimeric complexes are bridging two Cd atoms.

[d] Ref. 37. [e] Ref. 38. [f] Ref. 35. [g] Ref. 32. [h] Ref. 28. [i] Ref. 29. [j] Ref. 33. [k] Ref. 34. [l] Ref. 31.

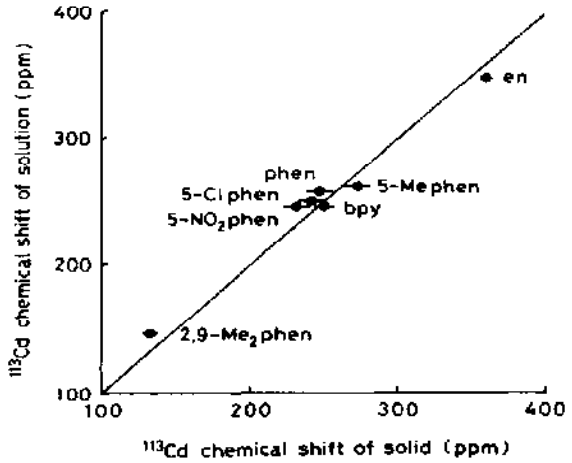

Fig. 2. Comparison of the solid- and solution-state ^{113}Cd NMR chemical shifts for CdL_3; L = bidentate chelate ligands as indicated. Horizontal lines indicate line widths of the solid-state NMR signals. From ref. 39.

complexes containing N-donor L ligands. Although the solution results will be discussed in more detail below, it is significant to point out that, for all cases examined, the shifts observed for complexes at low temperature (where slow-exchange spectra were obtained) agreed well with the shifts observed in the solid state spectra. These results can be seen clearly in Fig. 2, where solution shifts are plotted against solid state shifts (see also Table 6). For the CdL_3 complexes given in Table 6, a change in pK_a from 3.22 (L = 5-NO_2phen) to 5.95 (L = 4,7-$(CH_3)_2$phen) resulted in a change in solid-state ^{113}Cd shift from 243 to 267 ppm, respectively.

TABLE 6

^{113}Cd NMR chemical shifts for CdL_3 complexes (L = bidentate ligand) and pK_a values of L for solid- and solution-state experiments [a]

L	pK_a	^{113}Cd δ (ppm)	
		Solution	Solid
5-NO_2phen	3.22	243	229
5-Clphen	4.07	247	239
phen	4.93	254	244
5-CH_3phen	5.27	259	270
2,9-$(CH_3)_2$phen	5.85	143	129
4,7-$(CH_3)_2$phen	5.95	267	
2,2′-bipy	4.18	243	247
4,4′-$(CH_3)_2$(2,2′-bipy)	5.39	254	265

[a] Acetonitrile, $T = 23°C$, 0.05 M complexes; see ref. 39 for further details.

Cd–CdO samples have been examined using selective saturation, Hahn spin-echo, and 2D NMR experiments [40]. The broad ^{113}Cd NMR signal observed was shown to comprise individual lines arising from a distribution of CdO crystallites having different Cd(0) concentrations [40].

Single crystal studies

Ellis and co-workers [41] pioneered single crystal ^{113}Cd NMR studies on Cd coordination compounds. Initially, $3CdSO_4 \cdot 8H_2O$ and $Cd(NO_3)_2 \cdot 4H_2O$ salts were examined at 44 MHz, and at this field strength, small asymmetric shielding tensor parameters could be identified for $3CdSO_4 \cdot 8H_2O$ (Table 7). Included in Table 7 are the direction cosines and angles determined from X-ray crystallographic analyses.

Other crystalline samples were examined similarly [42] (Table 7), and the shielding tensor components for complexes containing exclusively O-donor atoms are compared graphically in Fig. 3. For complexes with monodentate ligands, the following structure–shielding tensor correlations were observed. First, tensor elements of similar magnitude had similar orthogonal environments. Second, the least shielded tensor element was aligned nearly orthogonal to planes containing coordinated water oxygens. Third, if no water molecules were coordinated to Cd, the least shielded element was oriented to maximize the short Cd–O bond shielding contribution. Fourth, the most shielded tensor element was oriented nearly perpendicular to the longest Cd–O bond. In addition, from recent studies of cadmium glycinate monohydrate [43], it was found that tensor elements can be influenced by current densities located on the ligand support structures of bidentate chelate ligands. No correlations between bond length dispersion and chemical shift

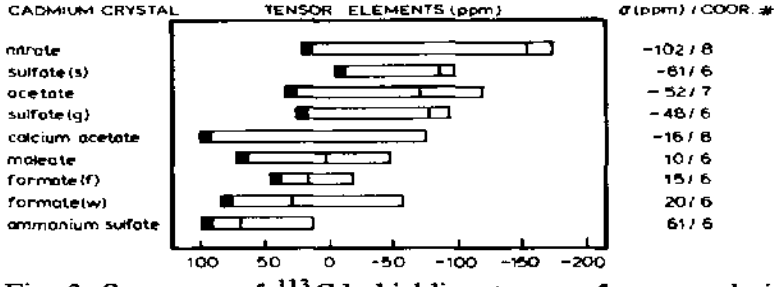

Fig. 3. Summary of ^{113}Cd shielding tensors for oxocadmium compounds determined using single crystal, solid-state NMR experiments. Vertical lines indicate the position of individual shielding elements. The deshielding element of each tensor is designated by either a cross-hatched bar (indicating predominant short-bond shielding contributions) or a solid bar (indicating intramolecular shielding contributions which are dominated by water oxygens). Sulfate suffixes correspond to cadmium in general and special positions. From ref. 42.

TABLE 7

Principal elements of the ^{113}Cd shielding tensors (ppm) and corresponding direction cosines for compounds studied via single crystal X-ray diffraction and ^{113}Cd NMR spectroscopy

Compound	Tensor element [a]		Direction cosines [b]			Angles (°) [b]		
			a	*b*	*c*	*a*	*b*	*c*
$3CdSO_4 \cdot 8H_2O$ [c]	Special position							
	δ_{11}	−95.6	0.0299	0.9995	0.0090	88	2	90
	δ_{22}	−85.3	0.8336	−0.0199	−0.5520	34	91	124
	δ_{33}	−3.4	−0.5515	0.0240	−0.8338	124	89	146
	δ	−61.4						
	General position							
	δ_{11}	−93.1	0.4675	0.8082	−0.3580	62	36	111
	δ_{22}	−76.7	0.5277	0.0698	0.8466	58	86	32
	δ_{33}	25.5	0.7092	−0.5847	−0.3939	45	126	113
	δ	−48.1						
$Cd(NO_3)_2 \cdot 4H_2O$ [c]	δ_{11}	−174.4	0.0561	0.0036	0.9984	87	90	3
	δ_{22}	−154.3	−0.8552	0.5162	0.0462	149	59	87
	δ_{33}	22.2	0.5152	0.8564	−0.0320	59	31	92
	δ	−102.2						
$CdCa(OAc)_4 \cdot 6H_2O$ [d]	δ_{11}	−74.0	0.0115	−0.9998	0.0139	89	179	89
	δ_{22}	−73.6	0.9999	0.0116	−0.0017	1	89	90
	δ_{33}	101.2	−0.0019	0.0139	0.9999	90	89	1
	δ	−15.5						
$Cd(maleate)(H_2O)_2$ [d]	δ_{11}	−46.8	0.8012	−0.0055	−0.5983	37	90	127
	δ_{22}	3.8	0.5984	0.0126	0.8011	53	89	37
	δ_{33}	73.2	−0.0031	0.9999	−0.0134	90	1	91
	δ	10.4						
			Cd_w					
$Cd(formate)_2(H_2O)_4$ [d]	δ_{11}	−55.8	−0.9432	0.0719	0.3242	160	80	71
	δ_{22}	30.3	0.3319	0.2432	0.9114	71	76	24
	δ_{33}	85.1	0.0133	−0.9673	0.2533	89	165	75
	δ	19.9						
			Cd_f					
	δ_{11}	−18.8	−0.0014	−0.2046	0.9789	90	102	12
	δ_{22}	17.4	−0.4014	−0.8964	−0.1879	114	145	101
	δ_{33}	45.6	0.9159	−0.3932	−0.0808	24	113	95
	δ	14.7						
$Cd(NH_4)_2(SO_4)_2(H_2O)_6$ [d]	δ_{11}	13.7	0.3630	0.4466	−0.8178	69	63	145
	δ_{22}	70.1	−0.4726	0.8446	0.2514	118	32	75
	δ_{33}	97.9	0.8030	0.2952	0.5177	37	73	59
	δ	60.6						

TABLE 7 (continued)

Compound	Tensor element [a]		Direction cosines [b]			Angles (°) [b]		
			a	*b*	*c*	*a*	*b*	*c*
$Cd(OAc)_2(H_2O)_2$ [d]	δ_{11}	−118.7	−0.5899	0.3428	−0.7311	126	70	137
	δ_{22}	−69.5	−0.5216	−0.8529	0.0210	121	148	89
	δ_{33}	33.5	0.6164	−0.3937	−0.6820	52	113	133
	δ	−51.6						
$Cd(tmtu)_2(NO_3)_2$ [e]	δ_{11}	−340	0.0228	−0.9995	−0.0227	89	178	91
	δ_{22}	308	0.1859	−0.0181	0.9824	79	91	11
	δ_{33}	327	−0.9823	−0.0266	0.1854	169	92	79
	δ	98						
$Cd(gly)_2H_2O$ [e]	δ_{11}	−117	0.5760	0.2752	0.7697	55	74	40
	δ_{22}	199	−0.7513	0.5492	0.3659	139	57	69
	δ_{33}	255	−0.3220	−0.7891	0.5231	109	142	58
	δ	112						
	δ_{11}	−116	−0.5688	0.3035	−0.7644	125	72	140
	δ_{22}	200	0.7614	0.5459	−0.3497	40	57	110
	δ_{33}	256	0.3112	−0.7810	−0.5416	72	141	123
	δ	113						

[a] Referenced to 0.1 M aqueous $Cd(ClO_4)_2$.
[b] See the appropriate references for details on the axis systems.
[c] Ref. 41. [d] Ref. 42. [e] Ref. 43.

anisotropy were observed. Instead, it was concluded that bond length dispersion, local site symmetry, and ligand type all contribute to the chemical shift anisotropy.

Bryant and co-workers [44] obtained values for the tensor elements identical to those found by Ellis and co-workers [42] for $Cd(OAc)_2 \cdot 2H_2O$; however, the alignments of the elements in the frame of the molecule were assigned differently. This discrepancy has recently been addressed [45] using the complex prepared with ^{13}C-enriched acetate. From the orientation dependence of the ^{113}Cd linewidths for each of the four distinguishable shielding tensors, the tensor elements were assigned unambiguously to lattice positions in the cadmium acetate crystal, confirming the assignments made originally by Ellis and co-workers [42].

Solid-state ^{113}Cd spectra of crystalline and powdered cadmium diethylphosphate have been reported [46]. By comparison of the NMR data with X-ray structural data, it was determined that the most shielded tensor element (−217 ppm) was aligned nearly perpendicular to the longest Cd–ligand bonds, a result consistent with the conclusions of Honkonen and Ellis [42] (vide supra). The ^{113}Cd powder spectrum for Cd-dimyristoylphosphatidic acid has also been presented [46].

(ii) Proteins

The first reported solid-state ^{113}Cd NMR spectrum for a protein was published in 1981 by Ellis and co-workers [47] for Cd-substituted Troponin-C (Tn C); details of the ^{113}Cd spectrum were not discussed. The solid-state ^{113}Cd NMR spectrum of Cd-substituted parvalbumin (Cd_2(Parv)) [5] gave a chemical shift which was ca. 20 ppm to higher field ($\delta = -120$ ppm) compared to the solution-state shift (-95 ppm). This difference was attributed to either chemical exchange (affecting the solution-state spectrum) or to structural differences at the metal binding site under the different sample conditions [5]. Armitage and co-workers [48] showed that the chemical shift of the Cd signals in the solid-state CP and CP/MAS spectra of Cd-substituted rabbit liver MT-1 was the same as the shift obtained from the solution-state spectrum. This confirmed that dynamic exchange processes were not influencing the solution-state shifts. Unfortunately, structural analyses based on the solid-state ^{113}Cd spectra could not be made due to the presence of multiple Cd binding sites and molecular motions.

The most detailed solid-state ^{113}Cd NMR study of metalloproteins to date was published by Ellis and co-workers [49], where Cd-substituted parvalbumin (Cd_2(Parv)) and concanavalin A (Cd_2(Con A)) were examined. The lyophylized powders of both metalloproteins gave very broad ^{113}Cd MAS spectra which indicated that the metal binding sites were considerably disordered under these conditions. Subsequent hydration by vapor diffusion resulted in narrower ^{113}Cd MAS NMR signals which demonstrated that the local structure about the metal had been restored. The ^{113}Cd CP/MAS spectrum obtained for Cd_2(Con A) is shown in Fig. 4. Analysis of spinning side band intensities allowed the values of the shielding tensor elements to

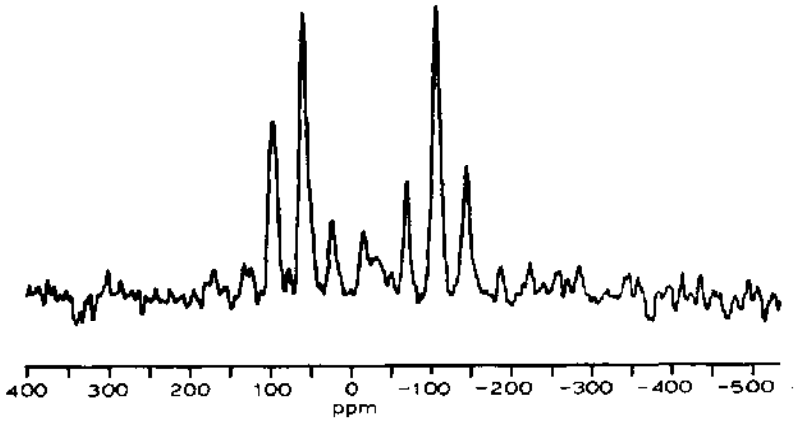

Fig. 4. ^{113}Cd CP/MAS spectrum of ^{113}Cd-substituted concanavalin A (ref. 49).

TABLE 8

Solid state ^{113}Cd NMR data for ^{113}Cd-substituted proteins [a]

	δ	δ_{11}	δ_{22}	δ_{33}	$\Delta\delta$	η
Cd_2(Parv) [b]	−120					
Cd_2(Parv)	−83.4	−10.65	−71.02	−168.5	−127.6	0.71
Cd_2(Con A) (S1)	59.1	104.0	103.1	−29.7	−133.2	0.00
(S2)	−108.4	−178.6	−113.4	−32.9	113.1	0.86

[a] From ref. 49 unless otherwise noted.
[b] From ref. 5.

be calculated for the two Ca sites in parvalbumin (here, the signals were unresolved) and the Mn (S1) and Ca (S2) sites in concanavalin A; see Table 8.

C. SOLUTION STUDIES

As for the previous section, studies of coordination compounds and metalloproteins will be presented separately. The studies on coordination compounds will be presented first, and will be grouped according to the type of donor atoms present (halides (X) and anions, alkyls (R), phosphines, S- and Se-donors, and N-donors).

(i) Coordination compounds

Oxoanions and halides

The first high-resolution ^{113}Cd NMR study for solution samples was published in 1973 by Maciel and Borzo [50], where the chemical shifts of a few Cd salts and Bu_2Cd (Bu = n-butyl) were reported. A more detailed study of Cd salts was published in 1974 by Kostelnik and Bothner-By [51]. The concentration dependence of the ^{113}Cd chemical shift was measured for Cd salts with NO_3, ClO_4, SO_4, I, Br, and Cl anions. In all cases, intermediate to fast exchange NMR spectra were observed (similar results were obtained for the ^{111}Cd nuclide [52]). Extrapolation of the shift-versus-concentration data to infinite dilution (Fig. 5) resulted in a common shift for all of the salts examined, which was designated as 0.0 ppm. This remains the chemical shift reference commonly utilized. On increasing the salt concentration, the complexes with NO_3, ClO_4 and SO_4 anions gave signals with shifts to higher field whereas the complexes with I, Br, and Cl gave downfield shifts. The slopes for ClO_4 and SO_4 were small, and solutions with these anions are generally employed for chemical shift referencing. In addition to anions, the effects of a wide range of ligands were examined and

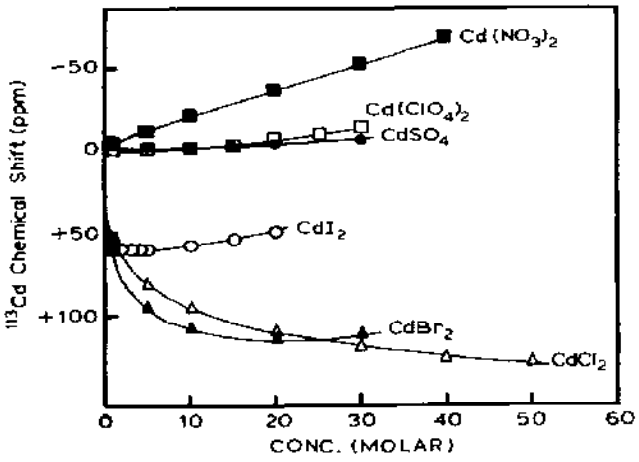

Fig. 5. ^{113}Cd NMR chemical shifts of Cd salts as a function of concentration (ref. 51).

an important general trend was discovered. Ligands which bind through oxygen cause increased shielding of the Cd nucleus whereas ligands which bind through nitrogen produce a marked deshielding of the Cd nucleus. Ligands which bind via sulfur produce very large deshielding.

From two detailed analyses of the fast-exchange ^{113}Cd chemical shifts of Cd halide solutions at ambient temperature, the shifts for CdX, CdX_2, CdX_3 and CdX_4 have been derived [53,54]. The method employed utilizes known equilibrium constant data and the relationship

$$\delta_{obs} = \sum_n P_n \delta_n \tag{5}$$

where P_n and δ_n are the population and shift of the CdX_n species. In the first study, by Drakenberg et al. [53], shifts were calculated for DMSO and H_2O solutions and the results are given in Tables 9 and 10, respectively. From these data, it was suggested that a change in coordination number occurred on formation of CdX_2 in DMSO but not in H_2O; a similar change

TABLE 9

Calculated ^{113}Cd NMR chemical shifts (ppm) for CdX_n species in DMSO [a]

X	[Cd] (M)	Cd^{2+}	CdX^+	CdX_2	CdX_3^-	CdX_4^{2-}
Cl	0.1–0.6	−27	31	204	398	442
Br	0.6	−27	11	373	285	351
I	0.6	−27	−14	286	124	44

[a] Shifts calculated using least squares analysis of fast-exchange data; for details see ref. 53.

TABLE 10

Calculated ^{113}Cd NMR chemical shifts (ppm) for CdX_n species in H_2O [a]

X	[X] (M)	CdX	CdX_2	CdX_3	CdX_4
Cl		63 [b]	98 [b]	282 [b]	
Cl	≤ 2.0	92	103	352	252
Cl	≤ 0.5	89 [c]	114 [c]	292 [c]	495 [c]
Cl	≤ 0.5	89 [d]	114 [d]	296 [d]	474 [d]
Br		62 [b]	83 [b]	186 [b]	399 [b]
Br	≤ 2.0	62	83	186	399
Br	≤ 0.5	72 [c]	75 [c]	365 [c]	379 [c]
Br	≤ 0.5	74 [d]	66 [d]	380 [d]	365 [d]
I		46 [b]	47 [b]	122 [b]	71 [b]
I	≤ 2.0	44		121	75
I	≤ 0.5	47 [c]		140 [c]	71 [c]
I	≤ 0.5	49 [d]		148 [d]	70 [d]
SCN		40 [b]	85 [b]	101 [b]	174 [b]

[a] Data from ref. 54 except as indicated.

[b] Data from ref. 53.

[c] Values obtained using CdX_4 benchmark shifts which were allowed to vary.

[d] Values obtained using CdX_4 benchmark shifts which were held fixed.

in coordination number was proposed to occur in H_2O on formation of CdX_3.

Ackerman et al. [54] evaluated the shifts for CdX_n species using solid state-derived shifts for CdX_4 compounds as benchmarks. In addition, the data were analyzed using low (< 0.5 M) and high (up to 2.0 M) anion concentrations (Table 10). Similar shifts were obtained at low anion concentrations for cases where the benchmark CdX_4 shifts were held constant or allowed to vary. The calculated dependence of CdI_n on the total I^- concentration is shown in Fig. 6. The shifts obtained with higher X concentrations were substantially different, however, and indicated that higher order species, e.g. CdX_5 and CdX_6, may be formed. Note that, except for the shift of $CdBr_3$, the values calculated by the two research groups are in reasonable agreement.

For supercooled aqueous solutions ($-80\,^\circ C$) containing cadmium iodide, distinct signals were observed which correspond to CdI_3 (122 ppm), CdI_4 (101 ppm), CdI_2 (43 ppm), CdI (20 ppm), and free Cd (or $Cd(NO_3)_n$, -86 ppm) [55], Fig. 7. These chemical shift values were in agreement with values assigned via least squares fitting of ambient temperature NMR data [54]. In more recent work, ^{113}Cd signals in the presence of a variety of Li salts containing O-donor anions were found to shift to lower field on reducing the sample temperature. For a given anion, this effect was independent of total salt concentration [56]. For some emulsions at low temperature, a high-field

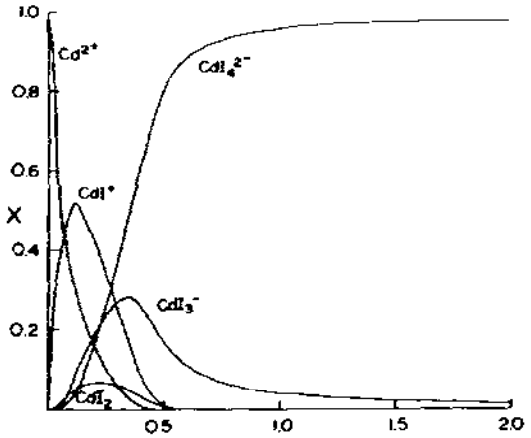

Fig. 6. Calculated dependence of the mole fractions of CdI_n species ($n = 0$–4) at ambient temperature on the total added I^- concentration; [Cd] = 0.10 M (ref. 54).

signal developed and intensified with time, and this signal was attributed to Cd in a droplet containing a portion of freezing solvent and (by Raoult's freezing law) a higher total salt concentration [56].

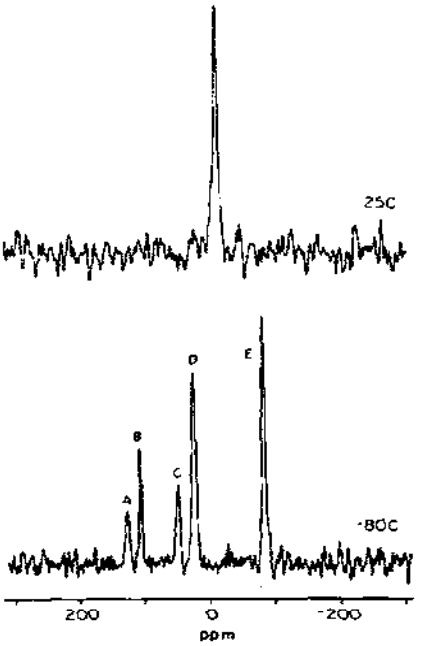

Fig. 7. ^{113}Cd spectra at 25 and $-80°$ of a water-in-oil emulsion whose aqueous component contained $Cd(NO_3)_2$ (0.01 M), NaI (0.018 M), and $LiNO_3$ (8 M). Signal assignments are as follows: A, CdI_3^-; B, CdI_4^{2-}; C, CdI_2; D, CdI^+; E, Cd^{2+} (ref. 55).

The ^{111}Cd and ^{113}Cd NMR spectra of CdX_4 (X = Cl, Br, I) and mixed-halo complexes have been examined using CH_2Cl_2 solutions and low temperatures [57], and the results are summarized in Table 11. Identical shifts were observed for the ^{111}Cd and ^{113}Cd isotopes. A first-order approach for calculating the chemical shifts (eqn. (6))

$$\delta_{calc} = \tfrac{1}{4}\left[n\delta(CdX_4) + (4-n)\delta(CdY_4)\right] \quad (6)$$

gave poor results, but an excellent fit was obtained when the pairwise additivity model [58] was employed. This procedure allows calculation of the chemical shift of a metal by summing the pairwise interaction parameters for all substitutents taken as adjacent pairs. For tetrahedral complexes, the shift is calculated by summing pairwise interaction parameters along the six edges of the tetrahedron. For comparison, the calculated shifts are given in Table 11.

Slow exchange ^{113}Cd NMR spectra were observed for halide binding to Cd(Ll) (Ll = $(BzCH_2)_3N$; Bz = 2-substituted benzimidazole) at ambient temperature [59]. The binding of a single halide caused a very large down-

TABLE 11

Experimental and calculated ^{113}Cd NMR chemical shifts (ppm) for CdX_4 complexes in CH_2Cl_2 at $T = -80\,^{\circ}C$ [a]

Complex	^{113}Cd δ	
	Experimental	Calculated
$CdCl_4$	438	438
$CdCl_3Br$	424	422
$CdCl_2Br_2$	404	403
$CdCl_3I$	394	394
$CdClBr_3$	381	379
$CdCl_2BrI$	367	366
$CdBr_4$	350	352
$CdBr_2ICl$	335	334
$CdCl_2I_2$	314	316
$CdBr_3I$	299	298
CdI_2ClBr	280	277
$CdBr_2I_2$	232	233
CdI_3Cl	203	207
CdI_3Br	153	154
CdI_4	62	64

[a] Experimental values obtained for a CH_2Cl_2 solution containing $CdCl_4 + CdBr_4 + CdI_4$; see ref. 57 for details. The values reported here have been corrected to the $Cd(ClO_4)_2$ standard (from a 4.5 M $Cd(NO_3)_2$ (aq) standard) by subtracting 73 ppm from the published values.

field shift compared to that expected from the above reports on halides. Downfield shifts increased in the order: I (177 ppm) < Br (211 ppm) < Cl (270 ppm), Fig. 8. Downfield shifts induced by CN, L-cysteine, and PhS of 240, 268, and 283 ppm, respectively, were also reported [59], and the results were discussed in terms of their potential for evaluating shifts of Cd-substituted metalloproteins [59] (vide infra).

The influence of halides on ^{113}Cd NMR spectra can clearly be seen from pH titration curves of $Cd(ATP)X_2$ ($X = ClO_4$, Cl) [60] as shown in Fig. 9. For the complex prepared with $CdCl_2$, raising the pH led to an upfield shift of the ^{113}Cd signal due to displacement of coordinated Cl whereas, for the complex prepared with $CdClO_4$, an increase in pH caused a downfield shift due to displacement of bound H_2O [60].

From analysis of the nuclear relaxation properties of aqueous $Cd(ClO_4)_2$, a rotational correlation time of 3.9×10^{-11} s at 25°C was obtained [61]. ^{113}Cd NMR was also evaluated as a probe for ion–polyelectrolyte interactions [62]. Fast-exchange spectra were obtained which were used to determine the fraction of bound ions, the exchange rate, and details about competition with Ca and Mg. The relaxation properties of Cd adsorbed on silica gels and zeolite–NaY provided information on the mobility and dynamic behavior of Cd in these systems [63].

Porphyrins

The biochemical significance of metals in metalloporphyrin-containing proteins has provided the impetus for a number of studies of Cd-substituted

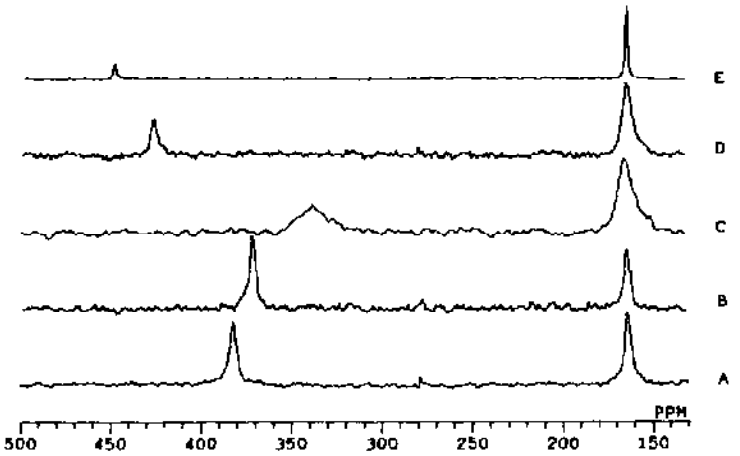

Fig. 8. ^{113}Cd NMR spectra obtained for DMSO-d_6 solutions (ambient temperature) containing $Cd(NO_3)_2$ (0.1 M), $(BzCH_2)_3N$ (L1, 0.1 M), and X anions (0.05 M; $X = Cl^-$ (A), Br^- (B), I^- (C), l-cysteine (D), PhS^- (E)). The upfield signals at δ 163 and the downfield signals are for Cd(L1) and Cd(L1)X, respectively (ref. 59).

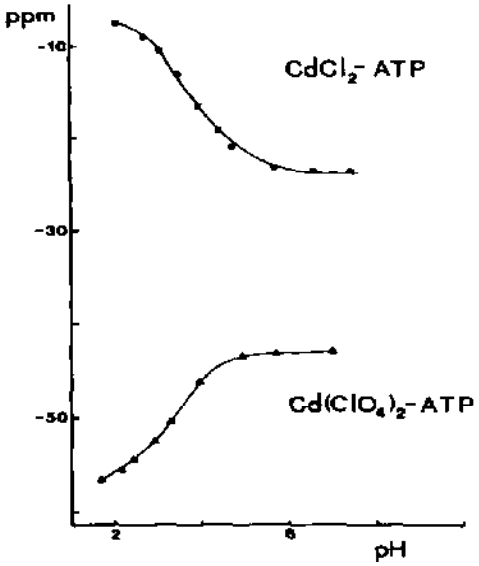

Fig. 9. ^{113}Cd chemical shifts of 0.5 M Cd salts in the presence of 0.5 M ATP as a function of pH (ref. 60).

porphyrins. ^{111}Cd was employed in the first study [64], where the adducts with ^{15}N-labeled tetraphenylporphyrin (TPP) and substituted pyridines were examined. ^{111}Cd chemical shifts and ^{111}Cd–^{15}N coupling constants are given in Table 12. To ensure complete formation of Cd(TPP)L species, a 10-fold excess of L was used, and the results demonstrated that ^{111}Cd NMR chemical shifts are sensitive to the basicity of L [64].

In more recent studies of Cd(TPP) adducts [36,65] solutions employed contained 1 : 1 molar amounts of Cd(TPP) : L and equilibrium effects could

TABLE 12

^{111}Cd NMR chemical shifts (ppm) and ^{111}Cd–^{15}N coupling constants (Hz) for ^{111}Cd(TPP)L complexes in $CDCl_3$ solution; L = substituted pyridine [a]

L	pK_a	^{111}Cd δ	$^1J(^{111}Cd-^{15}N)$
4-CNpy	1.90	9.31	147.6
3-Clpy	2.84	5.94	146.4
4-(COOMe)py	3.26	6.08	146.3
4-(COMe)py	3.51	6.84	146.0
py	5.17	0.00	142.5
4-Mepy	6.02	−0.35	141.0
4-NH_2py	9.12	−7.86	137.4

[a] Chemical shifts referenced to δ ^{111}Cd(TPP)py = 0.0 ppm. Solutions contained a 10-fold molar excess of L; see ref. 64 for details.

not be eliminated in evaluating correlations between ^{113}Cd chemical shifts and, for example, L basicity. When only the substituted pyridines are compared (Table 13), the changes in shift follow the same trend and are of the same magnitude as the changes observed for ^{111}Cd(TPP)L (Table 12). The relatively high shift (476 ppm) for unliganded Cd(TPP) was attributed to formation of polymers [36].

Perhaps the most enlightening studies of Cd(TPP) species are those of Ellis and co-workers, where solution- and solid-state properties were examined and compared [26,27]. Once again, ^{15}N-labeled TPP was employed, and ^{113}Cd chemical shifts and coupling constants are given in Table 14. The magnitude of the ^{113}Cd–^{15}N coupling constants was similar to the ^{111}Cd–^{15}N couplings observed for the ^{111}Cd(TPP)L complexes. In $CDCl_3$, an isotropic chemical shift of 426.8 ppm was observed for Cd(TPP)py whereas no ^{113}Cd signal was observed for the unliganded, Cd(TPP) complex due to insolubility. The solution shift compares favorably with the value obtained for the solid (432 ppm, see Section B(i)). The relaxation properties and correlation times for Cd(TPP)py and Cd(TPP)py-d_5 were also evaluated (Table 15).

Other N-donors

The ^{113}Cd chemical shift for Cd(EDTA) in aqueous media is independent of pH for values between 4–11 [66]. In this pH range, protons from water in

TABLE 13

^{113}Cd NMR chemical shifts for Cd(TPP) and its adducts [a] in $CDCl_3$

Complex	L	pK_a	^{113}Cd δ
			476 [b]
Cd(TPP)L	py	5.25	425
	4-picoline	6.02	423
	4-(COMe)py		432
	4-NH_2py	9.11	418
	3-Clpy	2.84	432
	piperidine	11.1	438
	imidazole	6.95	491
	1-Meimid	7.33	421
	1,2-Me_2imid		429
	THF		434
	Ph_3P		498
Cd(TPP)L_2	*p*-dioxane		435
	THF		425

[a] NMR solutions contained 1 : 1 or 1 : 2 molar amounts of Cd(TPP) : L; see ref. 36 for details.
[b] In solution at 35 °C containing no added L.

TABLE 14

NMR chemical shifts and coupling constants for Cd(TPP)(py) [a]

Parameter	Observed nucleus		
	^{113}Cd	^{15}N	^{13}C
Chemical shifts (ppm)	426.8	−170.9	150.6 (Cα)
			131.4 (Cβ)
			121.3 (Cγ)
Coupling constants (Hz)			
$^1J(^{113}Cd-^{15}N)$	+150.1	+150.1	
$^2J(^{113}Cd-C_\alpha)$			2.6 [b]
$^3J(^{113}Cd-C_\beta)$			−12.2
$^3J(^{113}Cd-C_\gamma)$			−10.7
$^4J(^{113}Cd-H_\beta)$	−5.0		

[a] References: ^{113}Cd = external 0.1 M $Cd(ClO_4)_2$ in D_2O; ^{15}N = external CH_3NO_3; ^{13}C = internal TMS. See ref. 26 for details.
[b] Sign undetermined.

the primary solvation sphere provide a dipolar relaxation mechanism for the ^{113}Cd nucleus. Evidence was presented for the formation of hydroxylated complexes at pH 13.8. Chemical exchange processes dominated the ^{113}Cd relaxation pathway for solutions at high pH [66].

Unlike the above findings for Cd(EDTA), studies of a similar compound, Cd(ChxDTA) (ChxDTA = cyclohexanediaminetetraacetate), employing selective ^1H irradiation and T_1 experiments, indicated that H_2O does not coordinate to Cd [67]. Only the acetate protons gave an observable $^1H-^{113}Cd$ nuclear Overhauser effect (NOE), and it was suggested that the lack of an observed NOE with the methine protons might be due to anisotropic motion of the Cd(ChxDTA) complex [67].

The ^{113}Cd NMR spectral properties of Cd complexes with EDTA, EGTA, 18-crown-6, and other macrocyclic N- and O-donor ligands have been examined [68]. In contrast to earlier studies of N-donor coordination com-

TABLE 15

Experimental ^{113}Cd NMR spin-lattice relaxation times (T_1) and nuclear Overhauser effects (η), and calculated values for η_{max}, T_1^{CSA}, and T_1^{DD} for Cd(TPP)py and Cd(TPP)py-d_5 [a]

L	Field (T)	T_1 (s)	η	η_{max}	T_1^{CSA} (s)	T_1^{DD} (s)
py	9.4	10.30	−0.5	−2.07	10.6	> 225
py-d_5	9.4	10.42	−0.06	−2.07	10.75	230–250
py	4.7	28.5	−0.26	−2.19	33.5	135–620

[a] Ref. 26.

pounds [70] and amino acids [98] (vide infra), it was concluded that a general correlation between the number of coordinated nitrogens and the ^{113}Cd chemical shift did not exist. It appears that the authors may have neglected to account for the influence of anions; in fact, the choice of CdX_2 salts used to obtain the ^{113}Cd chemical shift information was not published. The fact that one of the complexes examined [68] did not give a ^{113}Cd NMR signal in D_2O solution, even though the ^{13}C spectrum displayed ^{113}Cd–^{13}C coupling, provides strong evidence that exchange processes of the type $Cd(L) + X = Cd(L)X$ were probably in progress.

Cd complexes with Schiff base ligands have been examined [69], and the chemical shift results are summarized in Table 16. Note that, although it was not stated whether or not slow exchange spectra were observed, the shifts for the bis complexes (where the influence of anions and solvent should be minimal) are in the range expected for Cd coordinated to six secondary amine N atoms (eqn. (8), vide infra).

Summers and Marzilli [70] found that slow exchange ^{113}Cd NMR spectra could be obtained at ambient temperature for compounds containing N-donor ligands. Typical spectral data are shown in Fig. 10 and ^{113}Cd chemical shifts are summarized in Table 17. A chemical shift–donor atom relationship was established

$$\delta = 75A + 51B + 31C \quad (7)$$

where A, B, and C are the number of primary, secondary, and tertiary (or pyridine) N atoms coordinated to Cd, respectively, and the reference is 1.0 M $Cd(NO_3)_2$ in DMSO-d_6. The observed and calculated shifts usually agreed within 5%. These shifts can be converted to the $Cd(ClO_4)_2$ standard

TABLE 16

^{113}Cd NMR chemical shifts (ppm) for CdL_nX_2 complexes containing Schiff-base ligands L = 2,6-(R-N=C(Me))py [a]

R	X	^{113}Cd δ	
		mono	bis
Ph	NO_3	26.6	289.2
Ph	Cl	350.7	
p-$MeOC_6H_4$	Cl	348.9	
p-EtC_6H_4	OAc	69.1	
p-EtC_6H_4	Cl	349.6	
p-EtC_6H_4	I	270.1	
p-EtC_6H_4	NCS	295.1	
p-EtC_6H_4	BF_4		233.2

[a] See ref. 69 for details.

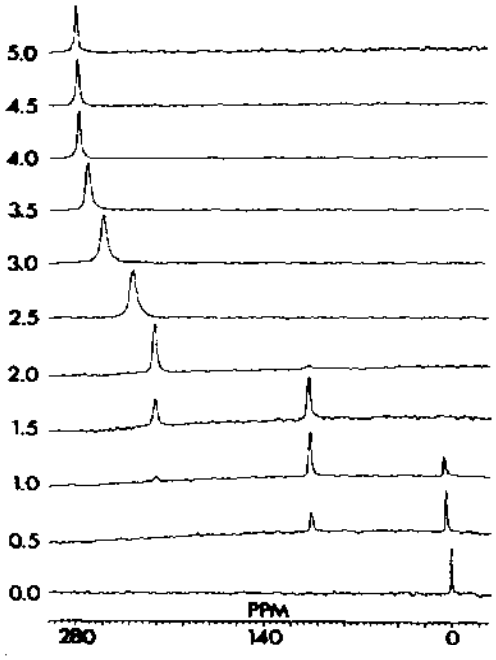

Fig. 10. ^{113}Cd NMR spectra of 1.0 M $Cd(NO_3)_2$ in DMSO-d_6 (ambient temperature) with N,N'-Me_2en at L : Cd ratios indicated at the left of each trace (ref. 70).

reference by subtracting 50 ppm. With relationship (8), the ligating atoms in Cd(MAMI) (MAMI = 5-(1,2,5-dithiazepan-5-ylmethylene)-4-methyl-2-ethylimidazole) were determined [71].

The study of N-donor ligands was extended to include ligands containing benzimidazole groups, including the tripodal ligand, Ll (Ll = $(BzCH_2)_3N$; Bz = 2-substituted benzimidazole) [59]. As expected, slow exchange spectra were observed for the equilibrium

$$Cd + L = Cd(L) \tag{8}$$

and with these data, eqn. (8) was modified to account for benzimidazole donors giving

$$\delta = 75A + 51B + 31C + 42D \tag{9}$$

where D is the number of benzimidazole-donor groups and the reference is 1.0 M $Cd(NO_3)_2$ in DMSO-d_6. To relate the shifts of models to shifts observed for proteins, eqn. (9) was modified to account for differences in solvent, anions, and chemical shift reference giving

$$\delta = 75A + 51B + 31C + 42D + 220E + 240F + 285G - 30H \tag{10}$$

where E is the number of bound Cl^- ligands (0 or 1) and $F = G = 0$; F is the number of bound CN^- ligands (0 or 1) and $E = G = 0$; G is the number

TABLE 17

^{113}Cd NMR chemical shifts (ppm) for $Cd(NO_3)_2$ compounds containing N-donor chelate ligands in DMSO-d_6 [a]

Ligand	^{113}Cd δ		
	mono	bis	tris
1,10-phenanthroline	61		
N,N,N',N'-Me_4en	66		
2,2',2''-terpy	88		
N,N,N',N'',N''-Me_5dien	92		
N,N''-Me_2en	103	219	278
N,N-Me_2en	106	226	
2-(NH_2CH_2)py	114		
N-Meen	126	262	359
en	149	290	403
N,N-Me_2dien	155	308	
dipropylenetriamine	200		
dien	207	386	
3,2,3-tetramine	256		
trien	262		
N,N-Me_2dien + *N,N*-Me_2en	272		
$(BzCH_2)_3N$ [b]	163		
$(MBzCH_2)_3N$ [b]	163		
$((BzCH_2)_2NCH_2CH_2OCH_2)_2$ [b]	113		
$(BzCH_2)_2NCH_2CH_2N(CH_2Bz)(C_2H_4OH)$ [b]	189		
$(BzCH_2)_2NH$ [b]	133		
$(BzCH_2)_2NCH_2CH_2OH$ [b]	115		

[a] Externally referenced to 1.0 M $Cd(NO_3)_2$ in DMSO-d_6; these shifts can be converted to the $Cd(ClO_4)_2$ (aq) reference by subtracting 50 ppm. Data from ref. 70 except as noted.
[b] Ref. 59.

of bound RS^- ligands (0 or 1) and $E = F = 0$; H is zero for less than 4 non-O donors and unity for 4 or more non-O donors.

Extensive comparisons of ^{113}Cd spectra obtained at low temperatures and in the solid have been made recently by Munakata et al. [39] for a large group of Cd compounds containing mono- and bidentate N-donor ligands. The influence of counterion, chelate ring size, and basicity were examined, and the chemical shifts are summarized in Tables 6 and 18. In every case, the shifts obtained at low temperatures and in the solid were in close agreement. The results for tris-diamine species (Table 18) displayed an influence of chelate ring size on ^{113}Cd chemical shift. Thus, deshielding decreased in the order: four- > five- > six- > seven-membered chelate rings. The influence of pK_a of L on ^{113}Cd shift was also demonstrated (see Fig. 11) where Cd deshielding increased with increasing pK_a of L [39]. As an example, a downfield shift of 8.8 ppm per pK_a unit was observed for

TABLE 18

^{113}Cd NMR chemical shifts (ppm) for CdL_n species (L = N-donor ligands) [a]

L	pKa	Cd	CdL	CdL_2	CdL_3	CdL_4
Ethanol, $T = -90\,^{\circ}C$						
4-Mepy	6.04	−21	11	42	72	101
4-CH_2CHpy	5.40	−21	11	42	71	98
4-Acpy	3.51	−21	10	40	67	93
4-CNpy	1.90	−21	9	39		
2-Mepy	5.09	−21	−2	17		
Water, $T = 23\,^{\circ}C$						
en	(7.08, 9.89)				347	
tn	(8.74, 10.52)				259	
tmd	(9.44, 10.72)				227	
N,N'-Me_2en	(7.01, 9.98)				229	

[a] See ref. 39 for details; tn = $NH_2(CH_2)_3NH_2$, tmd = $NH_2(CH_2)_4NH_2$.

$Cd(4\text{-Rpy})_4$ compounds. Note, however, that this actually translates to 2.2 ppm per pK_a unit for each individual 4-Rpy ligand. A substantially smaller influence (ca. 0.5 ppm per pK_a unit) is indicated from the CdL data (Table 18). It is also interesting to note that the trend (downfield shift for an

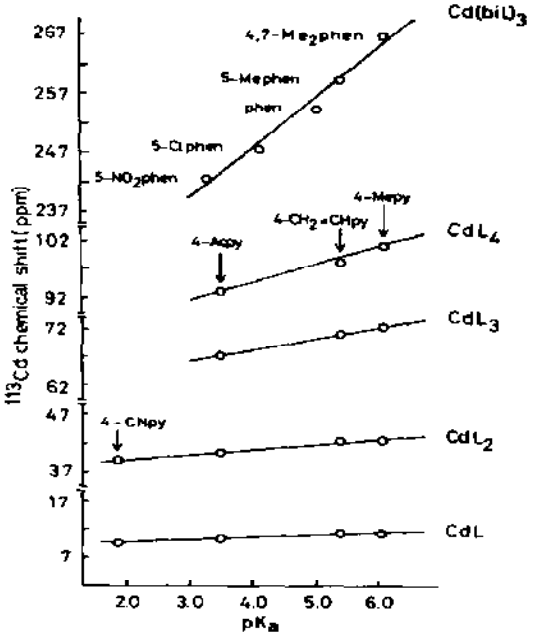

Fig. 11. Plot of ^{113}Cd chemical shifts of Cd complexes with 4-substituted pyridines (L) and 1,10-phenanthroline and its derivatives (biL) versus the pK_a values of the ligands (ref. 39).

TABLE 19

^{113}Cd NMR chemical shifts (ppm) for dialkylamido cadmium compounds, CdL_2, and adducts between neutral ligands (L′) and $Cd[N(SiMe_3)_2]_2$ [a]

Ligand	Solvent	^{113}Cd δ
L in CdL_2		
$N(SiMe_3)_2$	Neat	294
	Benzene	294
$N(SiMe_3)(t\text{-}Bu)$	Benzene	323
$N(SiPhMe_2)_2$	Benzene	264
$N(C_9H_{18})_2$	Benzene	362
L′ in $Cd[N(SiMe_3)_2]_2L'$		
py	Benzene	337
	MeC_6H_{11}	331
4-Mepy	Benzene	344
4-t-Bupy	Benzene	340
N-Meimid	Benzene	363
bipy	Benzene	353
Me_4en	Benzene	288

[a] See ref. 72 for details.

increase in pK_a) is opposite to that observed for 4-RpyCd(TPP) compounds [36,64].

A much more dramatic effect is observed when the shifts of 2-Mepy compounds are compared to the shifts of complexes containing 4-substituted pyridines (Table 18), with 2-Mepy producing much less deshielding in the mono and bis species. Since 2-substituted pyridines are sterically demanding ligands, it is likely that the reduced deshielding results predominantly from an increase in Cd–L bond distance. Similar high-field shifts were observed for complexes with the sterically demanding 2,9-$(Me)_2$phen ligand (Fig. 2).

^{113}Cd chemical shifts for Cd compounds containing dialkylamide ligands (here, the N-donor atoms are monoanionic) have been reported [72]. From the data given in Table 19, it is clear that the deshielding influence of N^- is much greater than for neutral N-donor atoms; e.g. compare the shift of $Cd[N(SiMe_3)_2]_2$ (294 ppm) to the shift of en (ca. 150 ppm). Shifts were also reported for adducts formed on addition of neutral N-donor ligands, including substituted pyridines. The binding of py to $Cd[N(SiMe_3)_2]_2$ resulted in a downfield shift of 43 ppm (Table 19).

S and Se donors

A number of Cd coordination compounds containing thiolate groups have been investigated as they serve as potential models of the metallothioneins. ^{113}Cd NMR spectra of Cd complexes containing bifunctional S- and O-donor

TABLE 20

^{113}Cd NMR chemical shifts (ppm) of some Cd–S complexes [a]

Compound	Solvent	pH	Concentration (M)	^{113}Cd δ
$Cd(glutathione)_2$	H_2O	9.5	0.5	318
$Cd(SCH_2CH_2OH)_2$	DMSO		0.2	655
$[Cd_{20}(SCH_2CH_2OH)_{16}](ClO_4)_4$	DMF		0.2	520
$[Cd_{20}(SCH_2CH_2OH)_{16}](ClO_4)_4$	H_2O		0.065	515, 382
$Cd(dtpp)_2$	Phenol		0.5	401
$[Cd(mnt)_2](Et_4N)_2$	DMSO		0.5	813
$Cd(Et_2dtc)_2$	DMSO		0.08	215
$[Cd(etxth)_3](Et_4N)$	$CHCl_3$		0.5	277

[a] See ref. 73 for details; Et_2dtc = *N,N'*-diethyldithiocarbamato, dtpp = *O,O'*-diisopropyldithiophosphinato, etxth = *O*-ethylxanthato, mnt = $S_2C_2(CN)_2$.

ligands were examined [73], Table 20. For $[Cd_{10}(SCH_2CH_2OH)_{16}]^{4+}$ (H_2O, 25 °C), two signals were observed at 515 and 382 ppm, and these signals were assigned to the Cd_{5-10} and Cd_{1-4} sites, respectively. Deshielding was found to decrease in the order: $Cd(SR)_4 > Cd(SR)_3 > Cd(SR)_2$.

^{113}Cd chemical shifts of thio-β-diketonate complexes with Cd and their py adducts were compared to the shifts of β-diketonates (Table 21) [74]. In acetone, the O-donor complexes gave signals upfield from the $Cd(ClO_4)_2$ reference, whereas the S-donor complexes gave signals in the range 191–237

TABLE 21

^{113}Cd chemical shifts (ppm) for Cd complexes with β-diketonates and thio-β-diketonates in various solvents, $T = 297$ K [a]

Compound	Solvent	Concentration (M)	^{113}Cd δ
$Cd(BTA)_2 \cdot 2H_2O$	Acetone	0.5	−24.0
	py	0.5	40.6
	4-Mepy	0.5	42.7
$Cd(TTA)_2 \cdot 2H_2O$	Acetone	0.5	−27.1
	py	0.5	39.4
	4-Mepy	0.5	41.7
$Cd(STTA)_2$	Acetone	0.05	191
	py	0.05	216
$Cd(SBB)_2$	py	0.05	237

[a] BTA = benzoyltrifluoroacetone, TTA = thenoyltrifluoroacetone, STTA = monothiothenoyltrifluoroacetone, SBB = monothiodibenzoylmethane; see ref. 74 for details.

ppm. Dissolution of the complexes with O-donor ligands into py resulted in downfield shifts of 64–67 ppm due to the formation of bis–py species, and the magnitude of the shift is as expected (31 ppm per py; eqn. (8)).

^{113}Cd chemical shifts for a large series of Cd-thiolate complexes have been examined [75]. In Table 22, data are presented for spectra obtained at ambient temperature and under conditions of 12-fold excess ligand. In general, the shifts were interpreted as resulting from the formation of

TABLE 22

^{113}Cd NMR chemical shifts (ppm) and peak widths at half-height for CdL_n complexes in the presence of 12-fold excess L; L = S donor [a]

LH	^{113}Cd δ	$W(1/2)$ (Hz)
MeSH	663	4
EtSH	648	4
n-PrSH	647	7
n-BuSH	644	12
i-PrSH	625	10
i-BuSH	622	12
BnzSH	646	10
$HOCH_2CH_2SH$	666	4
$NH_2CH_2CH_2SH$	659	4
$HOOCCH_2CH_2SH$	660	4
$MeCH(OH)CH_2SH$	659	9
$HOCH_2CH(OH)CH_2SH$	658	9
[L]$OOCCH(NH_2)CH_2SH$	623	10
[D]$OOCCH(NH_2)C(Me)_2SH$	577	10
$HOOCCH_2SH$	601	15
PhSH	583	7
$HSCH_2CH_2SH$	784 [b]	9
$HSCH_2CH(Me)SH$	780	47
$HSCH_2CH(Et)SH$	780	9
$HSCH_2CH(SH)CH_2OH$	782	15
$HSCH_2CH(SH)CH_2SO_3^-$	786	12
3-Medtb	796	4
$HSCH_2CH(SH)CH_2SH$	778	27
$HS(CH_2)_3SH$	663	9
$HSCH_2CH(OH)CH_2SH$	685	32
$HS(CH_2)_5SH$	648	37
$HSCH_2(CH(OH))_2CH_2SH$	674	17
$HS(CH_2)_5SH$	646	12
1,2-$(CH_2SH)_2$-4,5-$(Me)_2$benzene	631	22

[a] Aqueous solution; $T = 308$ K. See ref. 75 for details.

[b] Corrected value [189].

tetrahedral Cd complexes containing either four monothiolate or two dithiolate ligands [75]. Aliphatic monothiolates gave shifts in the range 622–663 ppm; substituents such as NH_2 or COOH caused some variation in ^{113}Cd chemical shifts (see Table 22).

Interestingly, the most shielded signal was observed for L = $HSC(Me)_2CH(NH_2)COO^-$ (577 ppm). Since this is the only ligand in which the SH group is attached to a tertiary carbon, the poorer deshielding could be due to poorer Cd–L bonding, the result of a steric effect. If only the aliphatic ligands are considered, a trend is observed where the deshielding decreases in the order: CH_3SH (663 ppm) > R–CH_2SH (644–648 ppm) > R,R′–CHSH (622–625 ppm) > R,R′,R″–CSH (577 ppm).

Complexes with ligands having vicinal thiolates gave shifts in the range 778–829 ppm, and it was suggested that a large chelate effect results only for ligands which can form 5-membered rings with Cd [75]. Mixed ligand systems were examined at reduced temperatures where slow-exchange spectra were obtained. The results (Table 23) indicate an additivity effect of L on ^{113}Cd chemical shift.

At room temperature, fast exchange ^{113}Cd spectra were observed for *O,O*-dialkyldithiophosphate (dtp) and dialkyldithiocarbamate (dtc) Cd complexes in CH_2Cl_2 solution [76]. On cooling, slow exchange spectra were obtained and the chemical shift and ^{113}Cd–^{31}P coupling constant results (for phosphine adducts) are summarized in Table 24. Although the exact nature of the complexes formed could not be determined, molecular weight mea-

TABLE 23

^{113}Cd NMR chemical shifts (ppm) for Cd–thiolate complexes in CD_3OD at 193 K [a]

Complex	^{113}Cd δ
$Cd(SCHMe_2)_4$	654.0
$Cd(SMe)(SCHMe_2)_3$	661.4
$Cd(SMe)_2(SCHMe_2)_2$	668.8
$Cd(SMe)_3(SCHMe_2)$	676.1
$Cd(SMe)_4$	682.8
$Cd(S(CH_2)_2S)(SCHMe_2)_2$	721.3
$Cd(S(CH_2)_2S)_2$	794.2
$Cd(SPh)_4$	595
$Cd(SPh)_3(SBnz)$	615.2
$Cd(SPh)_2(SBnz)_2$	634.2
$Cd(SPh)(SBnz)_3$	652.4
$Cd(SBnz)_4$	671.6

[a] See ref. 75 for details.

TABLE 24

^{113}Cd NMR chemical shifts (ppm) and $^{113}Cd-^{31}P$ coupling constants for Cd complexes containing S- and P-donors in CH_2Cl_2 solution [a]

Compound	T (°C)	^{113}Cd δ [b]	J (Hz)
$Cd(dtpb)_2$	30	352	
$Cd(dtpp)_2$	30	377	
$Cd(dtph)_2$	30	377	
$Cd(dtpb)_2(PBu_3)$	−70	402d	2145
$Cd(dtpb)_2(PBu_3)_2$	−90	457t	2015
$Cd(dtpp)_2(PBu_3)$	−90	402d	2145
$Cd(dtpp)_2(PBu_3)_2$	−110	477t	1840
$Cd(dtph)_2(PBu_3)$	−60	407d	2200
$Cd(dtph)_2(PBu_3)_2$	−90	377t	1940
$Cd(dtpb)_2(PChx_3)$	−90	382d	2170
$Cd(dtpp)_2(PChx_3)$	−60	387d	2150
$Cd(dtph)_2(PChx_3)$	−60	392d	2145
$Cd(S_2CN(iBu)_2)_2PChx_3$	−60	372d	1545
$Cd(S_2CN(Me)(Bu))_2PChx_3$	−60	367d	1595
$Cd(S_2CN(cC_5H_{11})_2)_2PChx_3$	−60	407d	1500

[a] Ref. 76; dtpb = *O,O'*-dibutyldithiophosphate, dtpp = *O,O'*-diisopropyldithiophosphate, dtph = *O,O'*-dicyclohexyldithiophosphate. Molecular weight experiments indicate that some of the complexes may be polymeric.
[b] d = doublet; t = triplet.

surements indicated that some of the complexes were extensively associated [76].

^{113}Cd NMR spectra of complexes containing phosphine oxides, sulfides, and selenides in liquid SO_2 were examined at low temperatures where slow exchange spectra were obtained [77]. Two-bond $^{113}Cd-O-^{31}P$ couplings (Table 25), were considerably smaller than $^2J(Cd-S-P)$ or $^2J(Cd-Se-P)$ coupling. The multiplicities of the signals observed at low temperatures

TABLE 25

$^{113}Cd-O-^{31}P$ coupling constants for phosphine oxide complexes in SO_2 solution [a]

Complex	T (K)	$^2J(^{113}Cd-O-^{31}P)$ (Hz)
$Cd(OP(Chx)_3)_4$	209	25.6
	308	28.0
$Cd((OPPh_2)_2CH_2)_3$	220	2.4
$Cd((OPPh_2)_2C_2H_5)_3$	205	14.2
$Cd(triphos(O_3))_2$	205	20

[a] See ref. 77 for details.

(Table 26) were as expected and demonstrated that slow exchange conditions prevailed. For the tetrahedral complexes given in Table 26, shielding decreased for donor atoms in the order: O ≫ Se > S. The chemical shift results for both the CdS_xSe_{4-x} and Cd_xSe_{3-x} species were analyzed using the pairwise additivity procedure (eqn. (7)) where, for the CdS_xSe_{4-x} data, $\Delta\delta_{S-S} = 11.3$ ppm and $\Delta\delta_{Se-S} = 4.8$ ppm and the corresponding values for CdS_xSe_{3-x} were 17.4 ppm and 8.0 ppm, respectively.

^{113}Cd chemical shifts for $Cd(SPh)_n(SePh)_{4-n}$ mixed ligand complexes in MeOH varied linearly from 541 ppm ($n = 0$) to 590 ppm ($n = 4$) (Table 27) [78]. $^{113}Cd-^{77}Se$ coupling constants also varied linearly from 126 Hz ($n = 0$) to 46 Hz ($n = 3$). The binding constant for PhSe was shown to be much greater than for PhS, and it was suggested that the high affinity of Se for Cd

TABLE 26

^{113}Cd NMR chemical shifts (ppm) and signal multiplicities for Cd complexes with phosphine oxides, sulfides, and selenides in liquid SO_2 [a]

Complex	T (K)	^{113}Cd δ [b]
$Cd((OPPh_2)_2CH_2)_3$	213	−7(s)
	306	−22(s)
$Cd((OPPh_2)_2C_2H_4)_3$	203	−27(sep)
$Cd((OPPh_2)_2C_2H_4)_2$	203	−13(s)
$Cd(OPPh(C_2H_4P(O)Ph_2)_2)_2$	203	18(t)
	306	4(s)
$Cd(OPChx_3)_4$	213	94(qnt)
	306	75(qnt)
$Cd(SPPh_3)_4$	203	577(qnt)
$Cd(SePPh_3)_4$	203	532(qnt)
$Cd(SP(o\text{-}MePh)_3)_4$	198	618(qnt)
$Cd(SP(o\text{-}MePh)_3)_3$	198	465
$Cd(SP(o\text{-}MePh)_3)_2$	198	277(t)
$Cd(SeP(o\text{-}MePh)_3)_3$	198	440(q)
$Cd(SeP(o\text{-}MePh)_3)_2$	198	130(t)
$Cd(SPChx_3)_4$	213	590(qnt)
$Cd(SPChx_3)_3$	213	503(q)
$Cd(SePChx_3)_4$	213	522(qnt)
$Cd(SePChx_3)_3$	213	450(q)
$Cd(SPChx_3)(SePChx_3)_3$	213	536.5
$Cd(SPChx_3)_2(SePChx_3)_2$	213	552.3
$Cd(SPChx_3)_3(SePChx_3)$	213	570.1
$Cd(SPChx_3)(SePChx_3)_2$	213	465.9
$Cd(SPChx_3)_2(SePChx_3)$	213	483.3

[a] Ref. 77; chemical shifts (originally reported relative to 4 M $Cd(NO_3)_2$ (aq)) have been changed here to the 0.1 M $Cd(ClO_4)_2$ reference by subtracting 65 ppm from the published values.

[b] s = singlet; t = triplet; q = quartet; qnt = quintet; sep = septet.

TABLE 27

^{113}Cd NMR chemical shifts (ppm) and ^{113}Cd–^{77}Se coupling constants for Cd complexes in MeOH at 213 K [a]

Complex	^{113}Cd δ	J (Hz)
$Cd(SePh)_4$	541	126
$Cd(SePh)_3(SPh)$	553.9	99
$Cd(SePh)_2(SPh)_2$	566.4	72
$Cd(SePh)(SPh)_3$	578.4	46
$Cd(SPh)_4$	590.0	

[a] See ref. 78 for details.

may be a factor in the antagonism of selenium compounds towards Cd toxicity in vivo [78].

In other studies, the $CdCl_2$ complex with the ionophore *N,N,N′,N′*-tetrabutyl-3,6-dioxaoctanedithioamide in CD_3CN gave a ^{113}Cd signal at ca. 350 ppm [79]. The ^{113}Cd spectrum of a DMSO solution containing Cd and 6-mercaptopurine displayed an asymmetric doublet at 554 ppm [80].

P donors

$Cd(PBu_3)_2X_2$ and $Cd_2X_4(PBu_3)_3$ complexes (X = Cl, Br, I) in CH_2Cl_2 and EtOH solution at reduced temperatures gave ^{113}Cd chemical shifts ranging from 105–602 ppm, Table 28 [81]. ^{113}Cd chemical shifts and ^{111}Cd–^{31}P coupling constants were reported for CdX_2L_2 complexes in CH_2Cl_2, where L = $PChx_3$ and PBu_3, Table 29 [82]. For $PChx_3$ complexes, slow-exchange spectra were obtained at 30 °C for the 1 : 1 adducts ($[CdX_2L]_2$ dimers), but the 1 : 2 adducts (CdX_2L_2) required cooling to −30 °C to give slow-exchange spectra. Linear correlations were found between the ^{113}Cd chemical shift and the electronegativity of X, suggesting that the shifts are largely determined by δ-bond effects [82]. Cd complexes with dicyclohexylphosphine, (1-(dicyclohexylphosphino))-*N*-phenylthioformamide, and mixed-ligand complexes of the type $CdX_2[PChx_3][PBu_3]$ (X = O_3SCF_3, ClO_4, NO_3, CF_3COO, CH_3COO, Cl, Br, I, SCN) gave shifts in the range 150–670 ppm, where complexes with coordinated I had the upfield-most shifts [83,84]. Chemical shifts and coupling constants are summarized in Tables 30–32.

Cd-cluster compounds

A number of compounds which contain multiple Cd atoms have been examined, in addition to the compound formed with $HSCH_2CH_2OH$ described above. A D_2O solution (pH 10.4; 298 K) containing the Cd complex with dicysteinoethylenediaminetetraacetic acid gave a ^{113}Cd spectrum with

TABLE 28

^{113}Cd and ^{111}Cd NMR chemical shifts and Cd–P coupling constants for $Cd(PBu_3)_2X_2$ and $Cd_2(PBu_3)_3X_4$ complexes in CH_2Cl_2 at reduced temperatures [a]

Complex	X	T (°C)	δ [b] (ppm)		J (Hz)	
			^{113}Cd	^{111}Cd	$^{113}Cd-^{31}P$	$^{111}Cd-^{31}P$
$Cd(PBu_3)_2X_2$	Cl	−85	602	602	1640	1570
	Br	−85	582	577	1510	1445
	I	−85	527	627	1370	1295
$Cd(PBu_3)_3X_4$	Br	−15	542	542	1650	1580
			422	417	2040	1945
	I	−10	507	502	1395	1330
			287	277	1730	1655
	I [c]	−30	427		1430	
			257		1640	
			105			

[a] See ref. 81 for details: Cd–P coupling constants for Cd complexes with phosphine ligands have also been measured using ^{31}P spectroscopy; see refs. 191–193.
[b] Shifts reported relative to 4.5 M $Cd(NO_3)_2$ (aq) have been corrected here to the $Cd(ClO_4)_2$ (aq) standard by subtracting 73 ppm from the published values.
[c] In EtOH solvent.

doublets due to $^{113}Cd-^{113}Cd$ coupling at 664 ppm and 260 ppm [85]. From an analysis using space filling models, a solution structure of the type Cd_3L_2 was suggested [85]. The $^{113}Cd-^{113}Cd$ coupling constant (80 Hz) was larger than those generally observed for Cd-substituted metallothioneins (20–50 Hz).

$^{111}Cd-^{113}Cd$ coupling constants of 45–47 Hz were observed by Dean and Vittal [86] for $[Cd_4(SPh)_{10}]^{2-}$, see Fig. 12. Since the $^{113}Cd-^{113}Cd$ coupling constant should be 4.6% greater, this value is within the range found in Cd-substituted metallothioneins, which supports the interpretation that Cd–Cd coupling in the protein results from coupling between CdS_4 kernels linked by bridging cysteinyl thiolate groups [86].

The effects on the ^{113}Cd NMR spectra of Zn and Se substitution in $[S_4Cd_{10}(SPh)_{16}]^{4-}$ have been investigated [87], where substitution of Se for S caused ^{113}Cd chemical shift changes of −37 ppm, −3 ppm to −1.5 ppm, and +1 ppm for substitutions which were one, three, and five bonds removed from Cd, respectively. Replacement of Cd by Zn caused a change in ^{113}Cd chemical shift of 13–5 ppm and −3 ppm for substitutions which were two bonds or over four bonds removed from Cd, respectively. The relevance of these findings to the ^{113}Cd NMR of Zn, Cd-metallothioneins has been discussed [87]. $^{111}Cd-^{113}Cd$ couplings in $[S_4Cd_{10}(SPh)_{16}]^{4-}$ were

TABLE 29

^{113}Cd NMR chemical shifts (ppm) and $^{(113,111)}Cd-^{31}P$ coupling constants (Hz) for CdX_2L_2 compounds in CH_2Cl_2 solution; L = $PChx_3$ and PBu_3 [a]

Compound	T (°C)	^{113}Cd δ	$^1J(^{113}Cd-^{31}P)$	$^1J(^{111}Cd-^{31}P)$
$L = PChx_3$				
$[CdCl_2L]_2$	30	452	2300	2200
$CdCl_2L_2$	−30	557	1635	1560
$[CdBr_2L]_2$	30	402	2045	1955
$CdBr_2L_2$	−30	512	1535	1460
$[CdI_2L]_2$	30	217	1805	1720
CdI_2L_2	−30	417	1390	1330
CdL_2	30	287	2200	2100
$[Cd(OAc)_2L]_2$	−30	162	2445	2340
$Cd(OAc)_2L_2$	−30	262	1875	1790
$[Cd(NO_3)_2L]_2$	30	97	2770	2650
$Cd(NO_3)_2L_2$	−30	252	2110	2020
$CdCl_2L_2$	−50	562	1660	1600
$CdIClL_2$	−50	507	1535	1470
CdI_2L_2	−50	427	1415	1345
$CdBr_2L_2$	−60	522	1570	1500
$CdIBrL_2$	−60	477	1490	1415
CdI_2L_2	−60	427	1410	1335
$CdCl_2L_2$	−65	562	1660	1600
$CdClBrL_2$	−65	542	1625	1550
$CdBr_2L_2$	−65	522	1585	1510
$[Cd(NO_3)L_2]_2$	30	272	2135	2040
$Cd(NO_3)_2L_2$	−65	257	2120	2065
$Cd(OAc)_2L_2$	−65	297	1940	1885
$L = PBu_3$				
$[CdCl_2L]_2$	−30		1690	1620
$CdCl_2L_2$	−85	602	1635	1570
$CdCl_2L_3$	−100	507	1600	1520
$[CdBr_2L]_2$	−15	422	2040	1945
$CdBr_2L_2$	−110	587	1545	1495
$CdBr_2L_3$	−110	492	1550	1500
$[CdI_2L]_2$	−110	207	1770	1695
CdI_2L_2	−110	537	1350	1305
CdI_2L_3	−110	472	1525	1455
CdL_2	30	267	2445	2320
CdL_3	−60	412	1690	1570
$[Cd(OAc)_2L]_2$	−70	147	2515	2410
		352	1905	1820
$Cd(OAc)_2L_2$	−70	347	1800	1750
$[Cd(NO_3)_2L]_2$	−50	57	2840	2700
		232	2460	2350
$Cd(NO_3)_2L_2$	−60	287	2200	2110
$Cd(NO_3)L_3$	−70	352	1750	1690
$CdBr_2L_3$	−110	492	1570	1500

TABLE 29 (continued)

Compound	T (°C)	^{113}Cd δ (ppm)	$^{1}J(^{113}Cd-^{31}P)$	$^{1}J(^{111}Cd-^{31}P)$
$CdIBrL_3$	−110	482	1545	1480
CdI_2L_3	−110	472	1510	1445
$CdCl_2L_3$	−110	507	1585	1510
$CdIClL_3$	−110	487	1555	1490
CdI_2L_3	−110	472	1520	1450
$CdClBrL_3$	−110	497	1580	
$CdIL_2$	0		1730	1650
$CdIL_3$	−110	572	1350	1290
CdI_2L_2	−110	472	515	
$Cd(OAc)L_2$	−80	362	1960	1875
$Cd(OAc)L_3$	−80	487	1385	1320
$Cd(NO_3)L_2$	−80	282	2310	2210
$Cd(NO_3)L_3$	−100	357	1750	1665
CdL_3	−100	417	1750	
$Cd(OAc)(NO_3)L_2$	−90	337	1900	1900
$Cd(NO_3)_2L_3$	−90	362	1770	1690
$Cd(OAc)_2L_2$	−90	352	1790	
$[Cd(OAc)_2L]_2$	−90	177	2330	
$Cd(OAc)(NO_3)L_3$	−90	427	1570	

[a] Chemical shifts reported relative to 4.5 M $Cd(NO_3)_2$ (aq) have been corrected here to the $Cd(ClO_4)_2$ reference by subtracting 73 ppm from the values published in ref. 82.

examined and a homonuclear Cd–Cd COSY spectrum was obtained [88]. ^{113}Cd spectra of $[Cd_x(SPh)_y]^{2x-y}$ species have also been reported [89].

^{113}Cd chemical shifts of clusters of the type $[(\mu-EPh)_6(CdX)_4]^{2-}$, (E = S

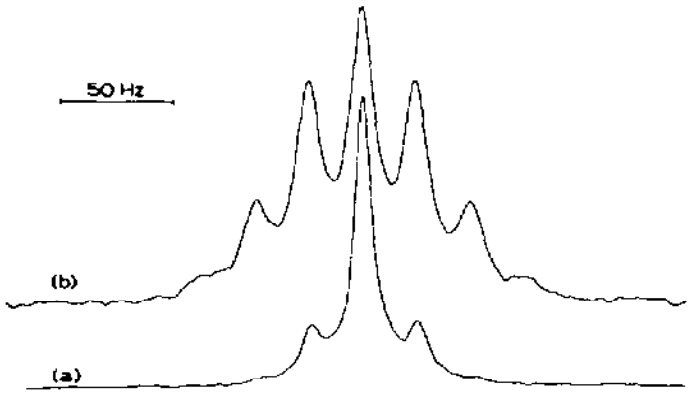

Fig. 12. ^{113}Cd NMR spectrum (295 K, in acetone) of $(Me_4N)_2[Cd_4(SPh)_{10}]$ (a) containing natural levels of Cd isotopes, and (b) containing enriched ^{113}Cd ($^{111}Cd:^{113}Cd:^{112}Cd$ = 0.13 : 1 : 0.85). From ref. 86.

TABLE 30

^{113}Cd NMR data for cadmium compounds with $PHChx_2$ (L) and (1-(dicyclohexylphosphino))-*N*-phenylthioformamide (L′) in CH_2Cl_2 at reduced temperatures [a]

Compound	^{113}Cd δ (ppm)	J(Cd–P) (Hz)	T (°C)
$[CdBr_2L]_2$	446	2005	−70
$[CdI_2L]_2$	293	1605	−50
$CdCl_2L_2$	672	1440	−90
$CdBr_2L_2$	623	1320	−70
CdI_2L_2	539	1210	−100
$CdClBrL_2$	659	1400	−120
$CdClIL_2$	620	1295	−120
$CdBrIL_2$	581	1265	−120
$CdCl_2L'_2$	652	1410	−100
$CdBr_2L'_2$	613	1280	−100
$CdI_2L'_2$	515	1090	−100
$[CdCl_2L']_2$	605	1535	−100
$[CdBr_2L']_2$	548	1430	−100
$[CdI_2L']_2$	429	1360, 1340	−100
$CdCl_2LL'$	669	1555, 1285	−100
$CdBr_2LL''$	635	1465, 1170	−100
CdI_2LL'	544	1260, 1000	−100

[a] Ref. 83.

or Se; X = Br or I) and mixed ligand species of the type $[Cd_4(EPh)_6L_4]^{2+}$ have been examined and the chemical shifts are summarized in Table 33 [90]. Mixed-ligand clusters of the type $[Cd_4(EPh)_x(L)_{10-x}]^{2-}$ and the mixed-metal clusters $[Cd_xZn_{4-x}(SPh)_{10}]$ gave ^{113}Cd spectra which indicated that the ^{113}Cd chemical shift is only slightly sensitive to whether the ligands bind terminally or are bridging, and that substitution of Zn has a relatively small effect on ^{113}Cd shifts [91]. Interestingly, similarly to metallothionein, no evidence was found for formation of a $CdZn_3$ combination [91]. The chemical shift values are summarized in Tables 33 and 34.

Dean et al. [92] recently examined the ^{113}Cd NMR spectra for complexes of the type $[\mu\text{-EPh})_6(CdL)_4]^{2-}$, E = S or Se, L = SPh, SePh, Cl, Br, or I; chemical shift values are given in Table 35. For a given L, the least shielded resonance is due to cadmium in a CdS_3L site whereas the most shielded resonance is due to $CdSe_3L$. The results indicated that the species in solution have terminally halogen substituted tetrameric adamantanoid structures analogous to those found for related structures in the solid state [92].

Alkyl–Cd compounds

Substituent effects have a significant influence on ^{113}Cd NMR chemical shifts in CdR_2 compounds [93] as can be seen from the results summarized

TABLE 31

^{113}Cd NMR data for Cd complexes with PBu_3 and $PChx_3$ at reduced temperatures [a]

Compound	n	Solvent	^{113}Cd δ (ppm)	J(Cd-P) (Hz)	T (°C)
$Cd(O_3SCF_3)_2(PChx_3)_n$	1	CH_2Cl_2	160	2540	−70
		MeOH	150	2580	−60
		Acetone	160	2500	−50
	2	CH_2Cl_2	357	2180	−60
		MeOH	352	2170	−60
		Acetone	354	2145	−50
$Cd(O_3SCF_3)_2(PBu_3)_n$	1	CH_2Cl_2	167	2630	−70
		MeOH	155	2730	−70
		Acetone	167	2610	−50
	2	CH_2Cl_2	379	2250	−60
		MeOH	385	2270	−70
		Acetone	371	2250	−50
	3	CH_2Cl_2	505	1730	−60
		MeOH	507	1720	−70
		Acetone	509	1690	−50
$Cd(ClO_4)_2(PChx_3)_n$	1	MeOH	156	2680	−70
		Acetone	170	2800	−70
	2	CH_2Cl_2	397	2240	−70
		MeOH	430	2140	−60
		Acetone	402	2160	−50
$Cd(ClO_4)_2(PBu_3)_n$	1	MeOH	163	2960	−60
		Acetone	160	2960	−50
	2	CH_2Cl_2	345	2500	−70
		MeOH	361	2480	−50
		Acetone	363	2450	−50
	3	CH_2Cl_2	506	1700	−80
		MeOH	493	1690	−50
		Acetone	520	1680	−50
$Cd(CF_3COO)_2(PChx_3)_n$	1	MeOH	181	2650	−70
	2	CH_2Cl_2	428	2000	−70
$Cd(CF_3COO)_2(PBu_3)_n$	1	CH_2Cl_2	194	2670	−70
		MeOH	170	2690	−70
	2	CH_2Cl_2	431	2080	−70
		MeOH	386	2180	−70
	3	CH_2Cl_2	485	1720	−70
		MeOH	486	1700	−70
$Cd(SCN)_2(PChx_3)_n$	2	CH_2Cl_2	549	1845	−70
$Cd(SCN)_2(PBu_3)_n$	1	MeOH	313	2250	−70
	2	MeOH	523	2000	−70
		Acetone	503	2010	−70
	3	CH_2Cl_2	538	1685	−100
		MeOH	544	1670	−70
		Acetone	534	1690	−70

[a] Ref. 84.

TABLE 32

^{113}Cd NMR data for $Cd(PBu_3)(PChx_3)L_2$ compounds in CH_2Cl_2 solution at reduced temperatures [a]

L	^{113}Cd δ (ppm)	J(Cd–P) (Hz)		T (°)
		$PChx_3$	PBu_3	
O_3SCF_3	383	2250	2200	−80
ClO_4	367	2360	2360	−70
NO_3	356	2220	2180	−70
CF_3COO	452	2060	2060	−70
CH_3COO	411	1990	1925	−70
Cl	656	1780	1650	−70
Br	623	1480	1630	−40
I	537	1460	1280	0
SCN	540	1940	1930	−70

[a] Ref. 84.

in Table 36. The replacement of R = Me by Et in CdR_2 results in an upfield shift of almost 100 ppm. This hypersensitivity of shift to substituent effects was attributed, in part, to inner shell contributions to the nuclear shielding constant [93]. Similar conclusions were drawn from the ^{113}Cd–^{13}C and ^{113}Cd–^{1}H coupling constants (Table 37). A 50 : 50 mixture of $CdMe_2$ and $CdEt_2$ gave three signals of relative intensity 1 : 2 : 1 (Fig. 13). The shift of the center resonance (593.06 ppm, Table 31), due to CdMeEt, was almost exactly in between the shifts of $CdMe_2$ (642.93 ppm) and $CdEt_2$ (543.20 ppm). The results confirmed that self-exchange occurs in mixed species of CdR_2 in the absence of catalyzing organic solvents. The moderate influence of solvents on the ^{113}Cd chemical shift of $CdMe_2$ was also examined [93] (Table 38).

TABLE 33

^{113}Cd NMR chemical shifts for $[Cd_4(EPh)_6L_4]^{2+}$ complexes in acetone [a]

E	L	^{113}Cd δ (ppm)
S	SPh	575
Se	SePh	519
S	Br	535
S	I	501
Se	Br	492
Se	I	441

[a] T = 295 K; see ref. 90 for further details.

TABLE 34

^{113}Cd NMR chemical shifts (ppm) for $[Cd_4(EPh)_x(L)_{10-x}]^{2-}$ at 295 K [a]

E	L	Solvent [b]	x										
			0	1	2	3	4	5	6	7	8	9	10
S	2-MePhS	actn	558	561	563	564	566	567	569	571	572	573	573
S	BuS	CH_3CN					631	622	613	604	595	585	577
S	$PhCH_2S$	actn								597	589	582	574
S	MeS	CH_3CN									598	588	578
S	PhSe	actn	519	525	531	537	544	549	554	559	564	569	574
S	PhTe	actn								552	558	567	574
Se	BuS	actn						605	588	571	553	536	519
Se	PhTe	actn								500	507	514	519

[a] See ref. 91 for details.

[b] actn = acetone.

TABLE 35

^{113}Cd chemical shifts (ppm) for $[(\mu\text{-EPh})_6(CdL)_4]^{2-}$ compounds in acetone at 295 K [a]

E	L	Concentration (M)	^{113}Cd δ
S	SPh	0.05	575
Se	SePh	0.02	519
		0.05	524
		Satd.	537
S	Cl	Satd.	551
S	Br	0.025	535
S	I	0.025	501
Se	Cl	Satd.	520
Se	Br	0.025	492
Se	I	0.025	441

[a] See ref. 92 for further details.

Heteronuclear double resonance methods were used to determine ^{113}Cd chemical shifts of a series of CdR_2 compounds [94] (Tables 36, 37). Although CH_2Cl_2 solvent was employed, where overlap existed, the shifts generally agreed with values published earlier [93]. Some relatively small differences were attributed to solvent effects [94]. Interestingly, the shift for R = iPr was 161 ppm to higher field than for R = nPr (Table 36), whereas the changes in shift for replacement of a hydrogen atom by a saturated carbon atom at the β and γ positions was found to be ca. +46 ppm and ca.

TABLE 36

^{113}Cd NMR chemical shifts (ppm) for CdR_2 compounds (R = alkyl) [a]

Compound	Solvent	^{113}Cd δ
$CdMe_2$	Neat	642.93
CdMeEt	Neat [b]	593.06
$CdEt_2$	Neat	543.20
$Cd(nPr)_2$	Neat	504.28
$Cd(nBu)_2$	Neat	489.11
$CdPh_2$ (1.0 M)	*p*-Dioxane	328.80
$CdMe_2$ [c]	CH_2Cl_2	643
$CdEt_2$ [c]	CH_2Cl_2	549
$Cd(iPr)_2$ [c]	CH_2Cl_2	436
$Cd(nPr)_2$ [c]	CH_2Cl_2	597
$Cd(nBu)_2$ [c]	CH_2Cl_2	599
$Cd(iBu)_2$ [c]	CH_2Cl_2	621

[a] From ref. 93 except as noted.
[b] From a 50:50 mixture of neat $CdEt_2$ and $CdMe_2$.
[c] From ref. 94.

TABLE 37

$^{1}H-^{113}Cd$ and $^{13}C-^{113}Cd$ coupling constants for CdR_2 compounds [a]

Compound	$J(^{13}C-^{113}Cd)$ (Hz)			$J(^{1}H-^{113}Cd)$ (Hz)	
	^{1}J	^{2}J	^{3}J	^{2}J	^{3}J
$CdMe_2$	−537.3			52.0	
$CdEt_2$	−498.0			51.6	
$Cd(nPr)_2$	−509.2	19.0	44.8		53.5
$CdMe_2$ [b]				52	
$CdEt_2$ [b]				53	60
$Cd(iPr)_2$ [b]					56
$Cd(nPr)_2$ [b]				50	55
$Cd(nBu)_2$ [b]				52	
$Cd(iBu)_2$ [b]				50	70

[a] From ref. 93 except as noted.
[b] From ref. 94.

−23 ppm, respectively. (Similar effects have been observed for dialkyl mercury compounds [94].) In all cases, $^{3}J(Cd-H)$ coupling constants were greater in magnitude than $^{2}J(Cd-H)$ coupling, and selective homonuclear decoupling experiments demonstrated that the couplings had opposite signs [94].

Double resonance methods were also employed in studies of methylcadmium alkoxides (CdMe(OR)) [95], Table 39. ^{111}Cd chemical shift and $^{111}Cd-^{1}H$ coupling data indicated that all of the compounds examined exist in a tetrameric structure, where each alkoxy group is attached to three chemically equivalent Cd atoms [95]. Complexation of $Cd(AsF_6)_2$ or

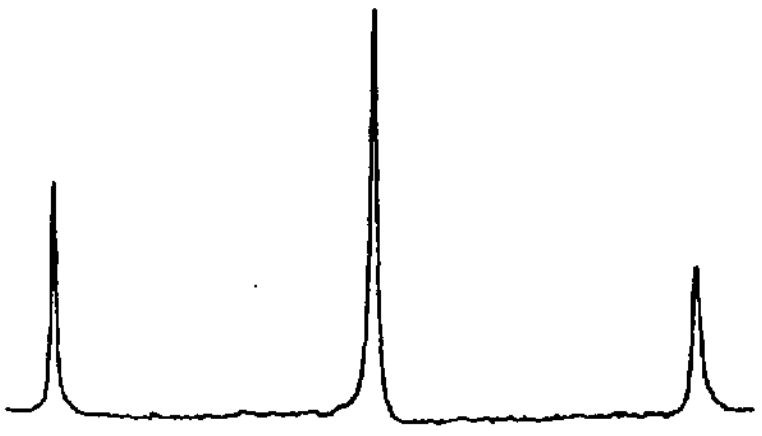

Fig. 13. ^{113}Cd NMR spectrum for an equimolar mixture of $CdMe_2$ and $CdEt_2$. The center resonance is assigned to the CdMeEt species (ref. 93).

TABLE 38

^{113}Cd NMR chemical shifts (ppm) for 1.0 M solutions of $CdMe_2$ [a]

Solvent	^{113}Cd δ	Solvent	^{113}Cd δ
THF	576.28	py	614.67
Diglyme	577.00	Et_2O	637.61
DMF	587.75	Neat	642.93
Dioxane	592.16	Benzene	644.96
Acetone	601.99	Toluene	644.96
Acetonitrile	605.55	CH_2Cl_2	646.06
Methyl formate	606.64	Cyclopentane	676.01
Ethyl acetate	609.68	Cyclohexane	677.60

[a] See ref. 93 for details.

$Cd(SbF_6)_2$ to an arene (hexamethyl- or hexaethylbenzene, pentamethylbenzene, durene, *p*-xylene, benzene, or toluene) was generally found to produce deshielding of the ^{113}Cd resonance and the NMR results were consistent with localized bonding of the arene to the cation [96]. NMR studies of dimethylcadmium in isotropic and anisotropic phases were used in combination with relativistic calculations to determine the Cd–C coupling tensor [97].

Complexes with amino acids

Ackerman and Ackerman [98] introduced the use of supercooled aqueous solutions to obtain slow-exchange ^{113}Cd NMR spectra for complexes formed with glycine. At room temperature, a solution containing $Cd(ClO_4)_2$, glycine, and $NaClO_4$ gave a single, broad ^{113}Cd NMR signal at ca. 150 ppm [98]. On cooling, the resonance split into three distinct signals which, at $-55\,^{\circ}C$, were separated by ca. 100 ppm; these signals were not unambiguously assigned. Spectra were obtained for similar solutions which contained various concentrations of glycine and $NaNO_3$. The shift of the downfield-most signal (262 ppm) was insensitive to the nature of the added salt (NO_3 or ClO_4) whereas the signals at ca. 155 and ca. 55 ppm were only slightly sensitive (ca. 10 ppm) to counterions [98].

One year later, Jakobsen and Ellis [99] unambiguously assigned the above signals for Cd complexes with glycine using supercooled solutions and ^{15}N-labeled glycine. Figure 14 shows the spectrum (spectrum a) obtained for a solution containing 0.1 M $Cd(ClO_4)_2$, 0.25 M glycine (95% ^{15}N-enriched), and 5 M $NaNO_3$ at $-40\,^{\circ}C$. Chemical shifts were virtually the same as those reported by Ackerman and Ackerman [98], and the multiplicities, due to ^{15}N–^{113}Cd coupling, allowed the respective complexes to be assigned. Thus, a quartet at 263 ppm due to $Cd(glycine)_3$, a triplet at 154 ppm due to

TABLE 39

^{113}Cd NMR data for methylcadmium alkoxides and related compounds in benzene solution [a]

Compound	Component [b]	Abundance (%)	^{113}Cd δ (ppm)	^{2}J(Cd–H) (Hz)	^{3}J(Cd–H) (Hz)
$Cd(Me)_2$		100	645	48.8	
CdMe(OMe)	O	40	322	82.5	9
	D	60	322	82.5	9
CdMe(OEt)	O	50	352	79.5	7.5
	D	50	352	79.5	7
CdMe(O-nPr)	O	50	345	79	
	D	50	349	79	
CdMe(O-nBu)	O	70	346	80.3	7.5
	D	30	350	80.4	
CdMe(O-iBu)	O	30	338	80.9	7.5
	D	70	342	81	7.5
CdMe(O-neo-C_5H_{11})		100	331	81.2	7.9
$(CdMeOCH_2)_2CH_2$	O		343	80	
	D		343	80	
CdMe(OCH_2Ph)	O	> 90	333	82.2	7.5
	D	< 10		82	7.5
CdMe($OCHPh_2$)		100	323	84.9	
CdMe($OCPh_3$)		100	316	86.5	
CdMe(O-iPr)		100	373	78.8	6.1
CdMe(O-2Bu)		100	370	77	7
CdMe(O-tBu)		100	386	77.3	
CdMe(OPh)		100	262	89.2	
[CdMe(OPh)py]$_2$		100	347		
CdMe(O-2,6-Me_2Ph)		100	264	90	
CdMe(S-iPr)		100	614		
CdMe(S-tBu)		100	601		

[a] The shifts reported here are corrected to the 0.1 M $Cd(ClO_4)_2$ reference by assigning $Cd(Me)_2$ a shift of 645 ppm; see ref. 95 for further details.
[b] O = Original species; D = component which developed after one week.

$Cd(glycine)_2$, and a doublet at 54 ppm due to Cd(glycine) were observed. The chemical shifts and coupling constants are summarized in Table 40.

^{113}Cd chemical shift-versus-pH profiles for Cd complexes with a series of amino acids and related ligands at room temperature have been obtained and compared [100]. A typical data set is shown in Fig. 15. The results for studies with glycine were consistent with formation of mono, bis and tris Cd complexes which contained bifunctionally coordinated glycine. As expected, complexes with the highest stability were those which contained ligands capable of forming 5-membered chelate rings with Cd. The ^{113}Cd spectra of glycylglycine, glycylglycyl-glycine, glycyl-γ-aminobutyric acid, and β-

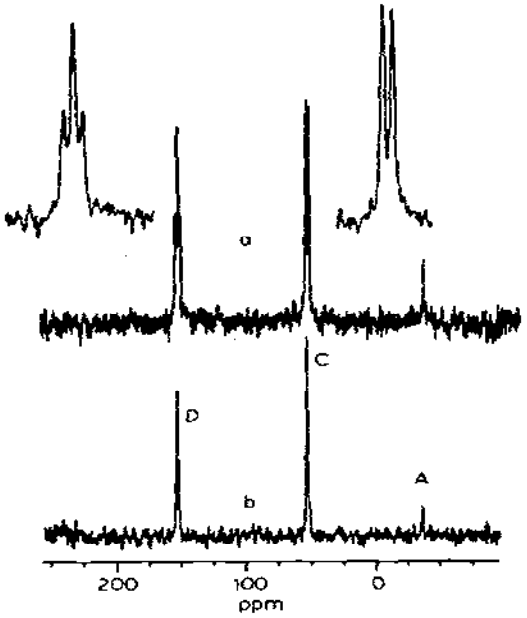

Fig. 14. ^{113}Cd spectra of super-cooled (−40 °C) aqueous solutions of 0.1 M $Cd(ClO_4)_2$ and 0.25 M glycine in 5 M $NaNO_3$, pH 7. (a) Obtained using 95% ^{15}N-enriched glycine; expansions of the doublet (C, due to the Cd(gly) species) and triplet (D, due to the $Cd(gly)_2$ species) are inserted. (b) Obtained using isotopically normal glycine. From ref. 99.

alanylglycine were investigated similarly [101] and no evidence was found for coordination of the peptide NH groups.

Fast exchange ^{113}Cd NMR spectra were obtained for the Cd complex formed with the tripeptide, glutathione [102]. The observed signal was sensitive to changes in the sample pH and to the Cd : glutathione ratio.

(ii) Proteins

Some of the Cd-substituted protein systems have received considerable attention, and it is beyond the scope of this review to examine all the work

TABLE 40

^{113}Cd NMR chemical shifts (ppm) and ^{15}N–^{113}Cd coupling constants (Hz) for $Cd(^{15}N\text{-Glycine})_n$ complexes in supercooled aqueous solution [a]

Compound	[^{15}N-Glycine] (M)	pH	^{113}Cd δ	^{1}J(N–Cd)
Cd(Glycine)	0.25	7.0	53.6	170
$Cd(Glycine)_2$	0.25	7.0	153.9	165
$Cd(Glycine)_3$	1.00	8.0	262.8	> 140

[a] See ref. 99 for further details.

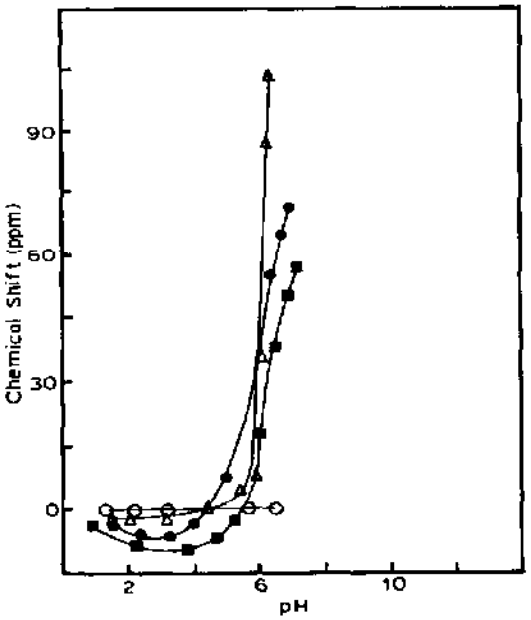

Fig. 15. ^{113}Cd chemical shift as a function of pH for 0.3 M $Cd(ClO_4)_2$ and 0.6 M methylamine (◆), glycine (●), glycine methyl ester (▲), and *N*,*N*-dimethylglycine (■). From ref. 100.

in detail. For such cases, details will be presented for the more recent work only, and the reader will be referred to the literature for information regarding earlier work. The main goal here is to summarize the ^{113}Cd chemical shift information which has been obtained and the sample conditions employed for each study. Then, it should be possible to make meaningful comparisons of shifts between different proteins and between proteins and coordination compounds.

The first data on ^{113}Cd-substituted metalloproteins was published by Armitage et al. in 1976 [1] and included the enzymes human carbonic anhydrase, bovine carbonic anhydrase, and alkaline phosphatase. Subsequently, more than twenty different metalloproteins have been examined. In some cases, the metal binding sites have been characterized by X-ray crystallography and, for these cases, attempts have been made to correlate NMR data with structural data. For proteins where X-ray structural data were not available, ^{113}Cd NMR was used to provide a first-approximation of the ligands at the metal binding sites. In many cases, ^{113}Cd NMR spectroscopy has provided new insights into protein–substrate interactions, conformational changes, metal displacement reactions, etc. The proteins are grouped here mainly according to the type of ligands at the metal binding sites. The three main groups are those which contain O donors exclusively, N donors (which may be in combination with O donors), and S donors (with

TABLE 41

Sample conditions and ^{113}Cd NMR spectral data for Cd-substituted proteins

Protein	Site	Ligands [a]	Form	pH	Buffer	Cd salt	δ (ppm)	Shift		Ref.
								f(pH)	$f(X^-)$	
O-DONOR SITES										
Calmodulin										
Cd_4(Cal)	HA1 [c]			7.0–5.3	None	ClO_4	−108	No	[b]	108
	HA2			7.0–5.3	None	ClO_4	−88	No	[b]	108
	LA1			7.0–5.3	None	ClO_4	[d]			108
	LA2			7.0–5.3	None	ClO_4	[d]			108
Cd_4(Cal)TFP [e]	HA1			7.0	None	ClO_4	−99.1 [f]	[b]	[b]	11
	HA2			7.0	None	ClO_4	−112.9 [f]	[b]	[b]	11
	LA1			7.0	None	ClO_4	−115.2 [f]	[b]	[b]	11
	LA2			7.0	None	ClO_4	−118.1 [f]	[b]	[b]	11
Parvalbumin										
Cd_2(Parv)	EF	1CO, 2COO, 2COO *, 1W		5.9	Tris-SO_4	SO_4	−93.8	No	No	122
	CD	1CO, 4COO, 1OH		5.9	Tris-SO_4	SO_4	−97.5	No	No	122
Troponin C										
Cd_2(sTnC)	HA1	6-oxygens [g]		6.4	cac [h]	ClO_4	−107.5	Yes	[b]	128
	HA2			6.4	cac [h]	ClO_4	−110.0	Yes	[b]	128
Cd_4(sTnC)	HA1			7	None [i]	Cl	−107.2	[b]	[b]	129
	HA2			7	None [i]	Cl	−112.7	[b]	[b]	129
	LA1 [j]			7	None [i]	Cl	−103.1	[b]	[b]	129
	LA2 [j]			7	None [i]	Cl	−109.9	[b]	[b]	129
Cd_2(cTnC)	HA1			7	None [i]	ClO_4	−107	[b]	No	130
	HA2			7	None [i]	ClO_4	−114	[b]	No	130
Intestinal Ca binding protein										
Cd(ICaBP)	EF-hand	3COO, nCO		8	None	[b]	−104	[b]	[b]	134

Cd_2(ICaBP)	EF-hand	1COO, *n*CO		8	None	[b]	−110	[b]	[b]	134
	pseudo EF-hand			8	None	[b]	−155	[b]	[b]	134
CdCa(ICaBP)	EF-hand			8	None	[b]	−110	[b]	[b]	134
Concanavalin A										
Cd : Cd(Con A)	S2	2CO, 2COO, 2W	Locked	5.2	Acetate	Cl	−125	No	No	104
Cd : Cd(Con A)S [k]	S2		Locked	5.2	Acetate	Cl	−133	[b]	[b]	104
Insulin										
Cd_3(InS)	Ca	6 COO		8.0	None	SO_4	−36	No	No	118
Zn_2Cd(Ins)	Ca	6 COO		8.0	None	SO_4	−36	No	No	118
Cd_2Ca(Ins)	Ca	6 COO		8.0	None	SO_4	[m]	No	No	118
Yeast inorganic pyrophosphatase										
Cd_2(PPase) [l]	HA			6.5	Tris-HCl	Cl	−23.0	No	No	119
Cd_6(PPase)	1			6.4	Tris-HCl	Cl	17.7	[b]	[b]	119
	2			6.4	Tris-HCl	Cl	−4.8	[b]	[b]	119
	3			6.4	Tris-HCl	Cl	−25.6	[b]	[b]	119
Cd_6(PPase)Pi_2	1			6.5	Tris-HCl	Cl	18.8	[b]	[b]	119
	2			6.5	Tris-HCl	Cl	−2.5	[b]	[b]	119
	3			6.5	Tris-HCl	Cl	−32.5	[b]	[b]	119
Cd_6(PPase)Pi_6	1			7.1	Tris-HCl	Cl	8.9	[b]	[b]	119
	2			7.1	Tris-HCl	Cl	−18.7	[b]	[b]	119
	3			7.1	Tris-HCl	Cl	−34.0	[b]	[b]	119
Cd_8(PPase)Pi_4	A			7.0	Mes [n]	Cl	12.2	[b]	No	120
	B			7.0	Mes [n]	Cl	−14.2	[b]	No	120
	C			7.0	Mes [n]	Cl	−16.5	[b]	No	120
	D			7.0	Mes [n]	Cl	−28.4	[b]	No	120
α-Lactalbumin										
Cd(α-Lact)				6.2–7.8	Tris-HCl	Cl	−80	No	[b]	131
Yeast enolase										
Cd_2(YE)	HA			7.2	None	NO_3	−43.2	Yes	Yes	132

TABLE 41 (continued)

Protein	Site	Ligands [a]	Form	pH	Buffer	Cd salt	δ (ppm)	Shift		Ref.
								f(pH)	$f(X^-)$	
Prothrombin fragment 1, factor X										
Cd_n(PF1)	H			[b]	None	ClO_4	10	[b]	No	133
	L1			[b]	None	ClO_4	−5	[b]	Yes	133
	L2			[b]	None	ClO_4	−18	[b]	Yes	133
Cd_n(PFX)	H			[b]	None	ClO_4	9	[b]	[b]	133
	L			[b]	None	ClO_4	−25	[b]	[b]	133
Serine proteases										
Trypsin		2COO, 2CO, 2W		6.5	None	ClO_4	−54.5	[b]	[b]	136
Trypsinogen		2COO, 2CO, 2W		6.5	None	ClO_4	−55.8	[b]	No	136
Chymotrypsin				6.5	None	ClO_4	0	[b]	[b]	136
Chymotrypsinogen				6.5	None	ClO_4	−10	[b]	[b]	136
Horseradish peroxidase										
Cd(HRP)	HA			6.3	None	Cl	−193	No	[b]	137
Phosphoglucomutase										
Cd(PGM_p) [o]				7.5	Tris-HCl	OAc	22	[b]	[b]	138
Cd(PGM_d)Glc-P_2 [o]				7.5	Tris-HCl	OAc	75	[b]	[b]	138
Cd_2(PGM_d)Glc-P_2 [o]				7.5	Tris-HCl	OAc	75	[b]	[b]	138
CdLi(PGM_d)Glc-P_2 [o]				7.5	Tris-HCl	OAc	75	[b]	[b]	138
Osteocalcin										
Cd(BGP)				6.0–9.0	Tris-HCl	Cl	0 –40	yes	[b]	121
Cd(BGP)Pi				8.0	Tris-HCl	Cl	0	[b]	[b]	121
Alkaline Phosphatase										
Cd_4(AP)Pi	C	4COO		9.0	Tris-HCl [p]	OAc	2	No	No	145
Cd_6(AP)Pi_2	C			9.0	Tris-HCl [p]	OAc	2	No	No	145
Cd_6(AP)·As [q]	C			6.0	Tris-HCl [p]	OAc	−2	[b]	[b]	146
Cd_6(AP)–As [q]	C			6.0	Tris-HCl [p]	OAc	−2	[b]	[b]	146

N-DONOR SITES										
Concanavalin A										
Cd:Cd(Con A)	S1	3COO, 2W, 1N	Locked	5.2	Acetate	Cl	46	[b]	No	104
Cd:Ca(Con A)	S1		Locked	5.2	Acetate	Cl	43	[b]	No	104
Cd:Pb(Con A)	S1		Locked	5.2	Acetate	Cl	32	[b]	No	104
Cd:Cd(Con A)S [k]	S1		Locked	5.2	Acetate	Cl	46	[b]	No	104
Insulin										
Cd_3(Ins)	Zn	3N, 3W		8.0	None	SO_4	165	Yes	Yes	118
Cd_2Ca(Ins)	Zn	3N, 3W		8.0	None	SO_4	165	Yes	Yes	118
Zn_2Cd(Ins)	Zn	3N, 3W		8.0	None	SO_4	[m]			118
Phospholipase C										
Cd(Pho C)	Str.			6.5	Acetate	Cl	85	No	No	140
Cd_2(Pho C)	Str.			6.5	Acetate	Cl	85	No	No	140
	Cat.			6.5	Acetate	Cl	115	Yes	Yes	140
CdZn(Pho C)	Cat.			6.5	Acetate	Cl	115	Yes	Yes	140
Alkaline phosphatase										
Cd_2(AP) [t]	A	3N, 1–2W*		6.0	Tris-OAc	Cl	117	Yes	Yes	17
	A			6.0	[r]	Cl	170	Yes	Yes	17
	A			6.5	Tris-OAc	OAc	120	Yes	Yes	143
	A			6.5	[s]	OAc	179	Yes	Yes	143
Cd_2(AP)	A			7.8	Tris-HCl [u]	OAc	144	Yes	Yes	144
	B	1N, 2COO		7.8	Tris-HCl	OAc	52	No	No	144
Cd_2(AP)Pi	A			6.5	Tris-HCl	OAc	142	Yes	Yes	144
	B			6.5	Tris-HCl	OAc	55	No	No	144
Cd_2(AP)As	A			6.3	Tris-HCl	OAc	163	[b]	[b]	146
	B			6.3	Tris-HCl	OAc	71	[b]	[b]	146
Cd_4(AP)	A			6.0	Tris-HCl	OAc	170	Yes	Yes	144
	A			7.5	Tris-HCl	OAc	142	Yes	Yes	144
	B			9.0	Tris-HCl	OAc	52	No	No	144
Cd_6(AP)·Pi_2	A			9.0	Tris-HCl	OAc	137	Yes	Yes	144
	B			9.0	Tris-HCl	OAc	64	No	No	144
	A			9.0	Tris-OAc	OAc	133	Yes	Yes	145

TABLE 41 (continued)

Protein	Site	Ligands [a]	Form	pH	Buffer	Cd salt	δ (ppm)	Shift		Ref.
								f(pH)	$f(X^-)$	
	B			9.0	Tris-OAc	OAc	64	No	No	145
Cd_6(AP)–Pi	A			9.0	Tris-HCl [u]	OAc	150	Yes	Yes	144
	B			9.0	Tris-HCl	OAc	68	No	No	144
	A			9.0	Tris-OAc	OAc	137	Yes	Yes	145
	B			9.0	Tris-OAc	OAc	70	No	No	145
Cd_6(AP)·As_2 [p]	A			7.8	Tris-HCl [u]	OAc	207	[b]	[b]	146
	B			7.8	Tris-HCl [u]	OAc	81	[b]	[b]	146
Cd_6(AP)–As_2 [p]	A			7.8	Tris-HCl [u]	OAc	192	[b]	[b]	146
	B			7.8	Tris-HCl [u]	OAc	90	[b]	[b]	146
Carbonic anhydrase										
Cd(BCA)		3N, W*		8.0	Tris-SO_4	[b]	214	Yes	Yes	1
				8.3	None	SO_4	224	Yes	Yes	151
Cd(BCA)OH					None	SO_4	274	Yes	Yes	151
Cd(BCA)H_2O					None	SO_4	219	Yes	Yes	151
Cd(BCA)HCO_3					None	SO_4	208	Yes	Yes	151
Cd(BCA)CN					None	SO_4	354 [w]	No	No	151
Cd(BCA)Neop [v]					None	SO_4	403 [x]	No	No	152
Cd(BCA)BS [v]					None	SO_4	387 [x]	No	No	152
Cd(HCAC)				8.1	Tris-SO_4	[b]	225	Yes	Yes	1
				8.1	None	SO_4	232	Yes	Yes	151
Cd(HCAC)OH		3N, W*			None	SO_4	275	Yes	Yes	151
Cd(HCAC)H_2O					None	SO_4	229	Yes	Yes	151
Cd(HCAC)HCO_3					None	SO_4	216	Yes	Yes	151
Cd(HCAC)CN					None	SO_4	354 [w]	No	No	151
Cd(HCAC)BS [v]					None	SO_4	390 [x]	No	No	152
Cd(HCAC)SH					None	SO_4	374 [ii]	No	No	152
Cd(HCAB)				9.1	Tris-SO_4	[b]	145	Yes	Yes	1
				8.3	None	SO_4	223	Yes	Yes	151

Cd(HCAB)OH		3N, W*		None	SO_4	274	Yes	Yes	151
$Cd(HCAB)H_2O$				None	SO_4	215	Yes	Yes	151
$Cd(HCAB)HCO_3$				None	SO_4	164	Yes	Yes	151
Cd(HCAB)CN				None	SO_4	411 [y]	No	No	150
Cd(HCAB)BS [v]				None	SO_4	355 [z]	No	No	152
Carboxypeptidase A									
Cd(CPA)		2N, COO*, W*	7.5	Tris-HCl [aa]	Cl	120 [bb]	[b]	[b]	154
Cd(CPA)PPPE [cc]			7.5	Tris-HCl [aa]	Cl	127	[b]	[b]	154
Cd(CPA)3PP [cc]			7.5	Tris-HCl [aa]	Cl	132	[b]	[b]	154
Cd(CPA)BzSuc [cc]			7.5	Tris-HCl [aa]	Cl	137	[b]	[b]	154
Cd(CPA)TGA [cc]			7.5	Tris-HCl [aa]	Cl	355	[b]	[b]	154
Cd(CPA)TLA [cc]			7.5	Tris-HCl [aa]	Cl	350, 339	[b]	[b]	154
Cd(CPA)3PP [cc]			6.9–7.5	Tris-HCl [aa]	Cl	133	[b]	[b]	17, 154
Superoxide dismutase									
Cd_2(SD)	Zn	3N, COO	6.0	None	[b]	170	[b]	[b]	17
			5.5	Acetate	Cl	311	[b]	[b]	18
$Cd_2Cu(I)_2$(SD)	Zn		4.6	None	[b]	9	[b]	[b]	17
			4.7–8.0	Acetate [dd]		320	No	[dd]	18
Bovine serum albumin									
Cd_2(BSA)	A		6.7	None [ee]	ClO_4	150	Yes	[b]	148
	B		6.7	None	ClO_4	28	Yes	[b]	148
S-DONOR SITES									
Horse liver alcohol dehydrogenase									
Cd_2(LADH)	str	4S(tetrahedral)	8.5	PO_4	SO_4	750	No	[b]	157
	cat	2S, 1N, W*	8.5	PO_4	SO_4	484	No	[b]	157
Cd_2(LADH)NAD^+	str		8–10	PO_4	SO_4	750	No	[b]	157
	cat		8–10	PO_4	SO_4	442	No	[b]	157
Cd_2(LADH)NADH	str		7–10	PO_4	SO_4	750	No	[b]	157
	cat		7–10	PO_4	SO_4	442	No	[b]	157

TABLE 41 (continued)

Protein	Site	Ligands [a]	Form	pH	Buffer	Cd salt	δ (ppm)	Shift		Ref.
								f(pH)	$f(X^-)$	
Cd_2(LADH)NAD^+ S [ff]	str			8.3	PO_4	SO_4	750	No	[b]	157
	cat			8.3	PO_4	SO_4	518	No	[b]	157
Metallothionine										
crab-Cd_6MT-1	cluster 1			9	Tris [u]	Cl	659.2	Yes	Yes	162
				9	Tris [u]	Cl	650.5	Yes	Yes	162
				9	Tris [u]	Cl	621.4	Yes	Yes	162
	cluster 2			9	Tris [u]	Cl	647.2	Yes	Yes	162
				9	Tris [u]	Cl	646.3	Yes	Yes	162
				9	Tris [u]	Cl	631.0	Yes	Yes	162
crab-Cd_6MT-2	cluster 1			9	Tris [u]	Cl	660.6	Yes	Yes	162
				9	Tris [u]	Cl	648.6	Yes	Yes	162
				9	Tris [u]	Cl	624.2	Yes	Yes	162
	cluster 2			9	Tris [u]	Cl	661.6	Yes	Yes	162
				9	Tris [u]	Cl	634.8	Yes	Yes	162
rabbit-Cd_7MT-2 [gg]	3-metal cluster			9	Tris [u]	Cl	668.8	Yes	Yes	172
				9	Tris [u]	Cl	659.0	Yes	Yes	172
				9	Tris [u]	Cl	649.2	Yes	Yes	172
	4-metal cluster			9	Tris [u]	Cl	671.3	Yes	Yes	172
				9	Tris [u]	Cl	630.9	Yes	Yes	172
				9	Tris [u]	Cl	625.0	Yes	Yes	172
				9	Tris [u]	Cl	611.3	Yes	Yes	172

Blue copper proteins								
Cd[azurin (*Pseudomonas*)]	2N, 1S, 1M	7.6	Tris-HCl	Cl	372	No	No	180
Cd[azurin (*Alcaligenes*)]	2N, 1S, 1M	7.7	Tris-HCl	Cl	379	No	No	180
Cd[stellacyanin]		8	Tris-HCl	Cl	380	No	No	180
Cd[plastocyanin (*Spinacea*)]	2N, 1S, 1M	8	Tris-HCl	Cl	432	No	No	180

[a] Determined by X-ray structural analysis: CO = carbonyl, COO = carboxyl, COO* = bidentate-binding carboxyl, W = water molecule, W* = water or substrate molecule, N = imidazole, S = cysteine, M = methionine. [b] Not reported.

[c] HA, LA refer to high affinity and low affinity binding sites, respectively. [d] Broadened beyond detection, except at low magnetic fields.

[e] TFP = antipsychotic drug, trifluoperazine: signal assignments to specific binding sites (HA1, HA2, LA1, LA2) were not made and those reported here may be interconverted.

[f] Chemical shifts of adducts with TFP and other drugs are dependent on the concentration of added drug.

[g] Site I: 1CO, 3COO, 1OH, 1W; Site II: 1CO, 4COO, 1OH; Sites III and IV: 2CO, 4COO. [h] cac = cacodylate buffer (0.05 M).

[i] Sample contained 0.1 M KCl; $T = 4°C$. [j] Low-affinity signals only observed at reduced temperatures. [k] S = mono or polysaccharide.

[l] Here, the high affinity site and the three distinct binding sites are labeled HA, 1, 2, and 3, respectively. Signals have not been assigned to specific binding sites in the molecule.

[m] No signal was detected for this site. [n] Mes (100 mM) = 4-morpholineethanesulfonate buffer.

[o] PGM_p, PGM_d represent the phosphorylated and dephosphorylated enzymes, respectively. Glc, Glc-P_2, Glc-6-P represent glucose, glucose-1,6-diphosphate, and glucose-6-phosphate, respectively.

[p] Buffer solutions also contained acetate and 0.1 M NaCl. [q] As = arsenate. [r] As above, plus 0.1 M NaCl. [s] As above, plus 0.3 M NaCl.

[t] Cd atoms occupy the equivalent A sites of each monomer. [u] Buffer solution also contains 0.1 M NaCl.

[v] Neop and BS are abbreviations for the inhibitors ^{15}N-neoprontosil and ^{15}N-benzenesulfonamide, respectively.

[w] $J_{Cd-C} = 1040$ Hz. [x] $J_{Cd-N} = 190$ Hz. [y] $J_{Cd-C} = 1060$ Hz. [z] $J_{Cd-N} = 210$ Hz.

[aa] 1.0 M NaCl. [bb] Signal only observed at reduced temperatures.

[cc] Substrate abbreviations: 3PP = 3-phenylpropionate; PPPE = L-phenylalanine phosphoramidate phenyl ester; BzSuc = D,L-benzylsuccinate; TGA = thioglycolic acid; TLA = thiolactic acid.

[dd] PO_4 buffer was also employed, and the sample was extensively dialyzed, which did not affect the ^{113}Cd chemical shift.

[ee] Solution contained 0.16 M NaCl. [ff] Substrate (S) = trifluoroethanol or pyrazole.

[gg] Reconstituted Cd_7MT. [ii] $J_{Cd-H} = 48$ Hz (ref. 13).

or without other types of donor atoms). ^{113}Cd chemical shifts and sample conditions are summarized in Table 41.

Calmodulin (Cal)

Calmodulin is a low molecular weight regulatory protein (17,000 Daltons) which, in biological processes, binds four equivalents of calcium. Reviews on structural aspects of Ca binding sites in proteins with homologous Ca binding domains [10] and Cd binding proteins in general [3] have appeared. ^{113}Cd NMR experiments on Cd-substituted Cal [106–117] indicate that two of the binding sites are "high-affinity" type sites, which yield sharp ^{113}Cd NMR signals, and the other two sites are low-affinity sites which give rise to extremely broad (undetected at high fields) signals. ^{113}Cd NMR chemical shifts for the high-affinity sites are −88 and −108 ppm at pH 7 for Cd_4(Cal) [108]. The resonance frequencies and intensities are unaffected by a lowering of pH to 5.3 (although the signals become broader); at lower pH values, the resonances disappear and a broad signal, due to free Cd, is observed. Addition of Zn results in broadening and loss of intensity for signals of the high-affinity sites, but Mg does not affect the ^{113}Cd NMR spectrum, even at high added Mg concentrations [108].

Addition of the hydrophobic antipsychotic drug trifluoperazine (TFP) causes a conformational change which results in sharp signals for all four

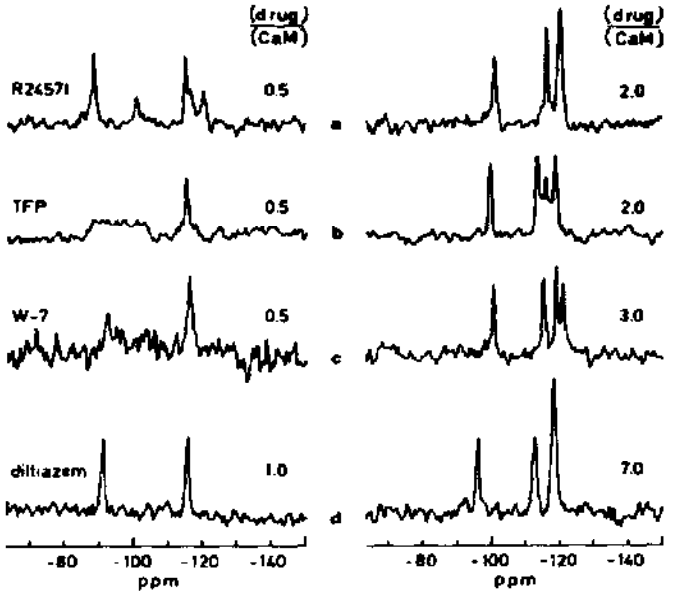

Fig. 16. ^{113}Cd NMR spectra of Cd_4(Cal) obtained after the addition of different drugs. The ratio of drug to Cal is indicated in the figure. For other sample conditions see ref. 11.

^{113}Cd NMR signals [109–113]. Chemical shifts of −99.7, −113.5, −115.8, and −118.7 ppm were observed for a solution where the TFP : Cd_4(Cal) ratio was 2 : 1. The chemical shifts were dependent on the concentration of added drug. Similar results were reported for studies with other drugs [11,109–113] as shown in Fig. 16, and the changes in the ^{113}Cd NMR spectra have been interpreted in terms of protein conformational changes.

The high- and low-affinity binding sites have been assigned to specific proteolytic fragments of Cal [114–116]. Proteolysis with thrombin results in fragmentation which separates the two high-affinity sites and causes a reduction in the affinity of both sites for Ca ions. Proteolysis with trypsin gives amino- and carboxy-terminal fragments which are conformationally similar to the native protein. Trifluoperazine binds to specific sites on both the carboxy- and amino-terminal fragments, although stronger binding occurs at the carboxy-terminal fragment [116].

Recently, Forsen and co-workers [117] found that one equivalent of the tetradecapeptide mastoparan binds strongly to Cd_4(Cal) which induces a conformation change in both the carboxy- and amino-terminal domains. The ^{113}Cd chemical shifts induced by binding of 10 different drugs to Cd_4(Cal) have been summarized in a recent review [11].

Parvalbumin (Parv)

Parvalbumin (M_r ca. 11,500) from carp muscle contains two Ca binding sites as determined by X-ray structural analysis. Octahedral Ca in the CD site is bound by four carboxyl groups, a peptide carbonyl, and a serine hydroxyl group. The EF site is similar except that serine is replaced by a molecule of water. The ^{113}Cd NMR spectrum of Cd_2(Parv) displays two distinct signals at −93.8 and −97.5 ppm [122]. The similarity of the chemical shifts indicated that the binding sites were similar, consistent with the X-ray structural data. The CD-site signal was insensitive to changes in pH or [Cl^-] which indicated that the Cd atom at this site was inaccessible to the external medium [122]. The shift of the EF-site signal was only very slightly affected by changes in the external medium. On the other hand, addition of Mg resulted in a shifting to higher field (ca. 3 ppm) of the EF site ^{113}Cd signal, suggesting that there is a secondary cation binding site close to the EF site [123]. The ability of lanthanide ions to compete with Cd, and their effect on the ^{113}Cd spectra have been investigated [124–127]. Measurement of ^{13}C–^{113}Cd couplings in the ^{13}C spectrum allowed the assignment of signals of carbonyl and carboxyl groups which are bound to Cd [125].

Troponin C (Tn C)

Troponin C (M_r 19,000) contains two high-affinity and two low-affinity metal binding sites. The high-affinity sites bind mainly Ca but also Mg,

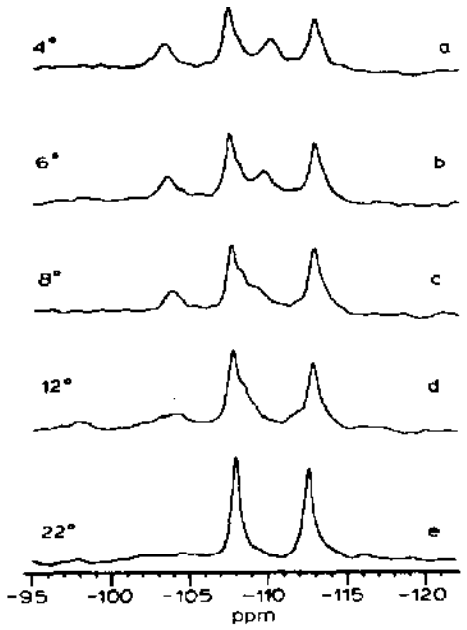

Fig. 17. Temperature dependence of the ^{113}Cd NMR spectrum of Cd-substituted skeletal troponin C. At 22°C, only the high-affinity site signals can be observed (ref. 129).

whereas the low-affinity sites bind Ca exclusively in the native protein. Two sharp ^{113}Cd NMR signals were observed for a solution of Tn C containing excess Cd, and these signals were attributed to Cd in the high-affinity sites [128]. The chemical shift values observed (−107.5 and −111.0 ppm; Table 36) were consistent with exclusively O-donor ligands and did not shift (but did exhibit loss of signal intensity) on addition of Ca or Mg [128].

All four ^{113}Cd signals in Cd_4(sTn C) (sTn C = Tn C from skeletal muscle) could be observed at reduced sample temperatures [129]. At 4°C, the two new resonances occurred at −103.1 and −109.8 ppm, Fig. 17. (In this work, the high-affinity site resonances were at −107.8 and −112.7 ppm, in agreement with the previously determined values.) In contrast, the low temperature spectrum of Cd_3(cTn C) (Tn C from cardiac muscle; see ref. 130) resulted in two sharp signals due to the two high-affinity sites (−107 and −114 ppm) and a very broad resonance slightly downfield from the −107 ppm signal, indicating that the third Cd binds less tightly to the single, low-affinity site in cTn C.

Intestinal Ca binding protein (ICaBP)

Native porcine intestinal Ca binding protein (M_r 9,000) binds two equivalents of Ca. At 5°C, addition of up to one equivalent of Cd to the apo-ICaBP resulted in a ^{113}Cd NMR signal at −104 ppm due to Cd bound

to the EF-hand site [134]. Further addition of Cd resulted in a second signal at −155 ppm (due to binding to the pseudo EF-hand site) and a concomitant upfield shift (to −110 ppm) to the EF-hand site signal. Interestingly, addition of Ca to Cd(ICaBP) resulted in a similar shift of the EF-hand site signal except that, for less than one equivalent of added Ca, two EF-hand site signals were observed at −104 and −110 ppm. This result was attributed to tighter binding of Ca in the pseudo EF-hand site [134]. At ambient temperature, the −155 ppm signal for Cd_2 (ICaBP) was not observed due to exchange broadening. Addition of Ca to Cd_2(ICaBP) resulted in replacement of Cd at the pseudo EF-hand site prior to substitution at the EF-hand site.

More recently, Forsen et al. [135] utilized site-directed mutagenesis to obtain four mutant forms of ICaBP. The mutations were restrained to the N-terminal (pseudo EF-hand) binding site in order to examine how the structure and chemistry in this region are affected by localized changes. Compared to the EF-hand site, the pseudo EF-hand site contains an extra Pro residue, and three of the mutants contained variations in this region of the molecule; the fourth mutant was prepared to determine the importance of a specific hydrogen bond. Among other findings, it was shown that modifications at the pseudo EF-hand site have little influence on the ^{113}Cd signal of the EF-hand site in Cd(ICaBP). In addition, the shift changes for the EF-hand site signal which accompany Cd binding to the pseudo EF-hand site were diminished in the mutants with modifications at the pseudo EF-hand site. Also, shifts for ^{113}Cd signals of the pseudo EF-hand site were highly sensitive to the mutations. In one case, where Pro-20 was replaced by Gly, the signal for the pseudo EF-hand site was observed at −88 ppm, which is 68 ppm downfield from the signal observed in the native protein (−156 ppm). For the two other cases, signals for this site were broadened beyond detection [135].

Concanavalin A (Con A)

Concanavalin A consists of identical subunits, each with a molecular weight of ca. 25,500 Daltons. In solution, dimers and tetramers are formed and the percentage of each species depends on pH, temperature, and ionic strength. Each subunit contains two sites which bind metals strongly: the S1 site, which binds Mn^{2+} in the native protein, and the S2 site which binds Ca^{2+}. As in the native protein, the Cd-substituted derivative binds saccharides and this binding is thought to be an important part of the biological activity of Con A. Two protein conformations have been observed for Con A, including an "unlocked" form where metals exchange rapidly between free and bound states, and a "locked" form, where the metals are tightly bound to the protein.

Ellis and co-workers have published three papers on the ^{113}Cd NMR spectral properties of Cd-substituted Con A [103–105], including studies of the locked and unlocked conformations in earlier work as well as a more recent detailed evaluation of the ^{113}Cd NMR relaxation and chemical exchange properties. The locked form of Cd_2(Con A) gives two ^{113}Cd NMR signals at 46 and −125 ppm [104]. The upfield-shifted signal is due to Cd in the calcium (S2) site and the downfield signal is from Cd in the manganese (S1) site. The chemical shifts of both signals were independent of added Cl^-. When one equivalent of Ca was added to a sample of Cd : Cd(Con A), the −125 ppm signal disappeared and the intensity of the signal due to free Cd increased. This binding of Ca caused a 3 ppm shift to higher field for the signal due to Cd in the S1 site of Cd : Ca(Con A). Pb was also found to compete for the S2 site, Fig. 18, and an upfield shift of 14 ppm for the ^{113}Cd signal of Cd in the S1 site of Cd : Pb(Con A) was observed. Zn was found to compete strongly at both the S1 and S2 sites of Cd : Cd(Con A). The binding of mono- and polysaccharides causes a similar, 8 ppm upfield shift of the S2-bound Cd signal but does not influence the shift of Cd in the S1 site.

Chemical exchange processes for Cd : Cd(Con A) were examined using a double saturation transfer experiment [105]. Analysis of data obtained at three field strengths revealed that chemical exchange processes contribute 14, 75, and 20% to the observed relaxation time constants for the signals due to Cd in the S1 site, for free Cd, and for the S2 site, respectively. The weak field dependence observed for the heteronuclear NOE is not due to internal motions but, instead, to chemical exchange processes [105].

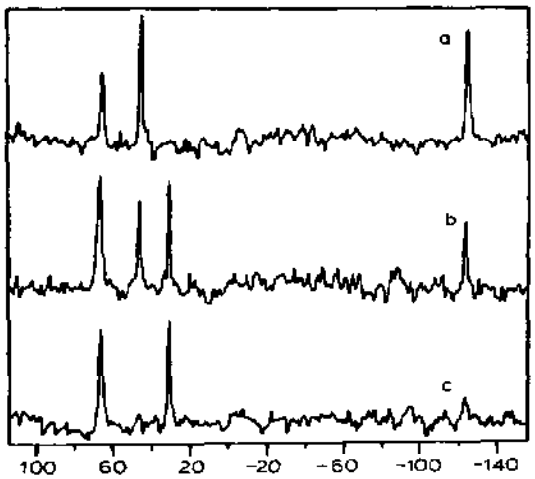

Fig. 18. (a) ^{113}Cd NMR spectra of Cd_2(Con A); (b) as in (a) except for the addition of 1.0 equivalents of Pb(II); (c) as in (a) except for the addition of 2.0 equivalents of Pb(II). From ref. 104.

Insulin (Ins)

Insulin consists of a hexamer (M_r (hexamer) ca. 40,000) which binds two equivalents of Zn and one equivalent of Ca. X-Ray crystallographic studies have shown that the Ca is bound by six glutamyl carboxyl groups and is inaccessible to solvent, whereas the equivalent (by symmetry) Zn atoms are each coordinated by three histidine imidazole groups and three molecules of water, Fig. 19. The ^{113}Cd NMR spectrum of Cd_3(Ins) (Ins refers to the hexamer) at pH 8.0 consists of two signals of relative area 2 : 1, Fig. 20 [118]. The more intense signal (for Cd in the Zn sites) occurs at 165 ppm, whereas the shift of the Ca-site signal is −36 ppm. As might be expected, the latter signal is insensitive to changes in sample pH or the presence of added Cl^-. On the other hand, the signal for the Zn sites is somewhat sensitive to changes in pH and [Cl^-]. As the sample pH was raised, the Zn-site signal shifted downfield and leveled off at 201 ppm. This change was attributed to deprotonation of coordinated water [118]. Addition of NaCl produced a small downfield shift to 177 ppm for an NaCl concentration of 1.0 M. Addition of one equivalent of Ca to a Cd_3(Ins) sample at pH 8.0 resulted in a dramatic loss of signal intensity for the Ca site; conversely, addition of two equivalents of Zn or Co(III) to Cd_3(Ins) resulted in spectra where only the Ca-site signal was observed, Fig. 20.

Yeast inorganic pyrophosphatase (PPase)

Yeast inorganic pyrophosphatase consists of a dimer of identical subunits (M_r ca. 35,000 per subunit), with each subunit capable of binding four divalent metal ions. Inorganic phosphate (Pi) is required for enzymatic

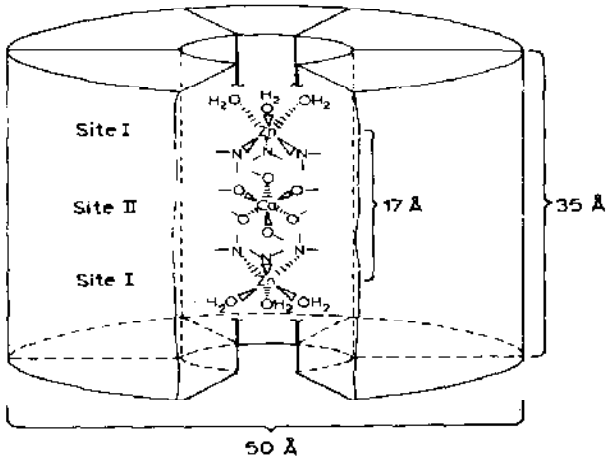

Fig. 19. Representation of the insulin hexamer showing the proposed Ca and Zn binding sites (ref. 118).

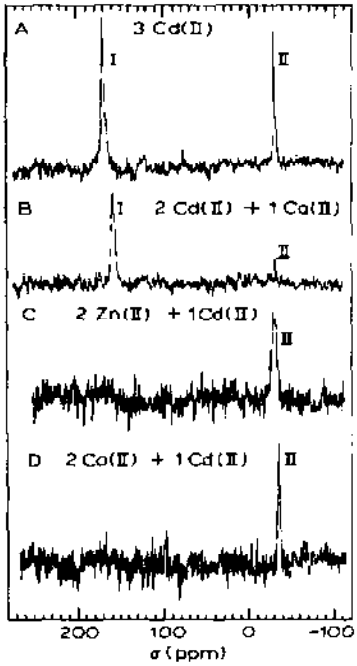

Fig. 20. (A) ^{113}Cd spectrum of a solution containing 2.6 mM insulin hexamer and 7.7 mM $CdSO_4$. (B) Sample conditions similar to (A) except for the addition of 2 equivalents of Ca. (C) Sample conditions similar to (A) except for the addition of 2 equivalents of Zn. (D) Spectrum of 2.7 mM insulin hexamer containing 1 equivalent of Cd and 2 equivalents of Co(III). From ref. 118.

activity. In initial ^{113}Cd NMR studies [119], tris-HCl buffer was employed and, as demonstrated later and described in detail in this review, Cl^- can sometimes profoundly influence ^{113}Cd chemical shifts. As such, comparison of the chemical shift values (Table 41) with those of other enzymes must be made with caution. The ^{113}Cd chemical shifts of the four resonances of Cd_8(PPase) (PPase represents the dimer) in the presence of excess Pi [120], in combination with ^{31}P NMR results indicated that two equivalents of Pi are bound by each subunit [120].

Osteocalcin (BGP)

Osteocalcin (mol.wt. 5,700), which binds Ca, is the only bone protein known to contain γ-carboxyglutamic acid (Gla) and is referred to as bone Gla protein (BGP). Tris-HCl buffer was utilized in ^{113}Cd NMR studies of Cd(BGP) [121] and, for the reasons mentioned above, interpretation of the ^{113}Cd chemical shifts is therefore difficult. A solution containing BGP with two equivalents of Cd gave a single, very broad resonance at ca. 20 ppm. A solution containing equimolar amounts of BGP, Cd, and Pi gave a narrower

resonance at ca. 0 ppm. It is noted here that, for model studies employing N-donor chelate ligands in DMSO-d_6, severe signal broadening can be induced by addition of Cl^- for some ligands. Thus, for osteocalcin, the presence of Cl^- may have not only affected the position of the Cd resonance observed, but the half-height width as well.

α-Lactalbumin (α-Lact)

α-Lactalbumins are Ca-binding proteins required for the biosynthesis of lactose in milk. Comparison of the ^{113}Cd chemical shift of the Cd-substituted protein (−79.5 to −80.5 ppm) with those of other proteins allowed the geometry and nature of the metal binding site to be determined [131]. Thus, the metal probably is probably bound by exclusively O-donor ligands.

Yeast Enolase (YE)

Native yeast enolase (M_r 93,000) is a dimeric enzyme which requires two equivalents of Mg per subunit for activity. Addition of Cd results in a single resonance at −30 to −43 ppm due to binding at the conformational site [132]. A broadening of the signal due to the catalytic site was attributed to rapid changes in the coordination geometry due to interconversion of substrate and product. The ^{113}Cd spectra under conditions of excess added Cd (which binds to an inhibitory site) were also examined [132].

Prothrombin fragment 1 and factor X

Bovine prothrombin fragment 1 is a cleavage fragment of prothrombin which binds Ca. Factor X, which also binds Ca, precedes prothrombin in the blood coagulation cascade. On addition of either $Cd(ClO_4)_2$ or $CdCl_2$ to fragment 1, a ^{113}Cd signal appeared at 10 ppm [133]. As the ratio of Cd : protein was raised above 4, new signals appeared between −5 to −25 ppm, and the shifts of these signals were dependent on the Cd salt employed. Similar results were obtained for factor X, which demonstrated that these proteins have similar high- and low-affinity binding sites [133].

Serine proteases

The Ca-binding sites of bovine trypsin, trypsinogen, chymotrypsin, and chymotrypsinogen have been examined [136]. Temperature and pH dependent chemical shift were observed for Cd-substituted chymotrypsin (0 ppm) and chymotrypsinogen (−10 ppm). Trypsin and trypsinogen gave sharper signals at −54.5 and −55.8 ppm, respectively, and these signals were insensitive to the presence of added inhibitors. X-ray structural studies revealed an octahedral coordination site for Ca comprising two carboxylates, two carbonyls, and two water molecules; the upfield ^{113}Cd chemical shifts observed are consistent with coordination exclusively by O-donor atoms.

Horseradish peroxidase (HRP)

Horseradish peroxidase is a heme enzyme, the activity of which is regulated by the binding of two equivalents of Ca. On addition of Cd to HRP, a ^{113}Cd NMR signal at -193 ppm was obtained due to the binding of Cd to a high-affinity site [137]. This unusually high-field resonance was attributed to Cd binding to an all-O-donor site where, perhaps, the overall anionic charge of the ligands was small. The second equivalent did not give rise to an NMR signal due to fast-exchange binding to a low-affinity site.

Phosphoglucomutase (PGM)

Phosphoglucomutase is a Mg-containing enzyme which catalyzes the interconversion of glucose-1-phosphate with glucose-6-phosphate. The downfield shift from 22 to 75 ppm on addition of glucose bisphosphate was attributed to replacement of one O donor by an N donor to Cd at some intermediate point in the catalytic process [138].

Phospholipase C (Pho C)

Phospholipase C is a monomeric enzyme (M_r 23,000) which contains two Zn binding sites. One site is thought to structurally stabilize the enzyme and the other site is probably involved in catalysis. When one equivalent of Cd was added to the apoenzyme, a signal at 85 ppm was observed resulting from Cd bound in the structural site [139]. Addition of one equivalent of Zn resulted in the replacement of Cd by Zn in the structural site, with the relocation of Cd to the catalytic site. The resulting spectrum displayed a single peak at ca. 115 ppm. Both signals were observed in the ^{113}Cd NMR spectrum of Cd_2(Pho C). The 85 ppm resonance was insensitive to changes in sample pH, temperature, and [I^-] [140]. The 115 ppm signal was only slightly sensitive to these changes and broadened with increasing temperature [140].

Alkaline phosphatase (AP)

The first report on the ^{113}Cd NMR of Cd-substituted alkaline phosphatase was published over a decade ago by Armitage, et al. [1]. Since then, numerous addition papers and reviews have appeared which have contributed significantly to the understanding of the structure and mechanistic features of this enzyme. Alkaline phosphatase consists of a dimer of identical subunits. Each subunit is capable of binding Cd in three different sites (A, B, and C). The A site contains three His ligands whereas the B site contains one His and two carboxyl groups and the C site contains three carboxyl and possibly one threonine (OH) ligand.

It would serve an injustice to attempt to summarize the detailed and complex ^{113}Cd results here. Interested readers are referred to the relevant

reviews [6,12–14] and to the original work [1,17,141–147], where ^{113}Cd NMR spectroscopy was used to monitor substrate binding effects, conformational equilibria, changes in binding site occupancy for systems with less than six equivalents of Cd, and anion and pH effects. As an example of the complexity of this system, consider the following. Cd_4(AP) (AP refers to the dimer) in 0.1M NaCl, pH 6.0, gives a very broad ^{113}Cd NMR signal at 170 ppm (due to Cd in the two A sites; the signal for Cd in the B sites is too broad to detect). When the pH is raised to 9.0, the A-site signal (now sharp) is observed at 143 ppm and a B-site signal is observed at 52 ppm. Addition of excess Pi results in a complex spectrum, where signals due to Cd_6(AP)–P (covalently linked Pi; $\delta = 150$ ppm (A), 68 ppm (B), 1.5 ppm (C)), Cd_6(AP) · P (noncovalently linked Pi; $\delta = 137$ ppm (A), 64 ppm (B), 1.5 ppm (C)), and Cd_2(AP)–P (Cd occupies the A and B sites of the same monomer while the binding sites of the other monomer are vacant; $\delta = 145$ ppm (A), 57 ppm (B)) are all observed simultaneously. Subsequent addition of two more equivalents of Cd resulted in the loss of signals due to the Cd_2(AP)–P species. Clearly, the ^{113}Cd chemical shifts for Cd-substituted AP are sensitive to the conformation of the enzyme. In addition, the chemical shifts of the A-site signals have been shown to be quite sensitive to added Cl^-, Fig. 21 [145].

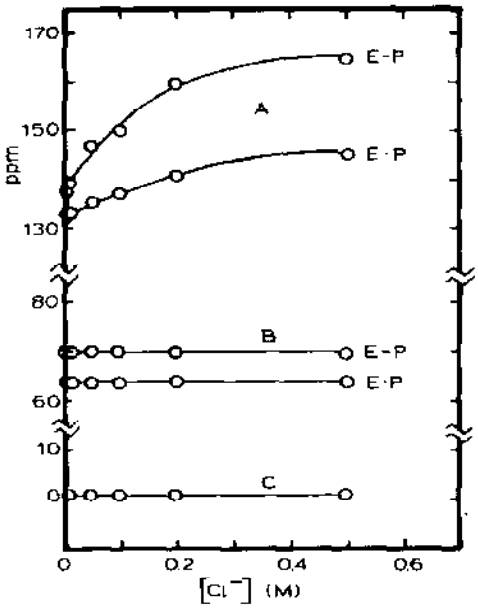

Fig. 21. Effect of chloride ion concentration of the ^{113}Cd chemical shifts for phosphorylated Cd_6(AP), pH 9. E·P and E–P refer to the non-covalently phosphorylated and covalently phosphorylated enzyme, respectively (ref. 145).

Bovine serum albumin (BSA)

Two signals were observed [148] for Cd_2(BSA) at 150 and 28 ppm. The chemical shifts were pH dependent in the range 5–7. Above pH 7, the shifts did not change. Titration with Cu or Zn resulted in displacement of Cd from the high-affinity (150 ppm) site. Based on the values of the chemical shifts, the high-affinity site was thought to contain two His ligands whereas the remaining site probably contains exclusively O-donor ligands.

Carbonic anhydrase (CA)

Carbonic anhydrases from human (HCA) and bovine (BCA) erythrocytes are monomeric proteins (M_r ca. 29,000), which contain a single Zn binding

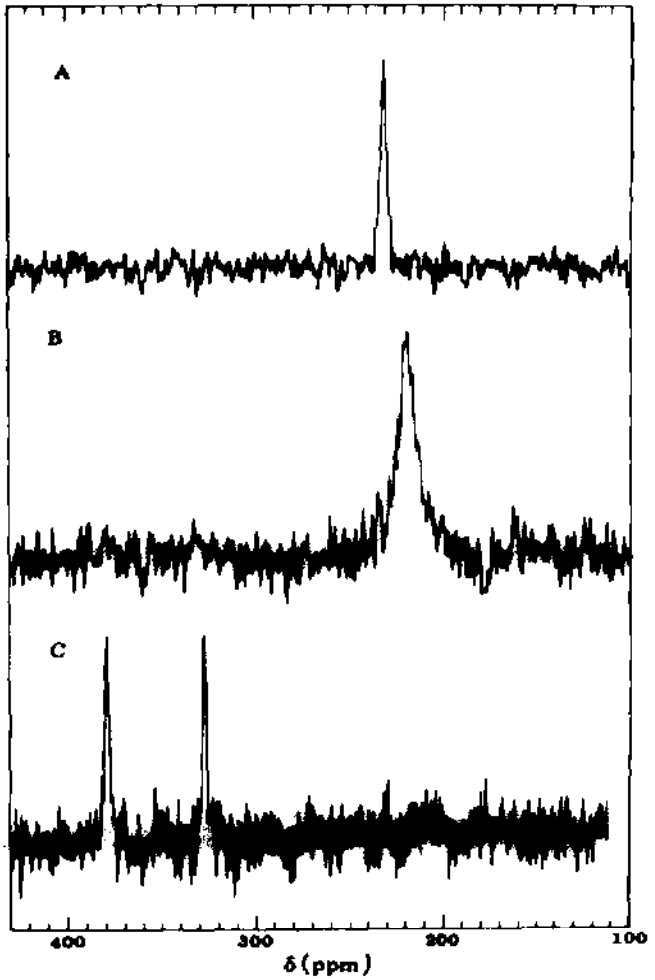

Fig. 22. ^{113}Cd NMR spectra of Cd-substituted human carbonic anhydrases. (A) Cd(HCAC); (B) Cd(HCAB); (C) Cd(HCAC) (3.0 mM) plus $Na^{13}CN$ (50 mM) (ref. 151).

site. In both the low-activity (HCAB) and high-activity (HCAC, BCA) isozymes, the Zn is bound by three His ligands and, presumably, water or hydroxide. In the original ^{113}Cd study of Cd(CA), it was noted that the chemical shifts were sensitive to the presence of halides and that changes in pH affected the ^{113}Cd NMR signals [1]. Later, chemical shift values for BCA (pH 8.0), HCAC (pH 8.1) and HCAB (pH 9.1–9.6) of 214, 225.7 and 145.5 were reported [17]. In a subsequent paper [149], HCAC and BCAB were reported to give ^{113}Cd signals at ca. 220 ppm for pH values between 5.5–10.0. HCAC either did not give an NMR signal, or gave an extremely broad signal over the same pH range and in the absence of anion inhibitors [149].

Sudmeier and Bell [150] reported that the ^{113}Cd chemical shifts for carbonic anhydrases were highly dependent on pH and HCO_3 concentration. In addition, they found that, on addition of ^{13}C-enriched KCN, an adduct was formed which gave a ^{113}Cd signal (doublet at 410 ppm, $^1J_{Cd-C} = 1060$ Hz) which was insensitive to changes in pH or anion concentration, Fig. 22. The ^{113}Cd shift dependence on pH and $[HCO_3^-]$ was carefully examined, and from a least squares fitting the chemical shift values for the OH^-, H_2O, and HCO_3^- adducts of Cd-substituted HCAC, HCAB, and BCA were determined [151].

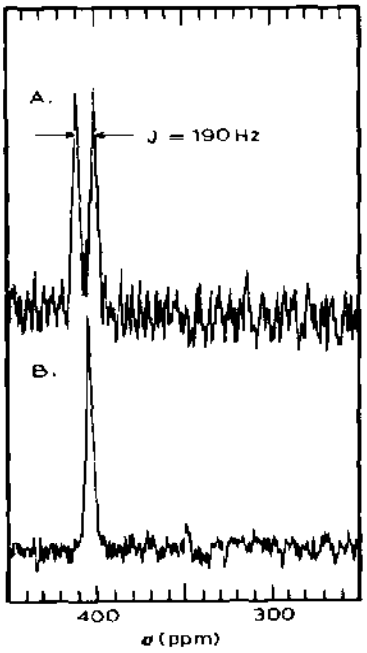

Fig. 23. ^{113}Cd NMR spectra of (A) 3.7×10^{-3} M BCA plus 1 equivalent of ^{15}N-labeled Neoprontosil, pH 8.9; (B) 5.3×10^{-3} M BCA plus 1 equivalent of unlabeled Neoprontosil, pH 9.1. From ref. 152.

Cd(CA) adducts with ^{15}N-labeled sulfonamide inhibitors also gave ^{113}Cd signals which were insensitive to changes in pH and halide concentration and displayed $^{113}Cd-^{15}N$ scalar coupling, Fig. 23 [152]. ^{15}N-Labeled 4-fluoro-*N*-hydroxybenzenesulfonamide coordinated to Cd in ^{111}Cd-substituted CA [153]. A ^{111}Cd chemical shift of -275 ppm (relative to dimethylcadmium) and a $^{111}Cd-^{15}N$ coupling constant of 249 Hz were reported [152].

Carboxypeptidase A (CPA)

Carboxypeptidase A, which binds a single equivalent of Zn, catalyzes the hydrolysis of peptides and esters. X-Ray structural studies have shown that the Zn is bound by two His residues, one Glu, and a molecule of water. Structural studies of inhibitor complexes revealed that the inhibitors displace the coordinated water and bind directly to the metal. At room temperature, Cd-substituted CPA does not display a ^{113}Cd signal due to rapid chemical exchange [17,154]. At reduced temperatures and with high NaCl concentrations, a single resonance was observed at 120 ppm [154]. At 298 K, and in the presence of O-donor inhibitors, single resonances were observed between 127–137 ppm. On the other hand, the coordination of the S-donor inhibitors thioglycolic acid and thiolactic acid resulted in ^{113}Cd NMR signals in the range 339–355 ppm [154].

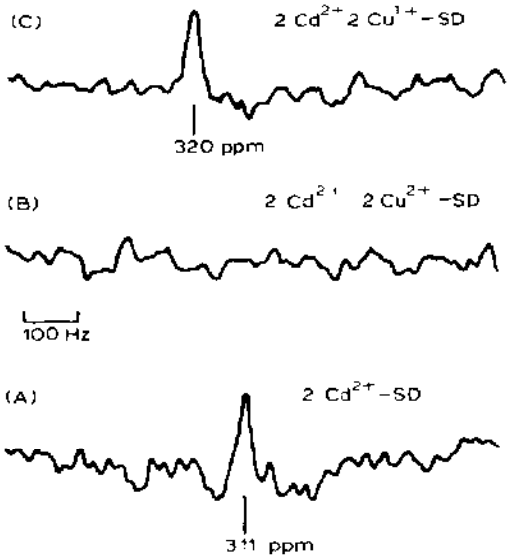

Fig. 24. ^{113}Cd NMR spectra of Cd-substituted superoxide dismutase. (A) $Cd_2(SD)$, with Cd in the equivalent Zn sites; (B) $Cd_2Cu(II)_2(SD)$, (no signals are observed due to line broadening effects of paramagnetic Cu(II)); (C) $Cd_2Cu(I)_2(SD)$. From ref. 18.

Superoxide dismutase (SD)

Superoxide dismutase from bovine erythrocytes has a molecular weight of ca. 32,000 and comprises two identical subunits. Each identical subunit binds one equivalent each of Zn and Cu. X-Ray crystallographic studies have revealed that the Zn and Cu atoms are ca. 6–7 Å apart, and that they are bridged by an anionic imidazole (for the Cu(II) form). Both Armitage et al. [17] and Bailey et al. [18] found that the Cd-substituted derivative of this form of the enzyme (where Cd occupies the Zn sites) gives no detectable signals in the ^{113}Cd NMR spectrum. This is most likely due to relaxation effects of the nearby, paramagnetic Cu(II). Armitage et al. [17] reported that Cd_2(SD), with vacant Cu sites, gave a ^{113}Cd spectrum with a single resonance at 170 ppm. Addition of Cu(II), with subsequent reduction, gave $Cd_2Cu(I)_2$(SD) which displayed a broad ^{113}Cd NMR signal at 9 ppm. In contrast, Bailey et al. [18] later reported shifts of 311 and 320 ppm for Cd_2(SD) and $Cd_2Cu(I)_2$(SD), respectively (see Fig. 24), and it was suggested that the presence of EDTA in the enzyme preparations may have led to erroneous results in the earlier work.

5-Aminolevulinic acid dehydratase (ALAD)

ALAD has a molecular weight of 280,000 Daltons and comprises eight subunits (ca. 35,000 Daltons each). Zn is known to enhance the activity of the enzyme. X-Ray crystallographic data are not available for this enzyme, and little is known about the nature of the metal binding sites. Although initial studies indicated that Cd-substituted ALAD gives rise to a sharp NMR signal [155], subsequent studies revealed that the signal observed was due to Cd bound to EDTA impurities [195].

Horse liver alcohol dehydrogenase (LADH)

LADH is a dimeric enzyme with two distinct Zn binding sites in each subunit. One Zn serves a structural role while the other may be involved in catalysis. The ^{113}Cd NMR signal for the noncatalytic site occurs at 750 ($\pm$2) ppm and this shift is independent of pH or added substrates [156,157]. The shift of the catalytic site signal, 484 ppm, is also independent of pH, except for pH values greater than ca. 10. On the other hand, the shift of the catalytic site signal is very sensitive to the presence of the coenzymes NAD^+ and NADH and also to substrates. A shift of 442 ($\pm$1) ppm was observed for both NAD^+ and NADH complexes with LADH, and this shift was independent of pH for values between 7.5 and 10.3. This upfield shift of 42 ppm was consistent with a conformational change of the enzyme induced by NAD^+ or NADH binding, and not to direct ligation of these coenzymes to Cd. Even more interesting is that this signal shifts back downfield by 75 ppm (to 518 ppm) on addition of the substrates trifluoroethanol or pyrazole

to LADH–NAD^+. The shift of the signal for the trifluoroethanol complex was independent of pH for values between 7–10. From these data, the authors concluded that the substrate analogues do not bind directly to Cd, and that the downfield shifts may result from deprotonation of one of the coordinated water molecules [157].

Metallothionein (MT)

Metallothioneins are relatively small proteins (M_r ca. 6,800) which are involved in metal detoxification and metabolism. Of the ca. 60 amino acids which make up MT, 20 are cysteines and there are no histidine residues present. For mammalian MT, two isozymes (MT-1 and MT-2) are present. Zn, Cd, and Cu(I) are the metals commonly found in native MT, with the proportion of each metal dependent on the origin of the protein. Metallothioneins typically contain 6–9 equivalents of metals. Review articles have appeared which deal with the ^{113}Cd NMR spectral properties of Cd-substituted metallothioneins, and the reader is referred to this literature [5,6,15] and to the actual work [158–179] for a more detailed presentation. Some of the major points are summarized below.

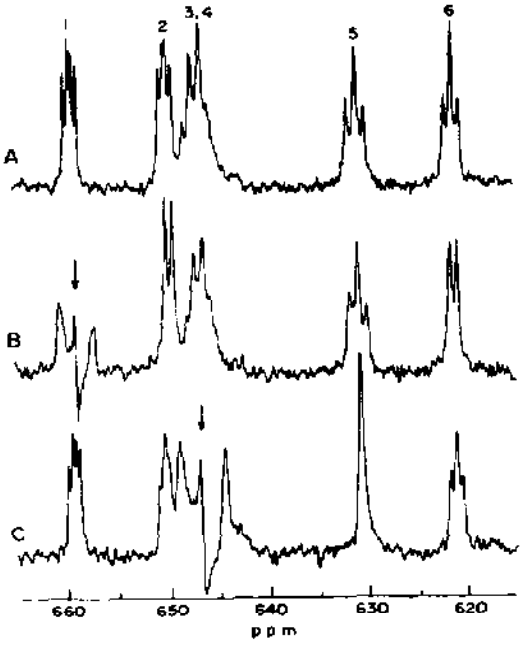

Fig. 25. (A) Proton-decoupled ^{113}Cd NMR spectrum of Cd-substituted crab MT-1. (B) and (C), as in (A) but with selective homonuclear decoupling at frequencies indicated by the arrows (ref. 162).

The first reports on ^{113}Cd-substituted MT appeared in 1978; Suzuki and Maitani [158] examined rabbit liver MT and Sadler et al. [159] examined rat liver MT. In these cases, ^{113}Cd-enriched MT samples were isolated after induction in vivo by administration of $^{113}CdCl_2$. Multiple signals were observed in the chemical shift range 550–700 ppm. The ^{113}Cd spectrum of rabbit liver MT-2 exhibited extensive ^{113}Cd–^{113}Cd scalar couplings [160]. Selective homonuclear ^{113}Cd decoupling experiments were used to determine that rabbit liver MT-2 contains two separate metal clusters, one cluster which contains four metals and another which contains three metals [160,161]. In this regard, all mammalian metallothioneins are similar. Based on the downfield chemical shifts and homonuclear scalar interactions, it was concluded that the Cd atoms are bridged by cysteine thiolate groups. These findings were corroborated by X-ray crystallographic studies on Cd,Zn rat liver MT-2 [190].

Metallothionein from human liver, calf liver, rat liver, and crab have also been examined using ^{113}Cd NMR spectroscopy. Crab MT binds six metal atoms, three each in two distinct metal clusters [162,164]. Homogeneous Cd-substituted MT-1 and MT-2 were obtained [162] and their ^{113}Cd spectra analyzed using homonuclear ^{113}Cd–^{113}Cd decoupling techniques, Fig. 25. From these data, the ^{113}Cd signals were assigned to specific clusters as shown in Fig. 26. Interestingly, native calf liver MT was found to contain Zn and Cu, and in vitro exchange with Cd results in the selective replacement of the Zn atoms only [166].

The isolated MT samples generally contained an inhomogeneous mixture of metals (usually Zn or Cu and Cd) which made analysis of the ^{113}Cd NMR spectra more difficult. In vitro methods for preparing MT containing only Cd have been described [167,172–174], and the effects of pH, temperature, and ionic strength on the ^{113}Cd spectra have been studied [173]. The presence of more than the seven expected Cd signals was originally interpreted as resulting from multiple configurational substates; later, however, it was shown that the extra signals probably result from polymers formed during the preparation of Cd_7(MT) [174]. The preparation of pure Cd_7(MT) enabled detailed analyses of the metal binding sites and geometries, and models of the Cd clusters have been presented; e.g. see refs. 171, 176, 177. In relation to this, ^{1}H–^{113}Cd heteronuclear multiple quantum coherence (HMQC), ^{113}Cd–^{113}Cd correlation spectroscopy (COSY), and other two-dimensional (2D) NMR methods have been applied (vide infra). ^{113}Cd NMR was also recently used to monitor the displacement of Cd in rat liver MT using mercuribenzoate [175]. The finding that native Zn,Cd cluster compositions could be obtained by simply mixing equimolar amounts of Cd_7(hepatic-MT) and Zn_7(hepatic-MT) enabled Otvos and co-workers [172] to develop an explanation for the observed in vivo response of hepatic Zn

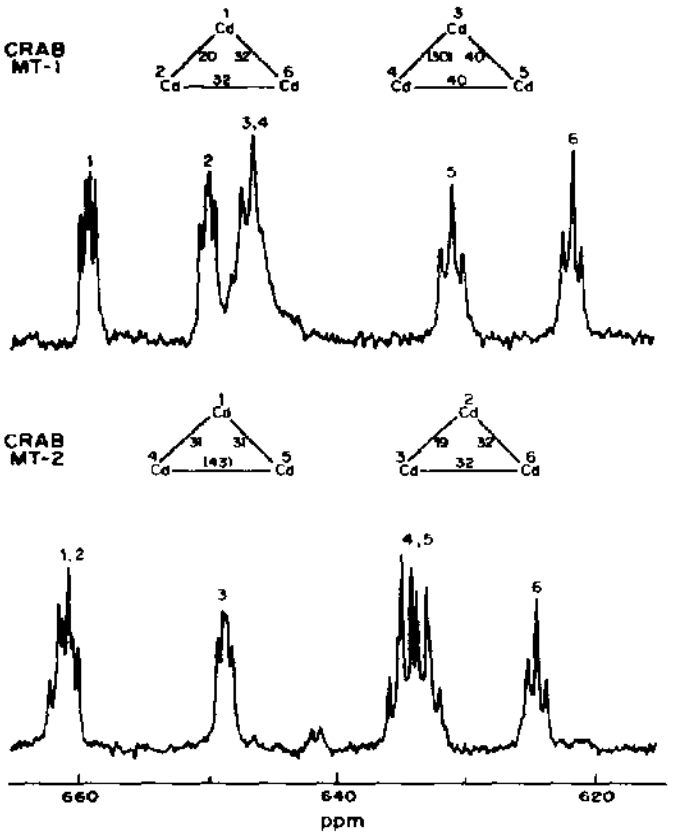

Fig. 26. Comparison of the proton-decoupled ^{113}Cd NMR spectra and corresponding cluster structures (represented schematically) for crab MT-1 and MT-2 (ref. 162).

and metallothionein levels to Cd administration. ^{113}Cd NMR chemical shift data for crab and rabbit liver metallothioneins are summarized in Table 41. ^{113}Cd NMR spectra for metallothioneins from plaice and *Cancer paqurus* have also been published [178].

Blue copper proteins

^{113}Cd spectra of the Cu proteins plastocyanin (*Spinacea*), stellacyanin (*Rhus vernicifera*), and two azurins (*Pseudomonas aeruginosa* and *Alcaligenes faecalis*) have been examined [180]. X-Ray structural studies on plastocyanin and azurin revealed that these proteins have similar metal coordination sites, where two histidines, one cysteine and one methionine provide N, S^-, and S donor atoms, respectively, in a distorted tetrahedron. Although X-ray data are not available for stellacyanin, spectroscopic results indicate that two N and one S^- donors are present; however, the absence of methionine had led to speculation that the fourth ligand may be a second S^-, a peptide N, or a disulfide group.

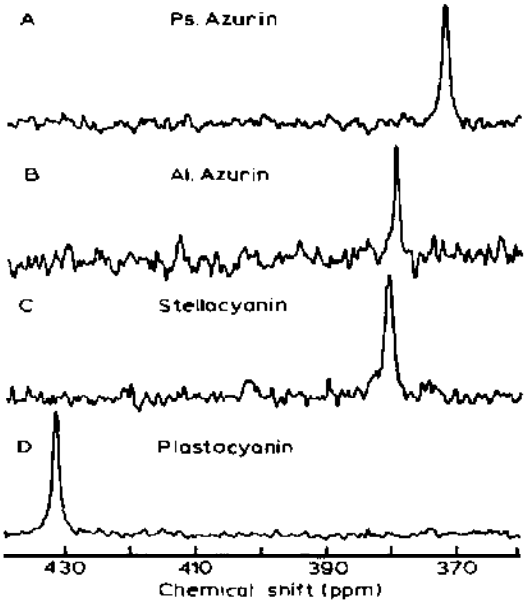

Fig. 27. Proton-decoupled ^{113}Cd NMR spectra of Cd-substituted blue copper proteins (ref. 180).

^{113}Cd NMR chemical shifts of 372, 379, 380 and 432 ppm were observed for *Pseudomonas* azurin, *Alcaligenes* azurin, stellacyanin, and *Spinacea* plastocyanin, Fig. 27. Since the shifts for the azurins and stellacyanin were nearly identical, it was concluded that the binding sites of these proteins must be highly similar, even though stellacyanin lacks a methionine [180]. Studies on model compounds [59] in combination with HMQC data for the copper proteins [181] indicate that methionine is not coordinated to Cd in the azurins but probably is coordinated to Cd in plastocyanin.

D. COMPARISON BETWEEN SOLID- AND SOLUTION-STATE CHEMICAL SHIFTS

(i) Coordination compounds

In addition to comparing solid- and solution-state chemical shifts, trends between chemical shifts and structural parameters (where they exist) will be pointed out.

Complexes with halides

Average solid-state chemical shifts of 474 ppm (Cl), 386 ppm (Br), and 86 ppm (I) for CdX_4 compounds have been calculated here using the data in Tables 1 and 2. For comparison, ^{113}Cd chemical shifts of 438 ppm (Cl), 350 ppm (Br), and 62 ppm (I) were observed using CH_2Cl_2 solutions at $-80\,^{\circ}C$

[57]; 474–495 ppm (Cl), 365–399 ppm (Br), and 70–75 ppm (I) shifts were derived from least-squares analyses of room temperature, aqueous solution data [53,54]; 442 ppm (Cl), 351 ppm (Br), and 44 ppm (I) shifts were derived from least-squares analyses of room-temperature, DMSO-d_6 solution data [53]; and a chemical shift of 101 ppm was observed for CdI_4 in an emulsion at $-80\,^{\circ}C$ [55]. Thus, the solid- and solution-state ^{113}Cd chemical shifts of CdX_4 complexes (tetrahedral in the solid-state) are in reasonably good agreement.

Complexes with N-donor ligands

Nearly identical ^{113}Cd chemical shifts have been obtained for CdL_3 complexes (L = phen, bipy, and their derivatives) in the solid- and solution-states (see Fig. 2) [39]. Note that the chemical shift values (243–267 ppm, except for the sterically hindered 2,9-Me_2phen complex) are much further downfield than expected (136 ppm, eqn. (8)) [70]. Binding of 1, 2, 3, and 4 equivalents of 4-Mepy to Cd in EtOH at $-90\,^{\circ}C$ results in downfield shifts from -21 ppm (for free Cd) to 11, 42, 72, and 101 ppm, respectively [39]. These shift changes of 32–29 ppm on sequential 4-Mepy binding are fully consistent with the expected 31 ppm shift [70]. Six distinct ^{113}Cd signals were observed for $Cd(imid)_n$ ($n = 1$–6) complexes in similar low-temperature binding studies [39]. For $n = 1$–6, downfield shifts induced by imid binding of 52, 47, 46, 42, 34, and 30 ppm, respectively, were observed; thus the average shift induced by imid binding, 42 ppm, agrees exactly with the value determined from ambient temperature, Me_2SO solution data [59]. As noted by Munakata et al. [39], the results suggest that no pronounced shifts occur due to geometric changes from tetrahedral to octahedral. The shift observed for $Cd(imid)_6$ in EtOH at $-90\,^{\circ}C$ (231 ppm) [39] is in excellent agreement with the solid-state shifts of 238 ppm for $Cd(imid)_6(NO_3)_2$ [22] and 230 ppm for $Cd(Meimid)_6(NO_3)_2$ [38]. In MeOH at ambient temperature, the $Cd(Meimid)_6(NO_3)_2$ complex gave a ^{113}Cd signal at 162 ppm (Table 5, ref. 38), and this upfield shift is probably due to fast exchange between complexes with less than six coordinated Meimid ligands.

Solid state ^{113}Cd chemical shifts of 380 and 361 ppm have been reported for $Cd(en)_3Cl_2 \cdot H_2O$ (refs. 22 and 39, respectively). The chemical shifts obtained for $Cd(en)_3$ complexes with a variety of counterions and in a wide range of solvents were in the range 346–353 ppm [39], and it appears that these complexes also have similar structures in the solution- and solid-states.

The isotropic solid-state chemical shift for $Cd(gly)_2 \cdot H_2O$ (112–113 ppm) [43] is in rather poor agreement with the shift of 154 ppm observed at $-40\,^{\circ}C$ for $Cd(gly)_2$ in supercooled aqueous solution [98,99]. Equation (10) gives a calculated shift value of 150 ppm. A solution-state shift of 54 ppm was observed for Cd(gly) [98,99] and the calculated shift is 75 ppm. A

solution containing a 10-fold excess of glycine gave a signal at 263 ppm which was assigned to $Cd(gly)_3$ [99]; here, agreement with the calculated shift (225 ppm) is fair at best.

Solid-state ^{113}Cd NMR signals in the range 97–117 ppm have been observed for $Na_2Cd(EDTA)$ [22]. A shift of ca. 86 ppm was observed for the complex in aqueous solution at pH 9 [66], and the calculated shift (eqn. (10)) is 62 ppm.

Amma and co-workers have systematically examined the solid- and solution-state spectra of numerous Cd compounds as summarized in Table 5. Except for the bipy complexes containing NO_3 anions, signals from the solution-state work given in Table 5 are always upfield from signals observed in the solid. The 72 ppm downfield shift observed when one NO_3 is replaced by H_2O in $Cd(bipy)_2(NO_3)_2$ [29,33] demonstrates the influence that O-donor ligands can have on the ^{113}Cd chemical shifts of solids.

Cd(TPP) gave a solid-state ^{113}Cd signal at 399 ppm but a solution-state spectrum could not be obtained due to insolubility [26]. The py adduct, Cd(TPP)py gave solid- and solution-state chemical shifts of 432 and 427 ppm, respectively [26], and the downfield shift of 33 ppm due to py binding is in excellent agreement with the predicted downfield shift change of 31 ppm [59]. Addition of py to $Cd[N(SiMe_3)_2]_2$ resulted in a downfield shift of 37–43 ppm (depending on the solvent) [72], which is also not far from the expected shift (31 ppm).

Porphyrins contain two neutral and two anionic N-donor atoms. Interestingly, the shift for Cd(TPP) (399 ppm) can be calculated reasonably using the data for dialkylamido compounds. Addition of 62 ppm (31 ppm per neutral N donor) to the shift for $Cd[N(C_9H_{18})_2]_2$ (362 ppm, Table 19) gives a value of 424 ppm for the calculated shift of Cd(TPP), which differs from the observed value by ca. 6%. Although additive ^{113}Cd chemical shift relationships have been found for compounds containing neutral N-donor ligands [59,70], and linear relationships between ^{113}Cd shift and n in $Cd(SPh)_n(SePh)_{4-n}$ complexes have been observed [77], the influence of N^- ligands on ^{113}Cd chemical shifts in CdL_n as a function of n has not been systematically investigated.

Complexes with S-donor ligands

Bis-(n-butylxanthate) and bis-ethylxanthate Cd complexes with Cd bound by 4 S-donor atoms in a tetrahedral geometry give solid-state ^{113}Cd signals at ca. 442 and 412 ppm, respectively (Tables 1 and 2) [22]. Shifts to much lower field (623–705 ppm) have been observed for Cd in the C site (tetrahedral, 4 S-donor atoms) of $Cd_{10}(SCH_2CH_2OH)^{4+}$ salts (Table 3) [25], and these shifts compare more favorably to those observed in solution for tetrahedral $Cd(SR)_4$ complexes (672, 590, 577, 590, 683, and 654 ppm for

$Cd(SBz)_4$, $Cd(SPh)_4$, $Cd(SPPh)_4$, $Cd(SPChx)_4$, $Cd(SMe)_4$, and $Cd(S\text{-}iPr)_4$, respectively; see Tables 23, 25 and 31 for sample conditions) [75,77,81].

There have been relatively few other solid-state ^{113}Cd NMR studies of coordination compounds which contain S-donor atoms. The CP/MAS spectrum of $Cd(N,N'\text{-dimethylthiourea})_4$ contained too many lines (due to the highly asymmetric, distorted geometry about Cd) to allow its analysis [30]. An isotropic shift of 98 ppm for $Cd(TMTU)_2(NO_3)_2$ (2 S-, 4 O-donor atoms) was reported [43], but no solution NMR data have been published. A solid-state shift of 263 ppm was reported by Amma and co-workers [31] for what appears to be the same compound.

(ii) Proteins

Solid-state shifts for the Cd-substituted proteins parvalbumin and concanavalin A were in good agreement with the solution-state shifts [5,49]. The solution-state shifts for the binding sites of these proteins were independent of pH and chloride ion concentration, and it is therefore probably not surprising that the solution shifts were virtually the same as the shifts in the solid. The solution- and solid-state shifts for Cd-substituted metallothionein were also in agreement, although the solid-state CP/MAS signal was extremely broad [48].

E. ^{113}Cd CHEMICAL SHIFTS FOR STRUCTURAL ANALYSES OF PROTEINS

A quantitative relationship between the ^{113}Cd chemical shift and structural features of metal binding sites in proteins, including ligand type and number, geometry, bond lengths, etc., has yet to be established. It was hoped that such a shift–structure relationship could be developed once a suitable number of compounds had been examined [6], and that this relationship could be used to predict coordination environments in proteins and the changes which occur during catalysis. General trends in ^{113}Cd chemical shifts have been helpful for studies of metal coordination environments in metalloproteins, where binding sites comprising exclusively O-donor ligands generally give ^{113}Cd signals in the range $+40$ to -180 ppm, sites with one to three N donors give shifts in the range 40 to ca. 300 ppm, and sites with S donors give signals with shifts from ca. 400 to 800 ppm. In general, coordination compounds can also be grouped in this manner.

Some attempts have been made to apply a more quantitative shift–structure relationship and this work is described below. In addition, an attempt will be made in this section to rationalize the shifts obtained for many of the Cd-substituted proteins in the light of recently published data on coordination compounds. Binding sites will be grouped according to the type of donor atoms present (O, N, or S).

(i) Sites with O-donor ligands

Morishima et al. [137] compared the ^{113}Cd chemical shifts and binding site data for a series of structurally (X-ray) characterized proteins and found that sites with less anionic character, e.g. more carbonyl or H_2O donors and less COO^- donors, gave ^{113}Cd signals to higher field. This is an interesting correlation which is opposite to what might be expected based on the concentration dependence of shifts for Cd salts with O-donor ligands [51]. For example, as mentioned above, the shift of all Cd salts with O-donor ligands at infinite dilution in H_2O is 0.0 ppm. Increasing the total concentration, or addition of oxoanions, results in upfield shifts of the Cd resonance. In DMSO (which coordinates to Cd via the O atom) and acetone, similar effects are observed [51], and for coordination compounds in solution, increasing the amount of coordinated oxoanions relative to neutral O-donor solvent molecules results in an upfield shifting of the ^{113}Cd resonance.

From the wide range of oxo-Cd compounds examined in the solid state, Ellis [2] found a general pattern between ^{113}Cd chemical shifts and the coordination number, where compounds with 6-coordinate Cd give shifts in the range 150 to -60 ppm whereas 7- and 8-coordinate Cd compounds give shifts in the range 0 to -60 ppm and 0 to -100 ppm, respectively [2]. No compounds containing exclusively O-donor ligands have been found which give shifts as high as -155 ppm or -193 ppm as observed for ICaBP and HRP, respectively.

Ellis and co-workers [43] also pointed out that the isotropic shifts of the Cd-oxo compounds examined to date are not sufficiently discriminating to allow structure–shift correlations. However, as described in the solid-state section (vide supra), correlations between structural features and principal shielding tensor parameters have been made [41–43].

(ii) Sites with N-donor ligands

Summers et al. [59] analyzed the shifts of some Cd-substituted metalloproteins using shift results derived from studies with coordination compounds. Shifts for the A and B sites of Cd-substituted AP, Cd(HCAC)CN, Cd(HCAC)SH, Cd(azurine), and Cd(plastocyanin) were consistent with shifts predicted using eqn. (10), and it was suggested that discrepancies in the literature for Cd-substituted SD could have resulted from Cl^- binding to Cd [59]. In the remainder of this section, the ^{113}Cd chemical shift data for the rest of the Cd-metalloprotein binding sites containing N-donor ligands, including adducts with substrates, inhibitors, etc., will be examined in terms of their compatibility with eqn. (10). Discussions will be limited to enzymes for which X-ray structural information is available.

Alkaline phosphatase

The shift for Cd in the A site of Cd_2(AP) in the absence of Cl^- (117–120 ppm) is in good agreement with the calculated shift of 126 ppm [59]. In the E · P form of the enzyme, phosphate is coordinated to the A-site Cd, and in the absence of Cl^-, a signal for this site was observed at ca. 133 ppm [145]; again this shift is in good agreement with Cd bound by 3 His ligands (Δ% (the percent error between the observed and calculated shifts) = 5%). In the E–P form, where phosphate is no longer coordinated to Cd, a shift of ca. 137 ppm was observed in the absence of Cl^- [145] and Δ% = 9%. The average shift of 129 ppm agrees almost perfectly with the calculated value of 126 ppm.

Cd in the B site of AP gives shifts of 52 ppm (Cd_2(AP)), 55 ppm (Cd_2(AP)Pi), 71 ppm (Cd_2(AP)As), 52 ppm (Cd_4(AP)), 64 ppm (Cd_6(AP) · Pi_2), 69 ppm (Cd_6(AP)–Pi_2), 81 ppm (Cd_6(AP) · As_2), and 90 ppm (Cd_6(AP)–As_2) (see Table 41). Shifts of the B site signals are unaffected by the presence of Cl^- [145]. It is clear that As binding produces shifts to much lower field than does Pi binding, and shifts obtained in the absence of Pi or As compare more favorably with the calculated shift value of 42 ppm. Since sites with O-donor ligands give a wide range of shifts (over 200 ppm), the correlation between observed and calculated shifts is poorer for sites with only one or two N donors and many O-donor ligands [59].

Carbonic anhydrases

In the absence of tightly binding inhibitors, all of the carbonic anhydrases give signals with pH- and [Cl^-]-dependent chemical shifts and, under these conditions, eqn. (10) fails. However, when CN^- or SH^- binds to Cd in Cd(HCAC), slow-exchange signals observed at 354 (^1J(Cd–C) = 1040 Hz) and 374 ppm (Table 41) are in excellent agreement with calculated shift values of 336 and 381 ppm, respectively. The CN adduct of Cd(BCA), which has a binding site nearly identical with that of HCAC, also gave a shift of 354 ppm (^1J(Cd–C) = 1040 Hz) which is in excellent agreement with the calculated value. The binding of the inhibitor ^{15}N-benzenesulfonamide (BS) to Cd(HCA) and Cd(BCA) resulted in ^{113}Cd signals at 390 (^1J(Cd–N) = 190 Hz) and 387 ppm (^1J(Cd–N) = 190 Hz), respectively (Table 41), and from this shift it appears that BS has a deshielding influence of ca. 290 ppm when a single molecule of BS binds to Cd.

HCAB, the low-activity form of HCA, has a somewhat different catalytic site. X-Ray structural studies of the native Zn enzyme revealed metal ligation to three His and a water molecule, similar to HCAC and BCA; however, residues Asn 67 and Thr 200 in HCAC are replaced by His 67 and His 200, respectively, in HCAB [188]. The ligand geometries of Zn(HCAC) and Zn(HCAB) are also somewhat different [151,152]. The shift of the ^{113}Cd

signal for Cd(HCAB)CN (411 ppm) is 57 ppm further downfield than observed for the high-activity enzymes (Table 41). In contrast, the signal for the BS adduct (355 ppm; ^1J(Cd–N) = 210 Hz) is ca. 34 ppm to higher field than observed for the HCAC and BCA enzymes. It is unclear at this time whether or not these anomalous results are due exclusively to differences in Cd coordination geometry.

Concanavalin A

The S1 site of Con A gives ^{113}Cd shifts in the range 32–46 ppm, and the shifts are not influenced by Cl^- [104]. The binding site contains one His, three COO, and two H_2O ligands, and the predicted shift of 42 ppm is in excellent agreement with the observed shifts.

Insulin

The Zn site of Ins gave a shift of 165 ppm under the conditions given in Table 41 [118]. Here, the shift was dependent on sample pH and the presence of Cl^-; thus, eqn. (10) cannot be employed. In a future experiment, it would be interesting to see if $^{13}CN^-$ binding would give a signal in which the shift is independent of pH and [Cl^-] as was found for carbonic anhydrase [150,151]. In this case, it should be possible to accurately predict the shift with eqn. (10), which accounts for the influence of CN^-.

Carboxypeptidase A

^{113}Cd spectra for Cd(CPA) were obtained in the presence of Cl^- [154] and the observed shift (120 ppm; data obtained using 1.0 M NaCl solutions) does not agree with the calculated value of 84 ppm. On the other hand, adducts with the tightly-binding S-donor inhibitors thioglycolic acid and D,L-thiolactic acid give shift values of 355 and 350, 339 ppm, respectively [154]. The 355 and 350 ppm shifts agree nicely with the calculated shift of 369 ppm ($\Delta\%$ = 4–5%); the 339 ppm shift for one of the isomers of thiolactic acid does not agree as well, which probably reflects a reduced ability of this isomer to coordinate to Cd in the enzyme pocket.

(iii) Sites with S-donor ligands

Good agreement was found between the observed and calculated ^{113}Cd chemical shifts for the blue copper proteins *Pseudomonas* azurin, *Alcaligenes* azurin, and stellacyanin [59]. The observed shift of *Spinacea* plastocyanin was further downfield than expected and implied that a Met sulfur was bound to Cd in this protein, and this finding was consistent with HMQC studies [59,181].

Cd in the structural site of LADH is bound by four Cys ligands in a tetrahedral geometry, and the observed shift (750 ppm) is insensitive to changes in pH or the binding of substrates [157]. For comparison, a shift of 683 ppm was observed for the tetrahedral $Cd(SMe)_4$ compound in MeOH at 193 K [75] and, for an aqueous solution at 308 K containing a 12-fold excess of MeSH, a signal was observed at 663 ppm [75]. Cd in the catalytic site of LADH gives an NMR signal with a shift that is significantly influenced by protein conformational changes induced by substrate and coenzyme binding. Currently, no model complexes of this type of site, which contains two Cys and one His donors, have been examined using ^{113}Cd NMR spectroscopy.

Cd cluster complexes containing S-donor ligands give shifts in the general region found for Cd-substituted metallothioneins [85–92]; in addition, some compounds give values for Cd–Cd couplings (Cd–S–Cd) similar to those observed in the proteins [86]. However, ^{113}Cd NMR chemical shifts obtained using models have not been used in a predictive manner to establish the coordination environment of the 6 or 7 Cd atoms in metallothionein, although studies with Zn–Cd derivatives have shown that neighboring metal atoms in Cd–MT and models can influence ^{113}Cd chemical shifts [87,90].

F. APPLICATION OF TWO-DIMENSIONAL NMR METHODS

Two dimensional (2D) $^{1}H-^{113}Cd$ heteronuclear multiple quantum coherence (HMQC) NMR spectroscopy is a powerful tool which can provide unambiguous information on the nature of Cd–L bonding and the identity of ligands coordinated to Cd. The method relies on $^{1}H-^{113}Cd$ scalar coupling (J), which must be maintained for a time period of the order of the reciprocal of the coupling constant ($1/J$). Very weak, long-range couplings between imidazole (H-2) or cysteine (CH_2S) protons and Cd are sufficient to give an HMQC correlation spectrum. Although rapid ligand exchange rates can preclude the detection of an HMQC correlation, the presence of an HMQC correlation provides unambiguous evidence for bonding between a particular ligand and Cd.

A total of four papers appeared in 1985 which demonstrated the applicability and utility of $^{1}H-^{113}Cd$ HMQC spectroscopy. Live et al. [182] obtained a 2D spectrum of ^{113}Cd-enriched Cd(EDTA) using a total acquisition time of ca. 3 min. A 2D $^{1}H-^{113}Cd$ HMQC spectrum of $^{113}Cd_6$(crab metallothionein) (3 mM) required 10 h of data accumulation [182]. Otvos et al. [183] published $^{1}H-^{113}Cd$ HMQC results for Cd_7(rabbit-liver metallothionein). Here, it was found that HMQC correlation peaks were sometimes missing (due to transverse relaxation and/or small coupling constants),

but could be detected by using several different delay periods in the pulse sequence (Δ, see ref. 183).

A more detailed study of Cd-substituted rabbit liver metallothionein was published by Wagner and co-workers [184]. A $^{1}H-^{113}Cd$ HMQC spectrum is shown in Fig. 28. Of the 20 Cys residues, 12 gave an HMQC correlation with a single ^{113}Cd resonance; in addition, the 8 remaining Cys residues gave HMQC correlations with 2 Cd signals, thus assigning these as bridging Cys residues. A 2D $^{113}Cd-^{113}Cd$ COSY spectrum (Fig. 29) allowed the homonuclear coupling pattern to be determined, which immediately allowed assignment of the Cd signals to two independent Cd-clusters as shown in Fig. 30. Heteronuclear $^{1}H-^{113}Cd$ coupling constants were determined by comparison of the ^{1}H-COSY data obtained using ^{113}Cd–MT and ^{112}Cd–MT; coupling constant values ranged from ≤ 5 Hz to 80 Hz. By combining these heteronuclear correlation data with ^{1}H NMR assignments, the topology and locations of the Cd–S clusters relative to the polypeptide structure were determined [176,177].

$^{1}H-^{113}Cd$ HMQC spectroscopy was also used to determine the ligands coordinated to Cd in Cd-substituted plastocyanin [185]. Multiple delay

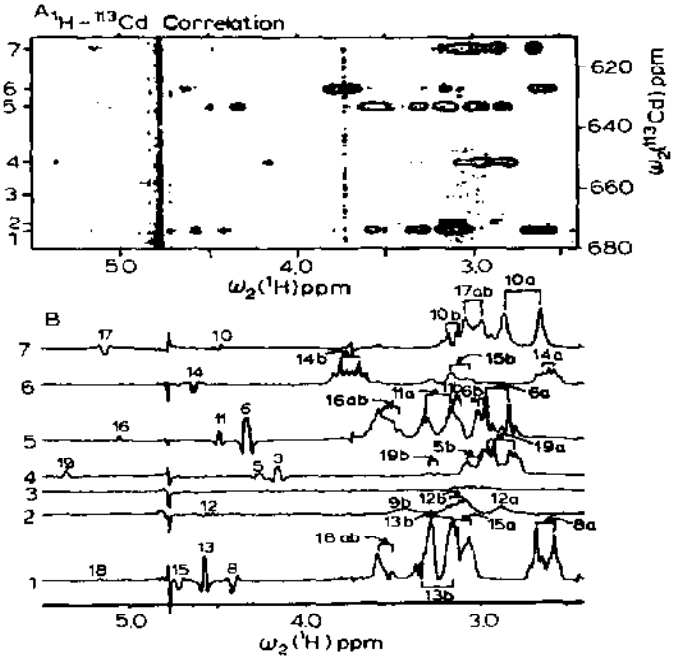

Fig. 28. Contour plot (A) and cross sections (B) of the ^{1}H-detected $^{1}H-^{113}Cd$ HMQC spectrum of MT-2. The cysteine signals are identified with arbitrary numbers according to the Hα chemical shifts, where α and β indicate the Hβ resonances with the larger and smaller coupling constant $^{3}J\alpha\beta$, respectively. Resonance splittings due to $^{1}H-^{113}Cd$ coupling are indicated with solid brackets. For further details see ref. 184.

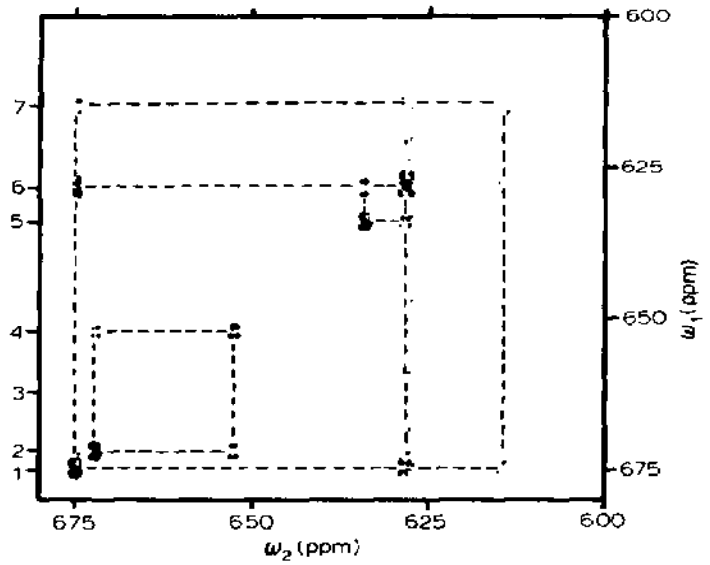

Fig. 29. $^{113}Cd-^{113}Cd$ double-quantum-filtered COSY spectrum of MT-2. Locations of the 7 Cd resonances are indicated on the left. $^{113}Cd-^{113}Cd$ connectivities are indicated with broken lines (ref. 184).

periods were used, and HMQC correlations with Cd were observed for His-37, His-87, Cys-84, and Met-92, confirming that these ligands were coordinated to Cd.

The HMQC method is also applicable to more labile Cd coordination compounds. The spectrum shown in Fig. 31 was obtained for a DMF solution at ambient temperature containing $Cd(ClO_4)_2$ (0.08 M) and equimolar amounts (0.02 M) of Et_4en and Meen [186]. Correlation peaks in the 2D plot allow assignment of the Cd signals and provide unambiguous information on the binding modes of these ligands [186].

The utility of X-filters in 2D ^{1}H-homonuclear correlation NMR experiments was recently shown to be useful for identifying scalar- or dipolar-cou-

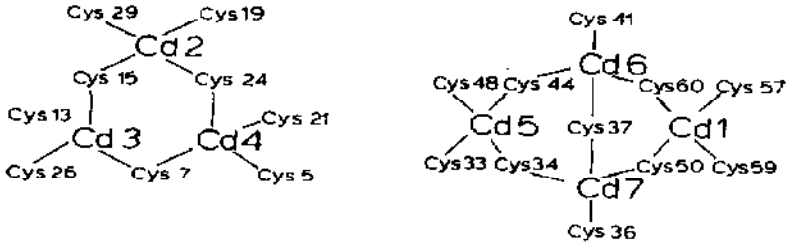

Fig. 30. Structures for the two metal clusters in MT-2 obtained using data from the $^1H-^{113}Cd$ and $^{113}Cd-^{113}Cd$ two-dimensional correlation NMR methods (ref. 184).

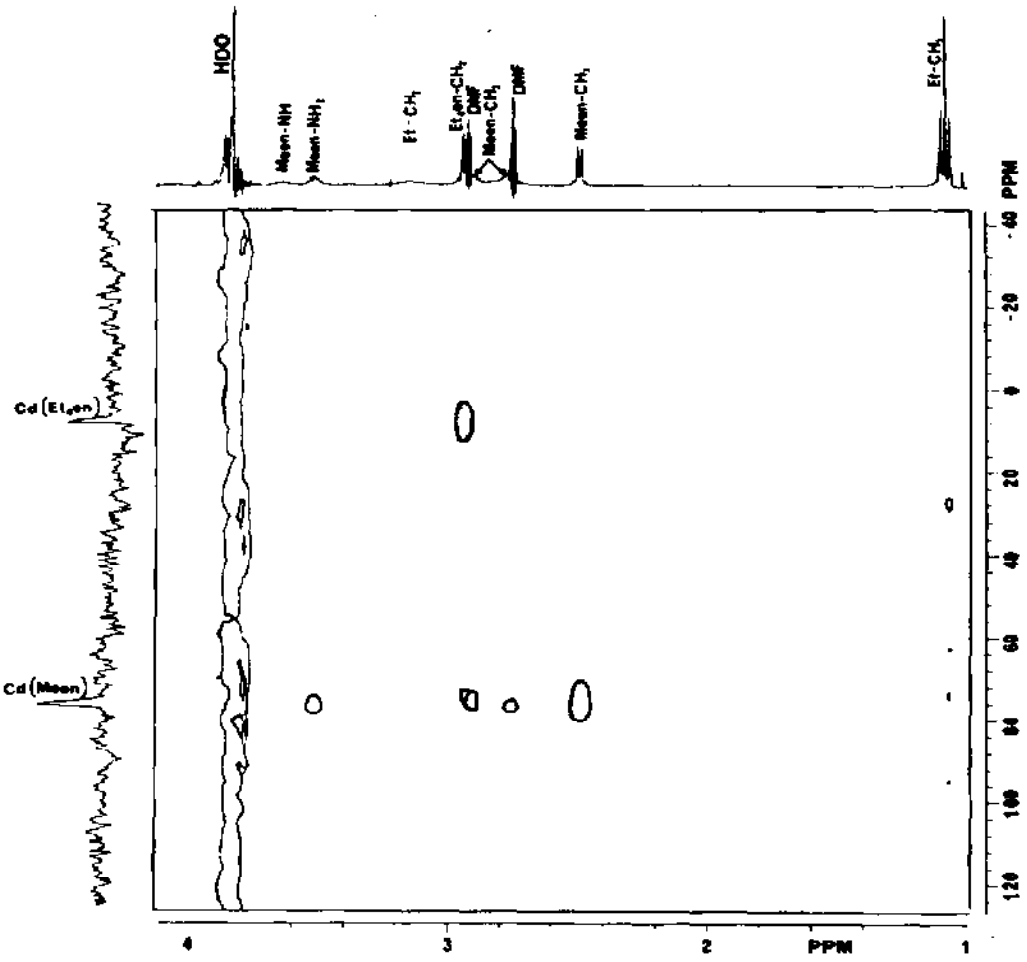

Fig. 31. $^{1}H-^{113}Cd$ HMQC NMR spectrum of a DMF solution (ambient temperature) containing $Cd(ClO_4)_2$ (0.08 M, natural isotopic abundance), *N*-Meen (0.02 M), and Et_4en (0.02 M). The normal 1D ^{1}H and ^{113}Cd spectra are shown at the top and side, respectively, of the contour plot (ref. 186).

pled protons which were also coupled to ^{113}Cd [187]. The methods were illustrated using a Cd(EDTA) sample and should prove extremely useful in future studies of Cd-substituted metalloproteins, especially where complex $^{1}H-^{113}Cd$ HMQC spectra are obtained.

G. SUMMARY

Despite the proven utility of ^{113}Cd NMR chemical shifts for qualitatively or, in some cases, semiquantitatively assessing the nature of ligands at metal binding sites in metalloproteins and for studying enzyme function and

mechanisms, it is likely that the full potential of ^{113}Cd spectroscopy as a metallobioprobe has yet to be realized. The development of a more quantitative relationship between structural parameters and ^{113}Cd chemical shift has been hampered in part by the lack of suitable model compounds and chemical dynamics [6]. As described throughout this review, these challenges are currently being met through applications of solid-state and low-temperature solution NMR methods and the design and study of less labile protein model compounds.

However, even for cases where dynamics and solvent or anion effects can be ruled out, it appears that ligand atom type and number, bond lengths, coordination geometry, and neighboring atoms (including other metals) all influence ^{113}Cd shifts. Studies of coordination compounds in solution have thus far provided useful information on the influence of donor-atom type and number on isotropic Cd chemical shifts. The influence on shift of coordination geometry and Cd–L bond lengths will probably only be adequately evaluated using the single crystal approach pioneered by Ellis and co-workers. Studies of the Cd ion bound exclusively by O-donor ligands will likely also be only adequately addressed through solid-state NMR methods due to lability problems with these ligands. In this area, model compounds with O-donor ligands which exhibit the unusual high-field shifts found for ICaBP and HRP are lacking.

^{113}Cd NMR chemical shift information alone is at present inadequate for unambiguous determination of structural features or structural changes at the metal binding sites of metalloproteins. In this regard, HMQC NMR spectroscopy promises to be a particularly useful tool for identifying the ligands which are coordinated to Cd. For cases where ligand exchange or nuclear relaxation rates are high (relative to $1/J$), however, this method will not work and determination of structural features may rely exclusively on chemical shift analyses. It is therefore important that both techniques be developed and utilized.

NOTE ADDED IN PROOF

Coleman [196] recently presented ^{113} Cd NMR results for Cd bound to the Zn domain of the protein product of gene 32 from bacteriophage T_4 (g-32P). The ^{113}Cd NMR chemical shift (638 ppm) is consistent with ligation via three S^- (Cys) and one N (His) donors. Ca^{2+}, Mg^{2+} and Cd^{2+} binding to the tryptic fragments of skeletal muscle troponin C have been investigated using ^1H and ^{113}Cd NMR [197]. ^{113}Cd-substituted pea and lentil lectins have also been studied [198].

ACKNOWLEDGMENTS

The author thanks Professors Joseph and Marilyn Ackerman, Philip A.W. Dean, Paul D. Ellis, and Sture Forsen for providing unpublished results. The help of Ken Seamon (Molecular Pharmacology, FDA) and support from members of the Biophysics Laboratory is also gratefully acknowledged.

REFERENCES

1 I.M. Armitage, R.T. Pajer, A.J.M. Schoot Uiterkamp, J.F. Chlebowski and J.E. Coleman, J. Am. Chem. Soc., 98 (1976) 3710.
2 P.D. Ellis, Science, 221 (1983) 1141.
3 H.J. Vogel, T. Drakenberg and S. Forsen, in P. Laszlo (Ed.), NMR of Newly Accessible Nuclei, Vol. 1, Academic Press, NY, 1983, p. 157.
4 P.D. Ellis, in J.B. Lambert and F.G. Riddell (Eds.), The Multinuclear Approach to NMR Spectroscopy, NATO ASI Ser., Ser. C, Vol. 103, 1983, p. 457.
5 I.M. Armitage and Y. Boulanger, in P. Laszlo (Ed.), NMR of Newly Accessible Nuclei, Academic, Press, NY, 1983, p. 337.
6 I.M. Armitage and J.D. Otvos, in L.J. Berliner and J. Reuben (Eds.), Biological Magnetic Resonance, Vol. 4, 1982, Plenum Press, NY, p. 79.
7 R. Garth Kidd, Annu. Rep. NMR Spectrosc. A, 10 (1980) 59.
8 J. Dechter, Prog. Inorg. Chem., 33 (1985) 393.
9 Y. Arata and T. Sawatari, Tampakushitsu Kakusan Koso, Bessatsu, (1983) 74.
10 K.B. Seamon and R.H. Kretsinger, in T.G. Spiro, (Ed.), Calcium in Biology, Wiley, New York, 1983, p. 1.
11 A. Andersson, T. Drakenberg and S. Forsen, in H. Hidaka and D.J. Hartshorne, (Eds.), Calmodulin Antagonists and Cellular Physiology, Academic Press, NY, 1985, p. 27.
12 J.E. Coleman, I.M. Armitage, J.F. Chlebowski, J.D. Otvos and A.J.M. Schoot Uiterkamp, in R.G. Shulman (Ed.), Biological Applications of Magnetic Resonance, Academic Press, NY, 1979, p. 345.
13 J.L. Sudmeier and D.B. Green, NATO Adv. Study Inst. Ser., Ser. C, 100 (1983) 35.
14 J.E. Coleman and P. Gettins, in T.G. Spiro (Ed.), Metal Ions in Biology, Vol. 5, Wiley, New York, 1983, p. 153. See Also: J.E. Coleman and P. Gettins, in A.V. Xavier (Ed.), Frontiers in Bioinorganic Chemistry, VCH, FL, 1986, p. 547; Adv. Enzymol. Rel. Areas Mol. Biol., 55 (1983) 381.
15 J.D. Otvos and I.M. Armitage, in A.A. Bothner-By, J.D. Glickson and B.D. Sykes (Eds.), Biochemical Structure Determination by NMR, Marcel Dekker, New York, 1982, p. 65; D.C. Dalgarno and I.M. Armitage, Adv. Inorg. Biochem., 6 (1984) 113.
16 R.G. Kidd and R.J. Goodfellow, in R.K. Harris and B.E. Mann (Eds.), NMR and the Periodic Table, Academic Press, NY, 1978, p. 195.
17 I.M. Armitage, A.J.M. Schoot Uiterkamp, J.F. Chlebowski and J.E. Coleman, J. Magn. Reson., 29 (1978) 375.
18 D.B. Bailey, P.D. Ellis and J.A. Fee, Biochemistry, 19 (1980) 591.
19 D.C. Look, Phys. Rev., 184 (1969) 705.
20 A. Nolle, Z. Naturforsch., Teil A, 33 (1978) 666.
21 T.T.P. Cheung, L.E. Worthington, P.D. Murphy and B.C. Gerstein, J. Magn. Reson., 41 (1980) 158.
22 P.G. Mennitt, M.P. Shatlock, V.J. Bartuska and G.E. Maciel, J. Phys. Chem., 85 (1981) 2087.

23 P.D. Murphy and B.C. Gerstein, J. Am. Chem. Soc., 103 (1981) 3282.
24 P.D. Murphy, W.C. Stevens, T.T.P. Cheung, S. Lacelle, B.C. Gerstein and D.M. Kurtz, Jr., J. Am. Chem. Soc., 103 (1981) 4400.
25 S. Lacelle, W.C. Stevens, D.M. Kurtz, Jr., J.W. Richardson, Jr. and R.A. Jacobson, Inorg. Chem., 23 (1984) 930.
26 H.J. Jakobsen, P.D. Ellis, R.R. Inners and C.F. Jensen, J. Am. Chem. Soc., 104 (1982) 7442.
27 P.D. Ellis, R.R. Inners and H.J. Jakobsen, J. Phys. Chem., 86 (1982) 1506.
28 P.F. Rodesiler and E.L. Amma, J. Chem. Soc., Chem. Commun., (1982) 182.
29 R.W. Turner, P.F. Rodesiler and E.L. Amma, Inorg. Chim. Acta, 66 (1982) L13.
30 P.F. Rodesiler, N.G. Charles, E.A.H. Griffith and E.L. Amma, Acta Crystallogr., Sect. C, 39 (1983) 1350.
31 E.A.H. Griffith, N.G. Charles, P.F. Rodesiler and E.L. Amma, Acta Crystallogr., Sect. C, 39 (1983) 331.
32 N.G. Charles, E.A.H. Griffith, P.F. Rodesiler and E.L. Amma, Inorg. Chem., 22 (1983) 2717.
33 P.F. Rodesiler, R.W. Turner, N.G. Charles, E.A.H. Griffith and E.L. Amma, Inorg. Chem., 23 (1984) 999.
34 N.G. Charles, P.F. Rodesiler, E.A.H. Griffith and E.L. Amma, Acta Crystallogr., Sect. C, 40 (1984) 1676.
35 P.F. Rodesiler, E.A.H. Griffith, N.G. Charles and E.L. Amma, Acta Crystallogr., Sect. C, 41 (1985) 673.
36 P.F. Rodesiler, E.A.H. Griffith, N.G. Charles, L. Lebioda and E.L. Amma, Inorg. Chem., 24 (1985) 4595.
37 P.F. Rodesiler, N.G. Charles, E.A.H. Griffith, K. Lewinski and E.L. Amma, Acta Crystallogr., Sect. C, 42 (1986) 538.
38 P.F. Rodesiler, N.G. Charles, E.A.H. Griffith, K. Lewinski and E.L. Amma, Acta Crystallogr., Sect. C, 42 (1986) 396.
39 M. Munakata, S. Kitagawa and F. Yagi, Inorg. Chem., 25 (1986) 964.
40 M.P. Shatlock and G.E. Maciel, J. Chem. Phys., 81 (1984) 895.
41 R.S. Honkonen, F.D. Doty and P.D. Ellis, J. Am. Chem. Soc., 105 (1983) 4163.
42 R.S. Honkonen and P.D. Ellis, J. Am. Chem. Soc., 106 (1984) 5488.
43 R.S. Honkonen, P.S. Marchetti and P.D. Ellis, J. Am. Chem. Soc., 108 (1986) 912.
44 S. Ganapathy, V.P. Chacko and R.G. Bryant, J. Chem. Phys., 81 (1984) 661.
45 P.S. Marchetti, R.S. Honkonen and P.D. Ellis, J. Magn. Reson., 71 (1987) 294.
46 V.W. Miner and J.H. Prestigard, J. Am. Chem. Soc., 107 (1985) 2177.
47 R.R. Inners, F.D. Doty, A.R. Garber and P.D. Ellis, J. Magn. Reson., 45 (1981) 503.
48 C.T. Hunt, Y. Boulanger, S.W. Fesik and I.M. Armitage, Bull. Magn. Reson., 6 (1984) 55.
49 P.S. Marchetti, P.D. Ellis and R.G. Bryant, J. Am. Chem. Soc., 107 (1985) 8191.
50 G.E. Maciel and M. Borzo, J. Chem. Soc., Chem. Commun., (1973) 349.
51 R.J. Kostelnik and A.A. Bothner-By, J. Magn. Reson., 14 (1974) 141.
52 H. Kruger, O. Lutz, A. Schwenk and G. Stricker, Z. Phys., 266 (1974) 233.
53 T. Drakenberg, N.-O. Bjork and R. Portanova, J. Phys. Chem., 82 (1978) 2423.
54 J.J.H. Ackerman, T.V. Orr, V.J. Bartuska and G.E. Maciel, J. Am. Chem. Soc., 101 (1979) 341.
55 M.J.B. Ackerman and J.J.H. Ackerman, J. Am. Chem. Soc., 107 (1985) 6413.
56 M.J.B. Ackerman and J.J.H. Ackerman, unpublished results, 1987.
57 R. Colton and D. Dakternieks, Aust. J. Chem., 33 (1980) 2405.

58 T. Vladimiroff and E.R. Malinowski, J. Chem. Phys., 46 (1967) 1830.
59 M.F. Summers, J. van Rijn, Y. Reedijk and L.G. Marzilli, J. Am. Chem. Soc., 108 (1986) 4254.
60 S. Biagini, M. Casu, A. Lai, R. Caminiti and G. Crisponi, Chem. Phys., 93 (1985) 461.
61 M. Holz, R.B. Jordan and M.D. Zeidler, J. Magn. Reson., 22 (1976) 47.
62 P. Linse, H. Gustavsson, B. Lindman and T. Drakenberg, J. Magn. Reson., 45 (1981) 133.
63 M. Monduzzi, A. Lai and L. Burlamacchi, Chem. Phys., 96 (1985) 419.
64 D.D. Dominguez, M.M. King and H.J. Yeh, J. Magn. Reson, 32 (1978) 161.
65 P.F. Rodesiler, E.H. Griffith, P.D. Ellis and E.L. Amma, J. Chem. Soc., Chem. Commun., (1980) 492.
66 C.F. Jensen, S. Deshmukh, H.J. Jakobsen, R.R. Inners and P.D. Ellis, J. Am. Chem. Soc., 103 (1981) 3659.
67 C.C. Bryden and C.N. Reilley, Inorg. Chem., 104 (1982) 2697.
68 A.D. Keller, T. Drakenberg, R.W. Briggs and I.M. Armitage, Inorg. Chem., 24 (1985) 1170.
69 E.C. Alyea, Inorg. Chim. Acta, 76 (1983) L239.
70 M.F. Summers and L.G. Marzilli, Inorg. Chem., 23 (1984) 521.
71 G.C. Baumann, M.F. Summers, J.P. Hutchinson, J. Zubietta and L.G. Marzilli, Inorg. Chem., 23 (1984) 3104.
72 E.C. Alyea and K.J. Fisher, Polyhedron, 5 (1986) 695.
73 R.A. Haberkorn, L. Que, Jr., W.O. Gillum, R.H. Holm, C.S. Liu and R.C. Lord, Inorg. Chem., 15 (1976) 2408.
74 T. Maitani and K.T. Suzuki, Inorg. Nucl. Chem. Lett., 15 (1979) 213.
75 G.K. Carson, P.A.W., Dean and M.J. Stillman, Inorg. Chim. Acta, 56 (1981) 59.
76 A.M. Bond, R. Colton, D. Dakternieks, M.L. Dillon, J. Hauenstein and J.E. Moir, Aust. J. Chem., 34 (1981) 1393.
77 P.A.W. Dean, Can. J. Chem., 59 (1981) 3221.
78 G.K. Carson and P.A.W. Dean, Inorg. Chim. Acta, 66 (1982) 37.
79 P. Hofstetter, E. Pretsch and W. Simon, Helv. Chim. Acta, 66 (1983) 2103.
80 E.A. Griffith and E.L. Amma, J. Chem. Soc., Chem. Commun., (1979) 1013.
81 R. Colton and D. Dakternieks, Aust. J. Chem., 33 (1980) 1677.
82 D. Dakternieks, Aust. J. Chem., 35 (1982) 469.
83 D. Dakternieks and C.L. Rolls, Inorg. Chim. Acta, 87 (1984) 5.
84 D. Dakternieks and C.L. Rolls, Inorg. Chim. Acta, 105 (1985) 213.
85 R.A. Bulman, J.K. Nicholson, D.P. Higham and P.J. Sadler, J. Am. Chem. Soc., 106 (1984) 1118.
86 P.A.W. Dean and J.J. Vittal, J. Am. Chem. Soc., 106 (1984) 6436.
87 I.G. Dance, Aust. J. Chem., 38 (1985) 1745.
88 I.G. Dance and J.K. Saunders, Inorg. Chim. Acta, 96 (1985) L71.
89 I.G. Dange, Inorg. Chim. Acta, 108 (1985) 227.
90 P.A.W. Dean and J.J. Vittal, Inorg. Chem., 24 (1985) 3722.
91 P.A.W. Dean and J.J. Vittal, Inorg. Chem., 25 (1986) 514.
92 P.A.W. Dean, J.J. Vittal and N.C. Payne, Inorg. Chem., 26 (1987) 1683.
93 A.D. Cardin, P.D. Ellis, J.D. Odom and J.W. Howard, Jr., J. Am. Chem. Soc., 97 (1975) 1672.
94 C.J. Turner and R.F.M. White, J. Magn. Reson., 26 (1977) 1.
95 J.D. Kennedy and W. McFarlane, J. Chem. Soc., Perkin Trans. 2, (1977) 1187.
96 L.C. Damude and P.A.W. Dean, J. Organomet. Chem., 168 (1979) 123.

97 J. Jokisaari, K. Raisanen, L. Lajunen, A. Passoja and P. Pyykko, J. Magn. Reson., 31 (1978) 121.
98 M.J.B. Ackerman and J.J.H. Ackerman, J. Phys. Chem., 84 (1980) 3151.
99 H.J. Jakobsen and P.D. Ellis, J. Phys. Chem., 85 (1981) 3367.
100 S.M. Wang and R.K. Gilpin, Anal. Chem., 55 (1983) 493.
101 S.M. Wang and R.K. Gilpin, Talanta, 32 (1985) 329.
102 B. Birgersson, R.E. Carter and T. Drakenberg, J. Magn. Reson., 28 (1977) 299.
103 D.B. Bailey, P.D. Ellis, A.D. Cardin and W.D. Behnke, J. Am. Chem. Soc., 100 (1978) 5236.
104 A.R. Palmer, D.B. Bailey, W.D. Behnke, A.D. Cardin, P.P. Yang and P.D. Ellis, J. Am. Chem. Soc., 19 (1980) 5063.
105 P.D. Ellis, P.P. Yang and A.R. Palmer, J. Magn. Reson., 52 (1983) 254.
106 E. Thulin, S. Forsen, T. Drakenberg, T. Andersson, K. Krebs and K.B. Seamon, in F.L. Siegel, E. Carafoli, R.H. Krestinger, O.H. MacLennon and R.H. Wasserman (Eds.), Calcium Binding Proteins: Structure and Function, Elsevier, New York, 1980, p. 241.
107 J.L. Sudmeier, J.L. Evelhoch, S.J. Bell, M.C. Storm and M.F. Dunn, in F.L. Siegel, E. Carafoli, R.H. Krestinger, O.H. MacLennon and R.H. Wasserman (Eds.), Calcium Binding Proteins; Structure and Function, Elsevier, New York, 1980, p. 235.
108 T. Andersson, T. Drakenberg, S. Forsen and E. Thulin, Eur. J. Biochem., 126 (1982) 501.
109 S. Forsen, E. Thulin, T. Drakenberg, J. Krebs and K. Seamon, FEBS Lett., 117 (1980) 189.
110 E. Thulin, S. Forsen, T. Drakenberg, T. Andersson, K.B. Seamon and J. Krebs, in F.L. Siegel, E. Carafoli, R.H. Krestinger, O.H. MacLennon and R.H. Wasserman (Eds.), Calcium Binding Proteins: Structure and Function, Elsevier, New York, 1980, p. 243.
111 A. Andersson, T. Drakenberg, E. Thulin and S. Forsen, Eur. J. Biochem., 134 (1983) 459.
112 A. Andersson, J. Drakenberg, E. Thulin, H. Vogel and S. Forsen, in B. de Bernard, G.L. Sottocasa, G. Sandri, E. Carafoli, A.N. Taylor, T.C. Varomar and R.J.P. Williams (Eds.), Calcium Binding Proteins, Elsevier, New York, 1983, p. 165.
113 S.-L. Bostrom, B. Ljung, S. Markh, S. Forsen and E. Thulin, Nature (London), 292 (1981) 777.
114 A. Andersson, S. Forsen, E. Thulin and H.J. Vogel, Biochemistry, 22 (1983) 2309.
115 S. Forsen, A. Andersson, T. Drakenberg, O. Teleman, E. Thulin and H.J. Vogel, in B. DeBernard et al. (Eds.), Calcium Binding Proteins, Elsevier, New York, 1983, p. 121.
116 E. Thulin, A. Andersson, T. Drakenberg, S. Forsen and H.J. Vogel, Biochemistry, 23 (1984) 1862.
117 S. Linse, T. Drakenberg and S. Forsen, FEBS Lett., 199 (1986) 28.
118 J.L. Sudmeier, S.J. Bell, M.C. Storm and M.F. Dunn, Science, 212 (1981) 560.
119 K.M. Welsh, I.M. Armitage and B.S. Cooperman, Biochemistry, 22 (1983) 1046.
120 K.M. Welsh and B.S. Cooperman, Biochemistry, 23 (1984) 4947.
121 R.V. Prigodich, T. O'Connor and J.E. Coleman, Biochemistry, 24 (1985) 6291.
122 T. Drakenberg, B. Lindman, A. Cave and J. Parello, FEBS Lett., 92 (1978) 346.
123 A. Cave, J. Parello, T. Drakenberg, E. Thulin and B. Lindman, FEBS Lett., 100 (1979) 148.
124 L. Lee and B.D. Sykes, Biochemistry, 22 (1983) 4366.
125 M.E. Bjornson, D.C. Corson and B.D. Sykes, J. Inorg. Biochem., 25 (1985) 141.
126 T. Drakenberg, M. Sward, A. Cave and J. Parello, Biochem. J., 227 (1985) 711.
127 D.C. Corson, L. Lee, G.A. McQuaid and B.D. Sykes, Can. J. Chem. Cell Biol., 61 (1983) 860.
128 S. Forsen, E. Thulin and H. Lilja, FEBS Lett., 104 (1979) 123.

129 P.D. Ellis, P. Strang and J.D. Potters, J. Biol. Chem., 259 (1984) 10348.
130 O. Teleman, T. Drakenberg, S. Forsen and E. Thulin, Eur. J. Biochem., 134 (1983) 453.
131 L.J. Berliner, P.D. Ellis and K. Murakami, Biochemistry, 22 (1983) 5061.
132 S.G. Spencer, J.M. Brewer and P.D. Ellis, J. Inorg. Biochem., 24 (1985) 47.
133 P.B. Kingsley-Hickman, G.L. Nelsestuen and K. Ugurbil, Biochemistry, 25 (1986) 3352.
134 H.J. Vogel, T. Drakenberg, S. Forsen, J.D.J. O'Neil and T. Hofmann, Biochemistry, 24 (1985) 3870.
135 S. Forsen, T. Drakenberg, E. Thulin, P. Brodin, T. Grundstrom, S. Linse, P. Sellers and K. Elmden, in A.W. Norman, T.C. Vanaman and A.R. Means (Eds.), Ca Binding Proteins in Health and Disease, Academic Press, NY, 1987, in the press.
136 E. Chiancone, T. Drakenberg, O. Teleman and S. Forsen, J. Mol. Biol., 185 (1985) 201.
137 I. Morishima, M. Kurono and Y. Shiro, J. Biol. Chem., 261 (1986) 9391.
138 G.I. Rhyu, W.J. Ray, Jr. and J.L. Markley, Biochemistry, 24 (1985) 2536.
139 K. Aalmo, J. Krane, C. Little and C.S. Storm, Biochem. Soc. Trans., 10 (1982) 367.
140 K. Aalmo, L. Hansen, E. Hough, K. Jynge, J. Drane, C. Little and C.B. Storm, Biochem. Int., 8 (1984) 27.
141 J.F. Chlebowski, I.M. Armitage and J.E. Coleman, J. Biol. Chem., 252 (1977) 7053.
142 J.D. Otvos and I.M. Armitage, Biochemistry, 19 (1980) 4031.
143 P. Gettins and J.E. Coleman, Fed. Proc., Fed. Am. Soc. Exp. Biol., 41 (1982) 2966.
144 P. Gettins and J.E. Coleman, J. Biol. Chem., 258 (1983) 396.
145 P. Gettins and J.E. Coleman, J. Biol. Chem., 259 (1984) 11036.
146 P. Gettins and J.E. Coleman, J. Biol. Chem., 259 (1984) 4987.
147 P. Gettins and J.E. Coleman, J. Biol. Chem., 259 (1984) 4991.
148 E.O. Martins and T. Drakenberg, Inorg. Chim. Acta, 67 (1982) 71.
149 A.J.M. Schoot Uiterkamp, I.M. Armitage and J.E. Coleman, J. Biol. Chem., 255 (1980) 3911.
150 J.L. Sudmeier and S.J. Bell, J. Am. Chem. Soc., 99 (1977) 4499.
151 N.B.-H. Jonsson, L.A.E. Tibell, J.L. Evelhoch, S.J. Bell and J.L. Sudmeier, Proc. Natl. Acad. Sci. U.S.A., 77 (1980) 3269.
152 J.L. Evelhoch, D.F. Bocian and J.L. Sudmeier, Biochemistry, 20 (1981) 4951.
153 M. Blackburn, B.E. Mann, B.F. Taylor and A.F. Worrall, Eur. J. Biochem., 153 (1985) 553.
154 P. Gettins, J. Biol. Chem., 261 (1986) 15513.
155 R. Sommer and D. Beyersmann, J. Inorg. Biochem., 20 (1984) 131.
156 B.R. Bobsein and R.J. Myers, J. Am. Chem. Soc., 102 (1980) 2454.
157 B.R. Bobsein and R.J. Myers, J. Biol. Chem., 256 (1981) 5313.
158 K.T. Suzuki and T. Maitani, Experientia Suppl., 34 (1978) 1449.
159 P.J. Sadler, A. Bakka and P.J. Beynon, FEBS Lett., 94 (1978) 315.
160 J.D. Otvos and I.M. Armitage, J. Am. Chem. Soc., 101 (1979) 7734.
161 J.D. Otvos and I.M. Armitage, Proc. Natl. Acad. Sci. U.S.A., 77 (1980) 7094.
162 J.D. Otvos, R.W. Olafson and I.M. Armitage, J. Biol. Chem., 257 (1982) 2427.
163 Y. Boulanger, I.M. Armitage, K.-A. Miklossy and D.R. Winge, J. Biol. Chem., 257 (1982) 13717.
164 I.M. Armitage, J.D. Otvos, R.W. Briggs and Y. Boulanger, Fed. Proc., 41 (1982) 2974.
165 Y. Boulanger and I.M. Armitage, J. Inorg. Biochem., 17 (1982) 147.
166 R.W. Briggs and I.M. Armitage, J. Biol. Chem., 257 (1982) 1259.
167 P.A.W. Dean, A.Y.C. Law, J.A. Szmanska and M.J. Stillman, Inorg. Chim. Acta, 78 (1983) 275.
168 Y. Boulanger, C.M. Goodman, C.P. Forte, S.W. Fesik and I.M. Armitage, Proc. Natl. Acad. Sci. U.S.A., 80 (1983) 1501.

169 J.K. Nicholson, P.J. Sadler, K. Chain, D.E. Holt, M. Webb and G.E. Hawkes, Biochem. J., 211 (1983) 251.
170 D. Neuhaus, G. Wagner, M. Vasak, J.H.R. Kagi and K. Wuthrich, Eur. J. Biochem., 143 (1984) 659.
171 C.T. Hunt, Y. Boulanger, S.W. Fesik and I.M. Armitage, Environ. Health, 54 (1984) 135.
172 D.G. Nettesheim, H.R. Engeseth and J.D. Otvos, Biochemistry, 24 (1985) 6744.
173 M. Vasak, G.E. Hawkes, J.K. Nicholson and P.J. Sadler, Biochemistry, 24 (1985) 740.
174 J.D. Otvos, H.R. Engeseth and S. Wehrli, Biochemistry, 24 (1985) 6735.
175 D.M. Templeton, P.A.W. Dean and M.G. Cherian, Biochem. J., 234 (1986) 685.
176 G. Wagner, D. Neuhaus, E. Worgotter, M. Vasak, J.H.R. Kagi and K. Wuthrich, J. Mol. Biol., 187 (1986) 131.
177 W. Braun, G. Wagner, E. Worgotter, M. Vasak, J.H.R. Kagi and K. Wuthrich, J. Mol. Biol., 187 (1986) 125.
178 D.P. Higham, J.K. Nicholson, J. Overnell and P.J. Sadler, Environ. Health, 65 (1986) 157.
179 J.D. Otvos and I.M. Armitage, in J.H.R. Kagi and M. Nordberg (Eds), Metallothionein, Birkhauser Verlag, Basel/Boston/Stuttgart, 1979, p. 249.
180 H.R. Engeseth, D.R. McMillin and J.D. Otvos, J. Biol. Chem., 259 (1984) 4822.
181 J.D. Otvos, personal communication, 1986.
182 D. Live, I.M. Armitage, D.C. Dalgarno and D. Cowburn, J. Am. Chem. Soc., 107 (1985) 1775.
183 J.D. Otvos, H.R. Engeseth and S. Wehrli, J. Magn. Reson., 61 (1985) 579.
184 M.H. Frey, G. Wagner, M. Vasak, O.W. Sorensen, D. Neuhaus, E. Worgotter, J.H.R. Kagi, R.R. Ernst and K. Wuthrich, J. Am. Chem. Soc., 107 (1985) 6847.
185 D.H. Live, C.L. Kojiro, D. Cowburn and J.L. Markley, J. Am. Chem. Soc., 107 (1985) 3043.
186 M.F. Summers, unpublished results, 1987.
187 E. Worgotter, G. Wagner and K. Wuthrich, J. Am. Chem. Soc., 108 (1986) 6162.
188 B. Notstrand, I. Vaara and K.K. Kannan, in C.L. Markert (Ed.), The Isozymes, Academic Press, NY, 1984, p. 575.
189 The correct chemical shift value for $Cd(S(CH_2)_2)S)$ (784 ppm) was published in a corrigendum: G.K. Carson, P.A.W. Dean and M.J. Stillman, Inorg. Chim. Acta, 108 (1985) 71.
190 W.F. Furey, A.H. Robbins, L.L. Clancy, D.R. Winge, B.C. Wang and C.D. Stout, Science, 231 (1986) 704.
191 B.E. Mann, Inorg. Nucl. Chem. Lett., 7 (1971) 595.
192 R.G. Goel, W.P. Henry and R.C. Srivastava, Inorg. Chem., 20 (1981) 1727.
193 R.G. Goel, W.P. Henry and N.K. Jha, Inorg. Chem., 21 (1982) 2551.
194 A. Nolle, Z. Phys. Chem., Abt. B, 34 (1979) 175.
195 D. Beyersmann, personal communication. S.S. Hasnain, E.M. Wardell, C.D. Garner, M. Schlosser and D. Begersmann, Biochem. J., 230 (1985) 625.
196 D. Giedroc, J.E. Coleman, 1987, in preparation.
197 T. Drakenberg, S. Forsen, E. Thulin and H.J. Vogel, J. Biol. Chem., 262 (1987) 672.
198 L. Bhattacharyya, P.S. Marchetti, P.D. Ellis and C.F. Brewer, J. Biol. Chem., 262 (1987) 5616.